

UCLA

UCLA Electronic Theses and Dissertations

Title

Axonal sprouting in a novel intracortical connection formed upon limb overuse after stroke: a circuit-specific transcriptomic study

Permalink

<https://escholarship.org/uc/item/9w5976qh>

Author

Nie, Esther Hang

Publication Date

2016

Supplemental Material

<https://escholarship.org/uc/item/9w5976qh#supplemental>

Peer reviewed|Thesis/dissertation

UNIVERSITY OF CALIFORNIA

Los Angeles

Axonal sprouting in a novel intracortical connection formed upon limb overuse after stroke:
a circuit-specific transcriptomic study

A dissertation submitted in partial satisfaction of the requirements for the degree
Doctor of Philosophy in Neuroscience

by

Esther Hang Nie

2016

© Copyright by

Esther Hang Nie

2016

ABSTRACT OF THE DISSERTATION

Axonal sprouting in a novel intracortical connection formed upon limb overuse after stroke:
a circuit-specific transcriptomic study

by

Esther Hang Nie

Doctor of Philosophy in Neuroscience

University of California, Los Angeles, 2016

Professor Stanley Thomas Carmichael, Chair

Stroke is the leading cause of adult disability and leaves millions of patients worldwide with chronic deficits in sensory, motor, and cognitive function. Although there are currently no pharmacological treatments for brain recovery after stroke, clinical trials have shown that a limb overuse paradigm, known as constraint-induced movement therapy (CIMT), can lead to significant and lasting motor improvements. This functional improvement is strongly associated with increased activity in the ipsilesional premotor cortex, but the exact neuronal connections and molecular processes that underlie this plasticity process are unknown.

The body of work within this dissertation identifies one potential mechanism of cortical axonal sprouting after limb overuse in a mouse model of stroke and forelimb overuse that approximates human CIMT. Via quantitative neuroanatomical mapping, we find that limb overuse drives the novel formation of a connection from retrosplenial cortex to premotor cortex (RSC-PMC). We then isolate the very neurons that comprise this connection by FACS (Fluorescence-Activated Cell Sorting) purification for RNA-Seq transcriptional profiling. The RSC-PMC

transcriptome is characterized by expression of activity-induced and growth-related genes, several of which are new to the context of CNS injury and plasticity. Pathway analyses indicate that limb overuse induces signaling in cell growth and tissue development, calcium signaling, and Ephrin A pathways. Upstream transcriptional regulators of the differentially expressed genes within RSC-PMC include NeuroD1, NeuroG3, YY1, and Otx2. Subsequently, top candidates from the 160 differentially regulated genes by limb overuse were functionally screened using CRISPR/cas9 in an in-vitro neuronal outgrowth assay. Two molecular hits were Otx2 and NeuroG3, genes previously associated with critical period onset/closure and neurogenesis, respectively. Finally, whole transcriptome comparison studies of the RSC-PMC across various plasticity paradigms indicate relationship to activity-dependent/learning transcriptomes and divergence from developmental growth programs. In parallel, we find that GDF10 (growth and differentiation factor 10) is an early trigger of axonal sprouting after stroke. Even in the absence of limb overuse, we find that in-vivo delivery of GDF10 increases axonal peri-infarct sprouting, forms synaptic contacts in premotor cortex, and results in improved behavioral recovery. Together, these studies identify potentially synergistic mechanisms to target in future therapeutic strategies for stroke.

The dissertation of Esther Hang Nie is approved.

Kelsey C. Martin

Neil G. Harris

Peyman Golshani

Stanley Thomas Carmichael, Committee Chair

University of California, Los Angeles

2016

In fond memory of Dr. Robin Fisher

TABLE OF CONTENTS

	PAGE
ABSTRACT OF THE DISSERTATION -----	ii-iii
LIST OF FIGURES -----	vi
LIST OF TABLES -----	vii
ACKNOWLEDGEMENTS -----	viii-ix
VITA -----	x-xi
CHAPTER 1. Introduction	1-34
1.1 Stroke initiates a dynamic state in surviving brain tissue-----	2
1.2 Constraint-induced movement therapy-----	13
1.3 Premotor cortex after primary motor stroke: a window of opportunity---	16
1.4 Harnessing the circuit and molecular mechanisms underlying CIMT -----	20
1.5 Figures-----	22
1.6 References-----	25
CHAPTER 2. Limb overuse after stroke induces axonal sprouting between retrosplenial cortex and premotor cortex	35-55
2.1 Introduction-----	35
2.2 Results-----	36
2.3 Discussion-----	38
2.4 Methods-----	43
2.5 Figures-----	47
2.6 References-----	52
CHAPTER 3. An activity-dependent and connection-specific transcriptome after stroke and limb overuse	56-94
3.1 Introduction-----	56
3.2 Results-----	57
3.3 Discussion-----	62
3.4 Figures-----	68
3.5 Methods-----	84
3.6 References-----	88
CHAPTER 4. CRISPR/cas9 in-vitro screening of candidate genes	95-122
4.1 Introduction-----	95
4.2 Results-----	96
4.3 Discussion-----	100
4.4 Figures-----	105
4.5 Methods-----	114
4.6 References-----	118
CHAPTER 5. GDF10 is a molecular signal for post-stroke axonal sprouting and improved motor recovery	123-53
5.1 Introduction-----	123
5.2 Results-----	124
5.3 Discussion-----	128
5.4 Figures-----	130
5.5 Methods-----	145
5.6 References-----	152
CHAPTER 6. Integration of findings and future outlook -----	154-62
6.1 References-----	160

LIST OF FIGURES

	PAGE
CHAPTER 1. Introduction	
Figure 1.1 Axonal sprouting after stroke -----	22
Figure 1.2 Constraint induced movement therapy -----	23
Figure 1.3 Premotor cortex comparative neuroanatomy-----	24
CHAPTER 2. Limb overuse after stroke induces axonal sprouting between retrosplenial cortex and premotor cortex	
Figure 2.1 Experimental timeline of neuroanatomic mapping studies -----	47
Figure 2.2 Limb overuse produces novel pattern of premotor connections-----	48
Figure 2.3 A second study reproduces PMC-RSC connectivity maps after limb overuse-	49
Figure 2.4 Corticospinal motor regions are distinct from RSC origin of PMC connection-----	50
Figure 2.5 Mapping the posterior medial region of interest to retrosplenial cortex -----	51
CHAPTER 3. An activity-dependent and connection-specific transcriptome after stroke and limb overuse	
Figure 3.1 Workflow from cell tracing to RNA-sequencing-----	68
Figure 3.2 FACS purification of Fluorogold-labeled neurons-----	69
Figure 3.3 FACS purification of RSC FG+ and NCAM+ neurons for RNA-Seq-----	70
Figure 3.4 Top 100 differentially expressed genes ranked across all comparisons -----	72-3
Figure 3.5 IPA pathway analyses -----	77-8
Figure 3.6 WGCNA gene modules-----	80-1
Figure 3.7 Transcriptome overlay analysis-----	82
CHAPTER 4. CRISPR/cas9 in-vitro screening of candidate genes	
Figure 4.1 Fluidigm qPCR candidate gene validation -----	106
Figure 4.2 CRISPR/cas9 gRNA and lentivirus workflow -----	107
Figure 4.3 Mutation detection using Cel-I nuclease-----	109-10
Figure 4.4 LentiCRISPRV2 transduction and cas9 expression -----	111
Figure 4.5 ImageExpress neurite tracing overlay -----	112
CHAPTER 5. GDF10 is a molecular signal for post-stroke axonal sprouting and improved motor recovery	
Figure 5.1 GDF10 enhances axonal outgrowth in primary neurons <i>in vitro</i> -----	130
Figure 5.2 GDF10 promotes axonal connections in peri-infarct cortex after stroke-----	131
Figure 5.3 Synaptic connections in peri-infarct cortex after GDF10 treatment-----	132-3
Figure 5.4 GDF10 promotes motor behavioral recovery after stroke -----	134-5
Figure 5.5 GDF10 is expressed in rodent, monkey and human peri-infarct tissue-----	136-7
Figure 5.6. GDF10 is upregulated in peri-infarct cortex neurons and extracellular space	138-9
Figure 5.7 Molecular transcriptome comparisons across various plasticity paradigms----	141
Figure 5.8 GDF10 canonical signaling pathways -----	142

LIST OF TABLES

	PAGE
CHAPTER 3. An activity-dependent and connection-specific transcriptome after stroke and limb overuse	
Table 3.1 Samples collected by FACS purification for RNA-Sequencing-----	71
Table 3.2 160 genes differentially regulated by limb overuse after stroke-----	74-76
Table 3.3 Upstream analysis of genes differentially regulated by limb overuse -----	79
Table 3.4 Expression profile sources used for transcriptome overlap analyses-----	83
CHAPTER 4. CRISPR/cas9 in-vitro screening of candidate genes	
Table 4.1 Candidate genes for Fluidigm qPCR validation-----	105
Table 4.2 Candidate gene gRNA sequences -----	108
Table 4.3 Neurite outgrowth candidate screen: Tau label for axons-----	113
Table 4.4 Neurite outgrowth candidate screen: MAP2 label for dendrites-----	113
CHAPTER 5. GDF10 is a molecular signal for post-stroke axonal sprouting and improved motor recovery	
Table 5.1 Sources of expression profiles for transcriptomic overlay analyses-----	140
Table 5.2. Differentially regulated genes within PTEN and PI3K pathways-----	143
Table 5.3 Axonal guidance genes differentially regulated by GDF10 -----	144

ACKNOWLEDGEMENTS

The work presented in this dissertation would not have been possible without the support of a fantastic cast of characters along the way. I will do my best in this finite space to express my infinite gratitude.

First and foremost, I humbly thank my graduate advisor Dr. Tom Carmichael for his guidance and active participation throughout the five years of my PhD training. In looking back, the Carmichael lab has grown enormously in the number of projects and personnel (and confocal microscopes) since I joined the lab. But through it all, Tom has always been an energetic, receptive, and engaging mentor. Tom's commitment to his trainees shines through in our near-daily encounters to chat, plan, or write science. His unique mentoring style is one that never micromanages, but specifically engages and cultivates student progress. This teaching philosophy allowed me to always feel well supported as a graduate student, but also gave me healthy room to grow intellectually and technically, to ultimately develop skills that drive independent scientific investigation. Finally, I respect Tom not only as an exemplar of a creative and productive physician-scientist, but also for his unshakable good spirit. Tom's one-of-a-kind MO is truly his winning trait, especially in the face of the myriad challenges in scientific research and patient-care.

To the cherished members of my dissertation committee: Peyman Golshani, Neil Harris, and Kelsey Martin, thank you for your support and discussions on this evolving project through the years. I left each committee or one-on-one meeting feeling inspired to pursue more. You are each an inspiration to me in different ways. To mentors I was lucky enough to meet early on: Sreeranga Chandra, Vinzenz Unger, and Robin Fisher, words cannot express my profound gratitude for your insights and encouragement. To our many collaborators and colleagues, including Giovanni Coppola, Riki Kawaguchi, Mark Anderson, Joe Loturco, Feng Zhang, Bryan Luikart, UCLA FACS and MSSR cores, thank you for the countless conversations, ideas, reagents and experiments we shared.

To all of the past and present members of Team Carmichael, thank you. In particular, I would like to thank Songlin Li and Justine Overman for their smiling support and guidance when I first joined the lab. Their pioneering work on post-stroke axonal sprouting very much drew me into what would become an exciting dissertation project. To all the other graduate students and many post-docs/fellows who overlapped with me on this ride: Justine, Jason, Sarah, Elif, Andrew, Harriet, Luca, David, Irene, Amy, Catherine, Kwon, Teena, Liang (just to name a few!), I will always remember our shared time, from SFN whiskeys to wee-hour experiments in the lab. To my NSIDP entering cohort of 2011, we really got lucky with a great bunch. You guys have immeasurably added to my rich graduate school experience. Tessa and Rachel, I'm glad we have a plan to freeze time after we all defend so this doesn't have to end.

Mom and Dad, thank you for everything from day one. Mom, not every daughter is so lucky to have a mother who embodies self-confidence, independent-thinking, and eternal optimism. Dad, thank you for your endless humor, strength of character, and advice to eat and drink and be merry. Thank you both for being my biggest champions, supporting me through adversity, and for always jointly cheering me on through every step of life, including this unique journey through the MSTP years.

Finally, thank you to Don for being a true partner to me throughout these PhD years. Your humor, patience, and zen...

The research presented in this project was supported by the Edwin and Catherine Davis Fund and National Institutes of Health NINDS (1 R01 NS077521). Graduate student support was provided through training grants from the UCLA Training Program in Neural Repair (NIH T32NS007449), AHA Western States Predoctoral fellowship (13PRE16910107), and NINDS Ruth L. Kirschstein NRSA (1F31NS086431).

Chapters 2-4 are elaborated from a manuscript currently under preparation:

Nie EH, Kawaguchi R, Coppola G, Carmichael ST. Limb overuse after stroke induces a unique molecular transcriptome of cortical reorganization in the retrosplenial cortex.

Manuscript in preparation

Data presented in Chapter 5 are published in the following research article. The written contents of Chapter 5 are an adapted and abridged version from this publication.

Li S*, Nie EH*, Yin Y, Benowitz LI, Tung S, Vinters HV, Bahjat FR, Stenzel-Poore MP, Kawaguchi R, Coppola G, Carmichael ST. GDF10 is a signal for axonal sprouting and functional recovery after stroke. *Nat Neurosci.* 2015; 12: 1737-45. *co-first authorship

VITA

EDUCATION

- 08/2009 to present David Geffen School of Medicine at UCLA, Los Angeles, California
Medical Scientist Training Program
- 08/2005 to 05/2009 Yale University, New Haven, Connecticut
B.S., Molecular Biophysics and Biochemistry
Distinction in the Major

HONORS & AWARDS

- 2016 Eva Kavan Prize for graduate research in basic neuroscience
- 2013-2016 NIH, NINDS F31 NRSA
- 2015 2nd place poster prize, 7th annual UCLA Neurology Science Day
- 2014 Advanced Techniques in Molecular Neuroscience Course, CSHL
- 2013-2015 Predoctoral Research Fellowship, American Heart Association
- 2012-2013 Training Program in Neural Repair NIH T32 training grant recipient
- 2013 Abstract selected for Hot Topics in Neuroscience SfN publication
- 2007-2009 Yale University Sheffield Scientific Scholarship
- 2005 Century Scholar for Scientific Research, Rice University
- 2005 National Merit Finalist and 2500 Scholarship recipient

RESEARCH

- 06/2010 to present S. Thomas Carmichael, M.D., Ph.D.
Dept. of Neurology, UCLA, Los Angeles, CA
Ph.D. Thesis lab; investigated circuit and molecular mechanisms of activity-dependent plasticity during limb overuse after stroke
- 07/2009 to 08/2009 Marie-Francoise Chesselet, M.D., Ph.D.
Dept. of Neurology, UCLA, Los Angeles, CA
MSTP rotation; examined role of hemoglobin in neurons
- 12/2006 to 05/2009 Sreeganga Chandra, Ph.D.
Dept. of Neurology, Yale School of Medicine, New Haven, CT
Studied the roles of synuclein proteins in Parkinson's disease
- 02/2008 to 07/2008 Haydn Allbutt, Ph.D.
Dept. of Physiology, University of Sydney, Sydney, Australia
Examined astrocytes loss in Parkinsons' disease rat model
- 06/2006 to 08/2006 Mark Henkemeyer, Ph.D.
Dept. of Dev. Biology,UTSW Medical Center, Dallas, TX
Summer Undergraduate Fellowship for Research
Studied nerve growth genes *Ephrin B1* and *B2* in double mutant mice

PUBLICATIONS & ABSTRACTS

Articles:

Nie EH, Kawaguchi R, Coppola G, Carmichael ST. Limb overuse after stroke induces a unique molecular transcriptome of cortical reorganization in the retrosplenial cortex. *Manuscript in preparation*.

Carmichael ST, Kathirvelu B, Schweppe CA, Nie EH. Molecular, cellular, and functional events in axonal sprouting after stroke. *Exp Neurol*. 2016; 16: 30029-2.

Li S*, Nie EH*, Yin Y, Benowitz LI, Tung S, Vinters HV, Bahjat FR, Stenzel-Poore MP, Kawaguchi R, Coppola G, Carmichael ST. GDF10 is a signal for axonal sprouting and functional recovery after stroke. *Nat Neurosci*. 2015; 12: 1737-45.

Greten-Harrison B, Polydoro M, Morimoto-Tomita M, Diao L, Williams AM, Nie EH, Makani S, Tian N, Castillo PE, Buchman VL, Chandra SS. $\alpha\beta\gamma$ -Synuclein triple knockout mice reveal age-dependent neuronal dysfunction. *Proc Natl Acad Sci*. 2010; 107: 19573-8.

*co-first authorship

Selected Abstracts and Presentations:

Nie EH, Kawaguchi R, Coppola G, Carmichael ST. Mechanisms of axonal sprouting in a cortical circuit induced by limb overuse after stroke. Presented at the 44th Annual meeting of the Society of Neuroscience, Chicago, IL, October 2015.

Schweppe CA, Nie EH, Li S, Carmichael ST. Stroke transcriptome-driven analysis of axonal outgrowth mechanisms. Presented at the 44th Annual meeting of the Society of Neuroscience, Chicago, IL, October 2015 and at the 27th Annual UCLA Brain Research Institute Poster Day, Los Angeles, CA, November 2015.

Nie EH, Coppola G, Carmichael ST. Activity-dependent formation of a novel premotor connection after ischemic stroke. Presented at the 9th World Congress International Brain Research Organization, Rio de Janeiro, Brazil, July 2015.

Nie EH, Carmichael ST. Activity-dependent mechanisms of cortical reorganization during limb-overuse after stroke. Presented at the Annual meeting of the American Society of Neurorehabilitation and 43rd Annual meeting of the Society for Neuroscience, San Diego, CA, November 2013.

Nie EH, Carmichael ST. Identifying activity-dependent cortical circuits in stroke recovery. Presented at the 42nd Annual meeting of the Society of Neuroscience, New Orleans, LA, October 2012, and at the 24th Annual UCLA Brain Research Institute Neuroscience Poster Day, Los Angeles, CA, December 2012.

CHAPTER 1

INTRODUCTION

Stroke: the clinical picture

Stroke is the number one cause of adult disability and has a worldwide prevalence greater than 33 million (Mozaffarian *et al.*, 2015). In the United State alone, 6.6 million adults are living stroke survivors who must cope with lifelong disabilities (Mozaffarian *et al.*, 2016). The myriad post-stroke debilities range from sensorimotor to cognitive to mood dysfunction. The only FDA approved drug for stroke is tissue plasminogen activator (tPA), an anti-clotting agent that must be administered in the first 4.5 hours after stroke. This equates to only about 1-3% of all patients receiving pharmacological treatment (DeMers *et al.*, 2012). Moreover, the death rate from stroke has actually been on the decline for several decades (Kelly-Hayes *et al.*, 2003). This shifts a substantial burden of care toward the growing number of people now living after one or more cerebrovascular accidents (CVA). These epidemiological trends highlight the significant need for therapies to enhance recovery after stroke, and to ultimately help address the unmet needs for long-term stroke survivors. The shift of clinical need toward caring for patients in the medium to long-term after stroke also motivates neuroscience research to target enhancing brain plasticity in the subacute or chronic period. The acute delivery of tPA serves to limit infarct size and cell death, but there are no pharmacological therapies that help patients improve function after the initial incident. Finally, as our society's population increasingly ages, the incidence of stroke is expected to more than double between 2010-2015 (Howard and Goff, 2012). Such a jarring statistic underscores the relevance and dire need for advances in this area of neural repair basic and translational research.

The following pages will review and synthesize neuroscientific research in three key background areas informing the rest of the dissertation. First, I will discuss the circuit, cellular, and molecular dynamics that characterize the post-stroke brain. Next, we will take a brief dive into classic and modern experiments in behavioral theory that form the rationale behind activity-dependent limb overuse therapy following brain injury. Finally, the last section will focus on the premotor cortex and its known and potential roles in motor recovery after brain injury. Together, these topics will springboard into the remainder of the dissertation: a focused investigation of premotor circuit rewiring and the molecular mechanisms underlying limb overuse therapy after stroke.

1.1 Stroke initiates a dynamic state in surviving brain tissue

During stroke, occlusion of a cerebral artery leads to focal ischemia and the resultant tissue damage leaves patients with deficits in motor function, sensation, and cognition. One longstanding belief about brain injury was that after cell death occurs in the central nervous system, the hardwired adult brain cannot repair and recover the lost function. However, many studies have since overturned this dogma by showing that neural injury thrusts surviving parts of brain into a structurally and functionally dynamic state. Neuronal growth, stem cell activation, and functional network remodeling are but a few examples of phenomena that illustrate the dynamic landscape following brain injury (Ohab *et al.*, 2006; Sozmen *et al.*, 2009; Tsai *et al.*, 2006). After stroke, the cortex adjacent to the infarct core is particularly dynamic: there is marked axonal sprouting (Carmichael *et al.*, 2001; Li *et al.*, 2010; Overman *et al.*, 2012), increased dendritic turnover (Brown *et al.*, 2007), and significant physiological changes in neuronal excitability (Clarkson *et al.*, 2010). Additionally, areas distant but connected to the site of injury also undergo considerable plasticity,

engaging mechanisms such as functional modulation and circuit rewiring (Dancause *et al.*, 2005; Grefkes and Fink, 2011). Examples of these substrates for post-injury brain plasticity, and their potential to promote recovery after injury are further explored here.

Peri-infarct cortex axonal sprouting

Axonal sprouting occurs robustly in the surviving cortex located adjacent to the stroke, a region termed the peri-infarct cortex (Carmichael *et al.*, 2001; Murphy and Corbett, 2009). The sprouting process is initiated in the first week after stroke (Li *et al.*, 2010), and has been demonstrated to occur between weeks in rodent (Li *et al.*, 2010; Overman *et al.*, 2012) to months in primate models of stroke (Dancause *et al.*, 2005). Axonal sprouting can be visually mapped by labeling and comparing total neuronal projection patterns in animals with or without stroke. For example, in an animal model of ischemic stroke to the forelimb motor cortex, one can introduce BDA, a neuronal tracer, to the peri-infarct cortex to label the sensorimotor projections. The identical neuroanatomical region of an uninjured animal can be mapped using the same neuronal tracer. These two sets of neuronal tracings can be quantitatively compared to each other to identify location and extent of neuronal sprouting after stroke (Carmichael *et al.*, 2001; Overman *et al.*, 2012), as depicted in Fig 1.1. In a landmark study that took cellular axonal sprouting toward a systematic molecular level of analysis, Li *et al.* used laser capture microdissection to isolate and genetically profile these sprouting neurons in the peri-infarct cortex in a rat model of stroke (Li *et al.*, 2010). From this study emerged the “molecular growth program” for axonal sprouting after stroke. One key finding was that axonal sprouting as a molecular process differs by age. That is, sprouting in a young adult mouse activated and suppressed unique sets of genes that were not the same ones seen in sprouting vs. nonsprouting neurons from an aged animal. Across both ages, interesting categories

of genes that were involved include growth factor, axonal pathfinding, and cellular adhesion molecules (Li *et al.*, 2010). However, in the aged brain, there was upregulation of Ephrin and myelin genes, both of which have classic roles in growth inhibition (Thiede-Stan and Schwab, 2015). Epidemiological and clinical evidence indicate that stroke recovery is an age-dependent process, in which young patients typically recover better than the elderly (Koennecke *et al.*, 2011; Kugler, 2003). Therefore, these recently identified age-dependent molecular differences in axonal sprouting represent a key area for current and future investigation of high clinical value.

Dendritic turnover after stroke

Stroke induces changes in dendritic spines in the peri-infarct cortex, a plasticity process that can be studied using chronic in-vivo imaging (Holtmaat and Svoboda, 2009). Dendritic spines turn over rapidly during development and dysregulation of this process can lead to developmental disease (Phillips and Pozzo-Miller, 2015) However, in the adult brain, where dendrites are relatively more stable, their structural changes can still occur during certain learning processes, circuit remodeling, and normal aging (Mostany *et al.*, 2013; Xu *et al.*, 2009; Yang *et al.*, 2009). After stroke, there is initially a net loss of peri-infarct dendritic spines, although the precise timing of acute spine loss is dependent on the stroke model and ranges from hours to days. In photothrombotic (PT) stroke (Carmichael, 2005), dendritic spines loss is detected within the first 24 hours after stroke, while in middle cerebral artery occlusion this effect is seen after 7 days (Brown *et al.*, 2007; Mostany *et al.*, 2010). This discrepancy may reflect the physiological differences of the size and extent of the ischemic penumbra: smaller and sharper border in PT (Brown *et al.*, 2007) and larger and more graded in MCAO. Nonetheless, across both models of stroke, the observed spine loss is temporary. Over time, peri-infarct dendritic growth and retraction either return to baseline or supersede control

levels. In the MCAO model, increased dendritic turnover was even found in areas as far as 2-3mm away from the infarct (Mostany *et al.*, 2010). Functionally, these remodeling dendrites may become a source for post-injury synaptogenesis with spared or sprouting neurons. Exciting yet unexplored areas in post-stroke spine dynamics include activity-dependent effects on spine turnover, spine-clustering dynamics during functional recovery, and the effects of epochs of spine “search mode” after injury.

Neurophysiological changes in excitability

In addition to structural plasticity in the peri-infarct cortex, there is also a shift in balance between excitation and inhibition in surviving stroke-affected tissue. One specific example of altered cellular physiology in peri-infarct neurons is overall diminished excitability, which occurs largely through heightened tonic GABA inhibition (Clarkson *et al.*, 2010). This peri-infarct inhibition seen initially after stroke is thought to be neuroprotective in the acute period, guarding against excessive glutamate signaling which can lead to excitotoxicity and cell death. However, after 3-5 days, reversing this inhibition using a GABA antagonist significantly helps improve motor recovery without negatively affecting lesion size (Clarkson *et al.*, 2010). Furthermore, increasing peri-infarct AMPA glutamatergic signaling can also induce BDNF growth factor release and further facilitate increased motor recovery after stroke (Clarkson *et al.*, 2011).

Excitatory signaling can also activate learning and memory mechanisms such as long-term potentiation, or LTP. LTP is the key cellular mechanism that underlies long-term memory formation, experience-dependent sensory encoding, and cortical learning. Complementary studies in rat brain slices indicate that 7 days after stroke, peri-infarct neurons exhibit prolonged excitatory potentials

and a tendency to undergo LTP-like changes (Hagemann *et al.*, 1998). Similarly, stroke patients who undergo transcranial magnetic stimulation (TMS) protocols that induce LTP-like phenomenon to the ipsilesional cortex show improved recovery in motor function, at least in the short-term (Chang *et al.*, 2015; Plow *et al.*, 2009). One idea is that these physiological changes may invoke mechanisms of metaplasticity after injury. Metaplasticity refers to the activity-dependent regulation of neuronal plasticity, to prepare for the future instances of plasticity (Hulme *et al.*, 2013). For example, homeostatic plasticity is an example of metaplasticity that a cell uses to make LTP less likely after previous LTP (and LTD less likely after previous LTD). Such plasticity functions as “synaptic scaling” to protect from runaway LTP and LTD, and to help maintain a cell’s intrinsic excitability within physiological range to enable future plasticity. During stroke, it is possible that the initial wave of injury-induced glutamate release may acutely decrease likelihood of future LTP, but upon increased GABA inhibition, the threshold for LTP is lowered. A role for metaplasticity, though not yet formally studied in peri-infarct cortex, may potentially reconcile the observations that peri-infarct neurons exhibit decreased intrinsic excitability but also show prolonged excitatory potentials once they are excited (Hagemann *et al.*, 1998). As we begin to understand how stroke injury modulates set points for LTP and LTD, molecular memory systems may be harnessed following injury to differentially reinforce or weaken synapses and enhance plasticity during recovery.

Plasticity in brain regions distant to the stroke

Stroke injury often occurs in a focal manner, depriving a specific region of brain distal to the clot of its blood perfusion and oxygenation. Although neurologists have focused on “localizing the lesion” to the core affected area, stroke is now increasingly understood as a disease of brain networks (Grefkes and Fink, 2011; Silasi and Murphy, 2014). Because the brain is organized in

densely connected neural networks, cell death caused by stroke inevitably affects a wider neural network than just the center of the lesion. “Diaschesis,” originally coined by Von Monakow in 1969, is a term that refers to depressed brain function at sites distant to injury (Von Monakow, 1969). Metabolic and functional imaging point to hypoactive areas distant from the injury site in both rodent and primate models of stroke (Carmichael *et al.*, 2004). This phenomenon likely happens because there is decrease synaptic input to that specific brain region. However, within our dense brain networks, redundant or related circuits can often be utilized to restore this lost synaptic input after injury. This is one mechanism that supports “vicariation,” or the process of a neighboring part of the brain taking over for the lost function of the injured area (Dancause and Nudo, 2011). Vicariation can be mapped using human fMRI brain imaging studies or by measuring regional cellular activity in preclinical models of stroke recovery. Diaschesis and vicariation are terms essentially used to describe complementary long distance reactions to the initial injury; the former underscores the loss in processing with brain structures connected to the stroke site, while the latter refers to the emergence of activity in a new part of the brain to take over or compensate for the lost function.

Another example of plasticity distant from the injury is post-stroke axonal sprouting in contralateral cortex. After cortical stroke in rodents, corticospinal motor neurons opposite that of the lesioned side, termed “contralesional” cortex, sprout projections to the ipsilesional striatum, denervated red nucleus, and spinal cord (Carmichael and Chesselet, 2002; Ishida *et al.*, 2016; Lindau *et al.*, 2014). Elegant studies have shown that corticospinal sprouting from the uninjured hemisphere functionally contributes to motor recovery. This sprouting increases innervation to the lower motor neurons in the spinal cord that have lost contralateral input after stroke, and increases motor

performance. Conversely, when the sprouted neurons are selectively blocked, motor recovery is abrogated (Wahl *et al.*, 2014).

While the intact, contralesional corticospinal tract in large volume strokes may sprout to denervated areas, other cortical circuits within the spared hemisphere after smaller strokes can actually form aberrant connectivity. For example, training of the nonparetic limb after unilateral stroke diminishes the outcome of rehabilitative training of the stroke-affected limb (Allred *et al.*, 2010; Allred and Jones, 2008; Allred *et al.*, 2005). Moreover, overuse of the stroke-unaffected limb is correlated with diminished forelimb representation of the peri-infarct cortex, and aberrant synaptogenesis perhaps from transcallosal neurons (Kim *et al.*, 2015). Conversely, muscimol-mediated inactivation of the contralesional cortex for 3-14 days improves behavioral outcome (Mansoori *et al.*, 2014). These findings are critical because the phenomenon of “learned nonuse,” or heightened reliance on the good limb after stroke, is common sequelae to hemiparesis, but may actually hinder circuit repair and motor recovery. In total, to truly dissect the role of contralateral cortex after stroke- whether it subserves or subverts recovery, necessitates an analysis of extent and location of the stroke along with relevant behavioral paradigms, both compensatory and rehabilitative.

Molecular changes in the post-stroke brain

Anatomical and molecular studies in the last 20 years have shown that stroke induces peri-infarct sprouting associated with a series of molecular changes in the affected tissue (Carmichael *et al.*, 2005; Carmichael *et al.*, 2001; Keyvani *et al.*, 2002; Kruger *et al.*, 2006). The earliest studies using curated gene expression panels showed that genes induced in the first few days after stroke include GAP43, CAP23, SPRR1 and c-jun (Carmichael *et al.*, 2005). GAP43, or growth associated protein, is

upregulated in growth cones during cortical and hippocampal development (Meiri, 1986; Skene *et al.*, 1986) and in CNS regeneration (Benowitz and Routtenberg, 1997). The correlation between c-jun induction and peri-infarct axonal sprouting are consistent with findings from a contemporaneous study that demonstrated c-jun is required for CNS neuronal regeneration after facial nerve injury (Raivich *et al.*, 2004). The expression of immediately early genes (IEGs) such as c-fos, c-jun, and ZIF268 had also been previously documented in various stroke models (Kogure and Kato, 1993), at both early and delayed times points (Johansson *et al.*, 2000). Mechanistically, ischemia-induced IEG upregulation is mediated by activation of NMDA receptors (Collaco-Moraes *et al.*, 1994). Since this is a molecular entry point for both excitotoxic cell death and neuroplasticity after survival, specific modulation of this system may help increase survival and enable plasticity of surviving tissue.

One week after stroke, several other genes involved in sprouting induction and maintenance are upregulated, including NGF1, p21 (cdk inhibitor), L1, and MARCKS (Carmichael *et al.*, 2005; Keyvani *et al.*, 2002). Of the queried genes in the peri-infarct cortex, transcription factors, immediate early genes, and growth/structural genes are turned on, while metabolic, ion channel, and genes tend to be downregulated in the 7-10 days after stroke (Keyvani *et al.*, 2002). Then in 2010, a milestone project advanced the earlier gene-by-gene studies of the peri-infarct region by acquiring the entire transcriptional profile of a sprouting neuron 7 days after stroke. For the first time, this work characterized an intrinsic growth program for post-stroke neuronal sprouting, and was done both with neuronal cell-type specificity and across the whole transcriptome, and in two age groups. This study underscored that growth factor, axonal pathfinding, and cellular adhesion molecules are key functional categories of genes induced by sprouting (Li *et al.*, 2010). One molecule in the growth factor category was IGF-1, or insulin-like growth factor, was shown to be upregulated in aged animals after stroke (Li *et al.*, 2010). A related protein, IGF-II, had previously been shown to be

upregulated at day 21 after stroke (Kruger *et al.*, 2006), and thus posited to have plasticity effects outside of the acute period targeted by neuroprotection. Mechanistic workup by in-vivo gain and loss of function studies indicated that while IGF-1 upregulation did not increase axonal sprouting, its blockade in the three weeks after stroke actually increased neuronal cell death and collapsed cortical projection patterns (Li *et al.*, 2010). This biological response suggests that post-stroke tissue is uniquely placed in a growth factor dependent state. Other growth factors, such as BDNF and NGF, are also induced in peri-infarct cortex and mediate functional recovery (Clarkson *et al.*, 2011; Keyvani *et al.*, 2002; Kleim *et al.*, 2003), though this likely involves more than just axonal sprouting and recruits parallel mechanisms like angiogenesis (Muramatsu *et al.*, 2012).

Axonal sprouting has both cell-intrinsic and cell-extrinsic components. Once an injured neuron is turned on to grow, concurrent extracellular matrix reorganization must permit the activated axon to sprout and find its path toward an eventual target. Carmichael *et al.* find that several growth inhibitory molecules such as CSPGs were concomitantly expressed at a low level in areas expressing high GAP43, a molecular signature permissive of axonal sprouting. However, growth inhibitory markers are not uniformly all downregulated after stroke. For example, neurocan, semaIIIa/NP1, ephrin-A5, and ephB1 are actually induced during the one month after barrel field stroke (Carmichael *et al.*, 2005). Curiously, some of these molecules such as ephrin-A5, are also induced in a similar distribution during barrel development, where they function to organize developing thalamocortical circuits (Bolz *et al.*, 2004). Conceivably, the adult brain after injury may in part recapitulate similar developmental processes that refine neuron pathfinding and circuit formation. Finally, at one month after stroke, growth inhibitory molecules found in peri-neuronal nets are upregulated. These molecules include brevican, phosphacan, and versican, and their induction may signal the end of an endogenous post-injury critical period for regenerative sprouting

(Carmichael *et al.*, 2005). This molecular change may correlate with the end of some spontaneous recovery or may even contribute to stabilization of the reorganized circuits. A better mechanistic understanding of the natural end of this plasticity period can help develop appropriate timing for future neural repair strategies.

Inspired by earlier studies in CNS and PNS regeneration, our molecular understanding of the changes underlying stroke neural repair has been incrementally growing since the late 1990s. The patterned induction and reduction of key molecules occur at temporally regulated epochs during the recovery period after stroke. Open questions in our molecular understanding of the post-stroke brain include 1) how cell-type and region-specific gene regulation together orchestrate repair after injury 2) assigning functional roles to the hitherto identified sprouting-related molecules to growth-promotion or inhibition, and/or circuit refinement and 3) characterizing how activity or experience-based neurorehabilitation therapies alter the cellular environment to promote functional circuit rewiring during neural repair.

The extent of injury matters

Studies across different stroke types and study models offer a multitude of potential mechanisms for recovery after stroke. How do we harness any useful information to determine the right timing, location, and frequency of a potential treatment? One strong theme that emerges from this growing body of work on post-injury neural repair is that mechanisms of circuit remodeling and functional recovery are related to the size and location of the stroke, as well as timing and frequency of rehabilitation. Classic studies from the early 20th century taught us that small cortical injuries in chimpanzees almost always resolve in functional recovery, and ablation of contralateral cortex does

not eliminate this recovery (Graham, 1913; Leyton, 1917). Many studies using smaller focal stroke models have confirmed that function does not map to contralateral cortex, but instead to nearby or connected regions on the ipsilesional hemisphere (Brown *et al.*, 2009; Nudo and Milliken, 1996). As discussed previously, in some cases plasticity in contralateral motor cortex can actually interfere with recovery.

On the other hand, large cortical injuries tend to recruit more input from contralesional side for functional recovery. In mice, large strokes result in robust axonal sprouting from the contralesional cortex to striatum and spinal cord (Carmichael and Chesselet, 2002; Wahl *et al.*, 2014). In rats that received different sized lesions and functionally recovered limb use, inactivating contralesional motor cortex revealed motor dysfunction only in animals that had suffered a larger stroke (Biernaskie *et al.*, 2005). Recruitment of contralesional cortex was again dependent on stroke size, with only larger strokes relying on contralesional cortex for regained function. Finally, patients with large cortical strokes also demonstrate a functional reliance on contralateral motor cortex; when TMS is used to perturb contralesional premotor and primary motor cortices, stroke patients show deterioration in limb motor function (Mohapatra *et al.*, 2016). From these contrasting studies, we can begin to build a hierarchy of circuit recruitment after stroke. Smaller strokes recruit ipsilesional, uninjured tissue for functional vicariation, but when this tissue is also destroyed, more distant regions such as contralateral cortex and subcortical regions are summoned for functional repair. In the motor system, these principles manifest when primary motor cortex (M1) stroke seems to first recruit remaining ipsilesional peri-infarct, then ipsilesional premotor cortex and supplemental motor areas, and finally contralateral cortex when compared across strokes of increasing size.

Future areas of research

The current discussion of the dynamic changes seen in post-stroke brain leaves open several areas for further investigation. At the systems level, future studies will enlighten how network structure and function change upon injury, and how they may be mutable to enhance recovery. For example, correlating pre- and post-synaptic changes in the peri-infarct tissue will help elucidate network effects of stroke injury and recovery. At the cellular level, no study to date has performed chronic in-vivo live imaging of a sprouting neuron after stroke. In order to do this, genetic tools are needed to differentially label the same neuron before and after stroke. These tools will enable experiments to visualize and track post-stroke structural changes on a cell-by-cell basis, and within the same animal before and after stroke. Finally, future basic research in the field will aim to understand the combinatorial and time-coordinated effects of molecular changes that limit or enhance post-stroke plasticity in the adult brain.

1.2 Constraint-induced movement therapy

Although there are no approved medications for stroke, one type of motor behavioral therapy has demonstrated efficacy in chronic stroke patients. The 2006 EXCITE clinical trial found that constraint-induced movement therapy, or CIMT, results in significant and lasting motor recovery (Wolf *et al.*, 2006) in patients months to years after their stroke. CIMT is a neurorehabilitative paradigm comprised of two parts: 1) constraint of the healthy limb and 2) focused overuse of the stroke-affected limb. The paradigm directly combats a common phenomenon after stroke known as “learned non-use,” or the tendency to give up trying to use one’s paretic limb after injury (Morris *et al.*, 1997; Taub *et al.*, 2014). Next, I will offer a brief review of the classic studies from which modern day CIMT was conceived.

Learned nonuse and cortical plasticity: a historical perspective

The behavioral psychologist Edwin Taub is often credited with developing CIMT based on his sensory deafferentation experiments in the 1980s. In these studies, monkeys that had undergone unilateral sensory deafferentation (via dorsal rhizotomy) developed a heightened reliance on the unaffected limb and opted to not use the deafferented limb, despite still having fully intact musculature and motor circuitry (Taub, 1980). This prominent behavioral effect was termed “learned nonuse.” The chronic tissue-level changes that occurred in the brain after learned-nonuse was immense: cortex normally innervated by sensory afferents from the hand was now almost completely taken over by neighboring input from the face. In the macaque, this equated to a region about 8-10 mm wide that had taken on new topographic representation (Pons *et al.*, 1991; Taub, 1980). Later experiments in primates who had undergone medically needed limb amputation, which induced overuse of one limb, also showed analogous plasticity in motor cortex. Electrical stimulation of primary motor cortical regions that once mapped to muscles of the amputated limb now elicited responses of nearby muscles or body representations in all animals tested (Wu and Kaas, 1999). Furthermore, neuroanatomical tracing in these primates revealed a wider cortical territory of M1 neurons corresponding to the amputated limb (Kaas and Qi, 2004). Injection of retrograde tracers into proximal muscle groups near the amputation stump labeled spinal neurons that typically innervated the distal limb muscles. These anatomical changes provide evidence of the structural plasticity that can accompany behavioral changes after injury. In summary, these studies indicate that both sensory and motor cortex in the adult animal can profoundly reorganize upon peripheral injury and behavioral shaping.

Dr. Taub helped develop a vocabulary to describe the effects of learned nonuse after injury, and eventually popularized the translational concept of CIMT as neurorehabilitation for patients.

However, a much less cited study from decades before Taub was actually the first to pioneer the combined use of limb constraint and patterned behavioral activity to treat cortical injury. Since before the twentieth century, clinicians have observed limited amounts of “spontaneous” behavioral recovery after brain injury. In a landmark study in 1917, Ogden and Franz set out to identify factors that could enhance the limited degree of functional recovery after motor cortex injury in macaque monkeys. After cauterization of M1, several methods of treatment were tested for efficacy in restoring motor function, including muscular massage, sensory stimulation, limb restraint, and application of “irritating” stimuli to paralyzed limbs to induce limb withdrawal. Repeatedly, the best recovery from unilateral lesion of motor cortex occurred after combined use of the latter two approaches: restraining the unaffected limb in a jacket and behaviorally coaxing of the animal to use its paretic limb (Ogden and Franz, 1917). At first, animals would use compensatory shoulder and arm muscles for gross, imprecise movement of the injured arm, but after three weeks the monkeys could “pick up small objects from the floor and convey them to [the] mouth” (Ogden and Franz, 1917) as depicted in Fig1.2. Goal-oriented movements with the once paretic right side were “as accurate, precise, and forceful as those of a normal animals” (Ogden and Franz, 1917). At two months after injury the injury, one rehabilitated animal as “observed to catch with the right hand a fly that had alighted in the monkey’s cage,” with readily appreciated “coordination and quickness” (Ogden and Franz, 1917). On the contrary, Ogden and Franz found that general muscle massage, a popular recommendation by contemporaneous neurologists, did not bring about significant motor recovery. Constraint alone without behavioral reinforcement was also ineffective and animals remained paretic more than 6 months after injury. After functional recovery from the first M1 stroke, a second stroke was generated on the uninjured contralateral M1 to test if this region subserved the initial lost function. The effect, seen in Fig 1.2b, was onset of hemiparesis to the previously unaffected limbs, but the recovered function persisted. The finding indicated that plasticity after M1

stroke occurred elsewhere, perhaps on the ipsilesional cortex. These set of early studies, though simple in design and largely qualitative, were truly prescient and harbinger to a clinically translational behavioral therapy for stroke.

Nearly 100 years after Franz and Ogden, the EXCITE clinical trial enrolled patients to undergo two weeks of constraint rehabilitation that focused on structured task training using the stroke-affected limb. For 14 days, patients wore a constraint mitt on their unaffected forelimb for 90% of their waking hours, and on weekdays behavioral training was implemented for 6 hours per day. After two weeks of training, the stroke patients (even chronic patients more than 1 year out from their initial stroke) experienced significant motor improvement of their affected limb. These motor benefits were sustained when behavior was reassessed 1 year later (Wolf *et al.*, 2008). Although the clinical effects of limb overuse after stroke were prominent, the specific circuits and molecules involved in the process of recovery remain unidentified.

1.3 Premotor cortex after primary motor stroke: a window of opportunity

Defining premotor cortex across species

The term “premotor cortex” generally describes a brain region in frontal cortex distinct from and usually anterior to primary motor cortex (M1) that supports aspects of motor function. Premotor cortex has been shown to anticipate and facilitate M1 activity, coordinate interhemispheric signaling, and regulate motor function after injury (Cerri *et al.*, 2003; Darling *et al.*, 2011; Vallone *et al.*, 2016). In the rodent, intracortical microstimulation (ICMS) motor mapping shows two distinct cortical areas that elicit forelimb movement (Tennant *et al.*, 2011). Named for their relative positions to each other, they are seen in the literature as caudal forelimb area and rostral forelimb area, or CFA and RFA, respectively. Both CFA and RFA send direct corticospinal efferents down to spinal

cord (Neafsey *et al.*, 1986), and RFA is commonly accepted as the rodent homolog of premotor cortex (Hira *et al.*, 2013). In primates and humans, premotor cortex is a general term that was traditionally classified as Brodmann Area 6 (Brodmann, 1905), and often subdivided into medial and lateral premotor cortex (McNeal *et al.*, 2010) (Fig1.3). Functionally, medial premotor cortex (also known as M2 or SMA, supplementary motor cortex) seems to be responsible for internally generated movements, since lesion to this area reduces spontaneous movements but does not hinder motor response to external cues (Halsband *et al.*, 1994). Lateral premotor cortex, which is important for action selection and motor planning, is further subdivided into dorsal and ventral premotor cortex, PMd and PMv, respectively (Barbas and Pandya, 1987; Hoshi and Tanji, 2007). A marked anatomical difference between PMd and PMv is that input connectivity comes from superior and inferior parietal lobules, respectively (Hoshi and Tanji, 2007). Briefly, PMd has a role in associative learning between sensory input and motor output (e.g. red light means stop). PMv is important for choosing specific grasp positions for fine motor tasks, and also includes mirror neurons- cells that are active observation of motor action in another subject (Rizzolatti and Sinigaglia, 2010). Finally, neuroanatomical tracing in primates shows that M1, M2, PMv and PMd all directly send layer V projections to the ventral horn of the spinal cord (Dum and Strick, 1991; Wise, 1996). These spinal connections may also explain the apparent spasticity and forced grasping seen upon premotor lesion (Fulton, 1934), and hypertonia and even clonus upon bilateral lesion (Travis, 1955).

Premotor cortex after stroke

In humans, non-human primates, and in rodent models of stroke, premotor cortex occupies a critical node in recovery circuits after stroke to the primary motor cortex. In stroke patients, fMRI studies show that brain activity significantly increases in ipsilesional premotor cortex during the recovery period (Cramer, 2008; Kleiser *et al.*, 2005). Increased fMRI activity of contralesional

primary and premotor cortices often is found in the acute period, but the patients who recover the best see a progressive loss of contralateral activity and a return of ipsilesional activity, especially of the premotor cortex (Cramer, 2008; Grefkes and Fink, 2011). Premotor cortex in these human fMRI studies maps to the M2 and PMv defined in primate anatomic and cytoarchitectonic studies. Consistent with fMRI studies in humans, selective M1 lesion in nonhuman primates increases activity in M2 to accomplish forelimb reach (Aizawa *et al.*, 1991). Anatomical studies in squirrel monkeys show that stroke induces significant axonal sprouting between the premotor and sensorimotor cortices (Dancause *et al.*, 2005). The premotor corticospinal projections often remain intact if M1 cortical stroke avoids the internal capsule, and can also reorganize following injury. For instance, a recent study in rhesus monkeys indicates medial premotor cortex sprouts connections to the ventral spinal cord after M1 stroke to the hand area (Morecraft *et al.*, 2016). Importantly, this structural change most likely contributes to functional recovery because 1) the sprouting selectively occurs in spinal laminae XII and IX of the spinal cord, where interneurons and lower motor neurons for intrinsic hand muscles are located and 2) secondary M2 ablation abrogates the motor functional improvements made after recovery. The studies reviewed here present overlapping findings in patients, primates, and rodent animal models that ascribe a role of premotor cortex to improved functional recovery after stroke. The next segment builds upon this work and further incorporates premotor cortex as an important functional element during post-stroke limb overuse.

Rehabilitation and the premotor cortex

Across patients and animal models, premotor cortex is activated during recovery after motor stroke. Patients who then undergo overuse training of the stroke-affected limb also exhibit significant motor improvement and retain high ipsilesional premotor activity (Johansen-Berg *et al.*, 2002). Moreover, when transcranial magnetic inhibition is applied to premotor cortex in subjects

without stroke and in patients with good motor recovery, only the rehabilitated stroke patients deteriorated in motor function (Johansen-Berg *et al.*, 2002). This effect shows that limb overuse rehabilitation specifically engages premotor cortex. A corresponding result had previously been seen in monkeys, whereby pharmacological inactivation of ipsilesional premotor cortex reintroduces the motor deficit in macaques that had recovered function after M1 injury (Liu and Rouiller, 1999). Finally, in mice after forelimb motor stroke, motor skill training using a forepaw prehension task can result in performance a pre-injury performance levels (Zeiler *et al.*, 2013). This motor recovery is correlated with an increase in premotor activity in the ipsilesional hemisphere, as evidenced by a marked loss of inhibitory neuronal markers in the premotor cortex (Zeiler *et al.*, 2013). However, if the animals incurred a second stroke, this time to ipsilesional premotor cortex, the forelimb motor deficit was reinstated, an effect not seen if contralesional premotor cortex was stroked. Neuroanatomically, stroke in rodent models also produces peri-infarct sprouting and new connections to premotor cortex (Li *et al.*, 2010). Mice that then overused their stroke-affected forelimb, an activity-based modification analogous to human CIMT, exhibit increased peri-infarct axonal sprouting toward premotor cortex (Overman *et al.*, 2012). Blocking this growth hinders motor recovery (Overman *et al.*, 2012).

After stroke, a dynamic cascade of repair processes take place within neural circuits spared from injury. The collection of studies described here, across human, primate, and rodent models, functionally link post-stroke motor recovery and limb overuse enhanced recovery to premotor cortex. This suggests activity-dependent axonal sprouting of new premotor circuits as one likely substrate of CIMT's efficacy in motor recovery. We hypothesize that the overlay of behavioral experience, in the form of activity-based rehabilitation, onto reorganizing neural circuits will elicit a circuit-specific molecular program for endogenous repair and improved functional recovery. Based

on its role in recovery, the premotor cortex is a compelling first target for the neural repair circuit mapping and molecular and functional studies.

1.4 Harnessing the circuit and molecular mechanisms underlying CIMT to promote recovery

In 1917, Ogden and Franz remarked: “Motor recovery after hemiplegia does not result if the animal is left to its own devices... and this management (or lack of management) is what is given to most human paralytic cases.” Dozens of studies across many models have since confirmed that behavioral recovery is enhanced with limb overuse after motor cortex injury (Darling *et al.*, 2010). For example, ICMS mapping in non-human primate models show that after a focal cortical lesion, skilled training of the paretic hand expands cortical representation of the hand area into neighboring wrist and elbow areas (Nudo *et al.*, 1996). This landmark study suggests a functional substrate for CIMT in primates. However, the circuit and molecular bases for such functional reorganization are not understood, but may encompass physical growth of new connections and/or modulation of existing synapses. While the exact neural circuit ensembles that underlie CIMT activity-based training are still unknown, the field suggests that the process involves reorganization of cortical circuits near or connected to the stroke (Grefkes and Fink, 2011; Schaechter *et al.*, 2012; Wittenberg *et al.*, 2012). Furthermore, we hypothesize that activity-dependent connections are formed in the adult brain by unique transcriptional and molecular processes that can be targeted during recovery.

Goals of the dissertation

Set within the highly dynamic landscape of the post-stroke brain, axonal sprouting has now been established as a key post-stroke phenomenon in the adult brain and is correlated with

functional improvement (Carmichael *et al.*, 2016; Starkey and Schwab, 2014; Wahl and Schwab, 2014). CIMT is also clinically therapeutic, but the critical gap in understanding in the field is now at the neural circuit level; the cortical circuitry and molecules mediating activity-based neural rewiring during rehabilitative limb overuse are yet unknown. This dissertation embarks upon experiments to address some of these outstanding questions in the field by mapping unique activity-dependent premotor circuits for circuit-specific molecular characterization and functional modification. The study has three main goals: 1) to map input connectivity to premotor cortex after limb overuse, 2) to determine the transcriptional profile of a plastic circuit found upon limb overuse, and 3) to establish mechanisms for candidate genes that drive CIMT-related premotor circuit plasticity. Together, the findings contribute toward a mechanistic understanding of a unique circuit elaborated by limb overuse therapy, and potentially highlight future molecular targets for adjuvant therapies during motor neurorehabilitation. The present work is the first in the field to investigate the circuit and molecular changes of premotor cortical reorganization that underlies activity-induced axonal sprouting in a model of stroke rehabilitation.

1.5 Figures

Figure 1.1

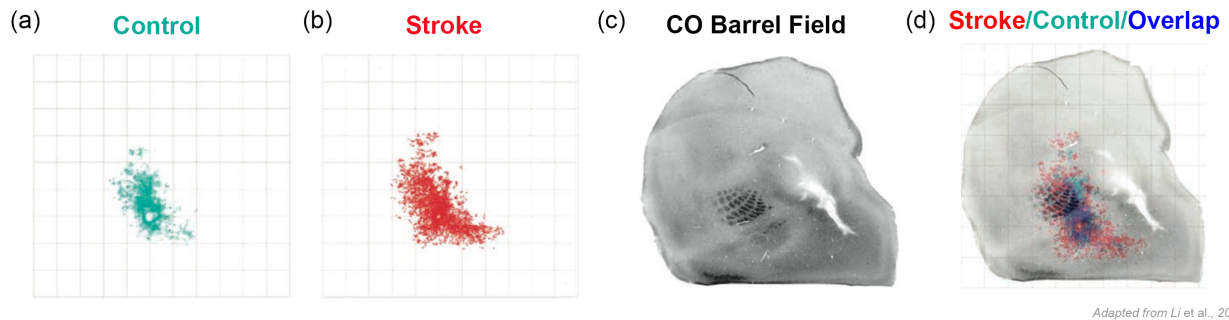


Figure 1.1 Axonal sprouting after stroke

a) BDA neuronal tracer-labeled connectivity map of barrel cortex in control animal without stroke
b) Connectivity map of the same area after MCAO to the barrel cortex; BDA now labels peri-infarct connections
c) Cytochrome oxidase (CO) labels thalamocortical connections in the barrel field cortex
d) Overlay of stereologically plotted population maps and CO stained section for anatomical localization.

Figure 1.2

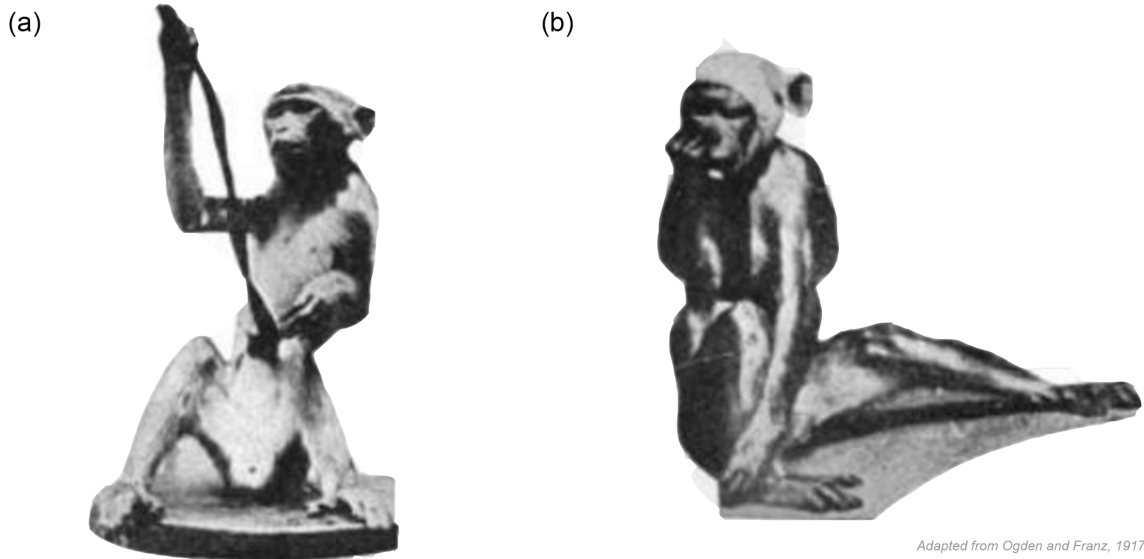
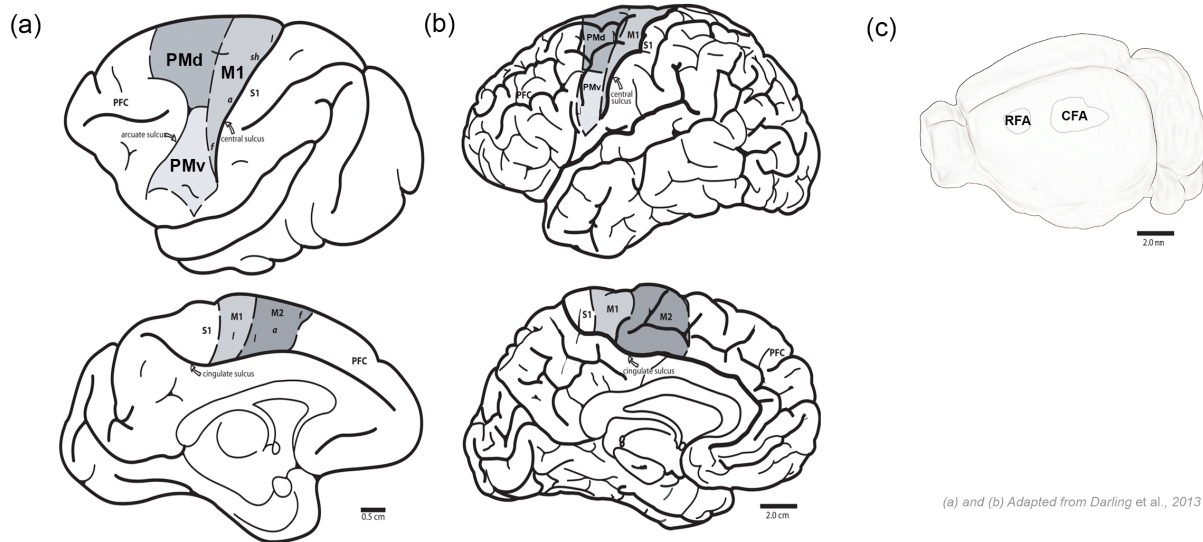


Figure 1.2 Constraint induced movement therapy

a) From Ogden and Franz's study, a macaque monkey after 26 days of limb constraint and coaxed usage of injured right arm. Fine motor grasp and limb strength are reported after complete destruction of contralateral M1 **b)** After motor recovery of the right limb, the contralesional M1 is injured in a second surgery. The monkey still uses its recovered right hand in fine motor tasks (here seen bringing hand to mouth), but the new stroke resulted in contralateral hemiparesis. This experiment indicates that after local M1 stroke, the remaining contralateral homotopic area is not responsible for observed recovery of motor function.

Figure 1.3



(a) and (b) Adapted from Darling et al., 2013

Figure 1.3 Premotor cortex comparative neuroanatomy

a) Nonhuman primate premotor cortex regions: M1=primary motor cortex; PMd= Dorsal premotor cortex (of lateral premotor cortex); PMv= Ventral premotor cortex (of lateral premotor cortex); M2=medial premotor cortex, also known as Supplementary Motor Area, SMA; S1=primary sensory area; PFC=prefrontal cortex. Top is lateral view and bottom is medial view **b)** Human premotor cortex regions: conventions are the same as in (a). **c)** Rodent premotor areas: RFA=rostral forelimb area; CFA=caudal forelimb area. Lateral view.

1.6 References:

- Aizawa, H., Inase, M., Mushiake, H., Shima, K., Tanji, J., 1991. Reorganization of activity in the supplementary motor area associated with motor learning and functional recovery. *Exp Brain Res* 84, 668-671.
- Allred, R.P., Cappellini, C.H., Jones, T.A., 2010. The "good" limb makes the "bad" limb worse: experience-dependent interhemispheric disruption of functional outcome after cortical infarcts in rats. *Behav Neurosci* 124, 124-132.
- Allred, R.P., Jones, T.A., 2008. Maladaptive effects of learning with the less-affected forelimb after focal cortical infarcts in rats. *Experimental neurology* 210, 172-181.
- Allred, R.P., Maldonado, M.A., Hsu, J., Jones, T.A., 2005. Training the "less-affected" forelimb after unilateral cortical infarcts interferes with functional recovery of the impaired forelimb in rats. *Restor Neurol Neurosci* 23, 297-302.
- Barbas, H., Pandya, D.N., 1987. Architecture and frontal cortical connections of the premotor cortex (area 6) in the rhesus monkey. *The Journal of comparative neurology* 256, 211-228.
- Benowitz, L.I., Routtenberg, A., 1997. GAP-43: an intrinsic determinant of neuronal development and plasticity. *Trends in neurosciences* 20, 84-91.
- Biernaskie, J., Szymanska, A., Windle, V., Corbett, D., 2005. Bi-hemispheric contribution to functional motor recovery of the affected forelimb following focal ischemic brain injury in rats. *The European journal of neuroscience* 21, 989-999.
- Bolz, J., Uziel, D., Muhlriedel, S., Gullmar, A., Peuckert, C., Zarbalis, K., Wurst, W., Torii, M., Levitt, P., 2004. Multiple roles of ephrins during the formation of thalamocortical projections: maps and more. *J Neurobiol* 59, 82-94.
- Brodman, K., 1905. Beiträge zur histologischen Lokalisation der Grosshirnrinde: dritte Mitteilung: Die Rindenfelder der niederen Affen. . *J Psychol Neurol.*, 177-226.
- Brown, C.E., Aminoltejari, K., Erb, H., Winship, I.R., Murphy, T.H., 2009. In vivo voltage-sensitive dye imaging in adult mice reveals that somatosensory maps lost to stroke are replaced over weeks by new structural and functional circuits with prolonged modes of activation within both the peri-infarct zone and distant sites. *The Journal of neuroscience : the official journal of the Society for Neuroscience* 29, 1719-1734.
- Brown, C.E., Li, P., Boyd, J.D., Delaney, K.R., Murphy, T.H., 2007. Extensive turnover of dendritic spines and vascular remodeling in cortical tissues recovering from stroke. *The Journal of neuroscience : the official journal of the Society for Neuroscience* 27, 4101-4109.

- Carmichael, S.T., 2005. Rodent models of focal stroke: size, mechanism, and purpose. *NeuroRx : the journal of the American Society for Experimental NeuroTherapeutics* 2, 396-409.
- Carmichael, S.T., Archibeque, I., Luke, L., Nolan, T., Momiy, J., Li, S., 2005. Growth-associated gene expression after stroke: evidence for a growth-promoting region in peri-infarct cortex. *Experimental neurology* 193, 291-311.
- Carmichael, S.T., Chesselet, M.F., 2002. Synchronous neuronal activity is a signal for axonal sprouting after cortical lesions in the adult. *The Journal of neuroscience : the official journal of the Society for Neuroscience* 22, 6062-6070.
- Carmichael, S.T., Kathirvelu, B., Schweppe, C.A., Nie, E.H., 2016. Molecular, Cellular and Functional Events in Axonal Sprouting after Stroke. *Experimental neurology*.
- Carmichael, S.T., Tatsukawa, K., Katsman, D., Tsuyuguchi, N., Kornblum, H.I., 2004. Evolution of diaschisis in a focal stroke model. *Stroke; a journal of cerebral circulation* 35, 758-763.
- Carmichael, S.T., Wei, L., Rovainen, C.M., Woolsey, T.A., 2001. New patterns of intracortical projections after focal cortical stroke. *Neurobiology of disease* 8, 910-922.
- Cerri, G., Shimazu, H., Maier, M.A., Lemon, R.N., 2003. Facilitation from ventral premotor cortex of primary motor cortex outputs to macaque hand muscles. *Journal of neurophysiology* 90, 832-842.
- Chang, M.C., Kim, D.Y., Park, D.H., 2015. Enhancement of Cortical Excitability and Lower Limb Motor Function in Patients With Stroke by Transcranial Direct Current Stimulation. *Brain Stimul* 8, 561-566.
- Clarkson, A.N., Huang, B.S., Macisaac, S.E., Mody, I., Carmichael, S.T., 2010. Reducing excessive GABA-mediated tonic inhibition promotes functional recovery after stroke. *Nature* 468, 305-309.
- Clarkson, A.N., Overman, J.J., Zhong, S., Mueller, R., Lynch, G., Carmichael, S.T., 2011. AMPA receptor-induced local brain-derived neurotrophic factor signaling mediates motor recovery after stroke. *The Journal of neuroscience : the official journal of the Society for Neuroscience* 31, 3766-3775.
- Cramer, S.C., 2008. Repairing the human brain after stroke: I. Mechanisms of spontaneous recovery. *Annals of neurology* 63, 272-287.
- Dancause, N., Barbay, S., Frost, S.B., Plautz, E.J., Chen, D., Zoubina, E.V., Stowe, A.M., Nudo, R.J., 2005. Extensive cortical rewiring after brain injury. *The Journal of neuroscience : the official journal of the Society for Neuroscience* 25, 10167-10179.

- Dancause, N., Nudo, R.J., 2011. Shaping plasticity to enhance recovery after injury. *Progress in brain research* 192, 273-295.
- Darling, W.G., Pizzimenti, M.A., Morecraft, R.J., 2011. Functional recovery following motor cortex lesions in non-human primates: experimental implications for human stroke patients. *J Integr Neurosci* 10, 353-384.
- Darling, W.G., Pizzimenti, M.A., Rotella, D.L., Hynes, S.M., Ge, J., Stilwell-Morecraft, K.S., Vanadurongvan, T., McNeal, D.W., Solon-Cline, K.M., Morecraft, R.J., 2010. Minimal forced use without constraint stimulates spontaneous use of the impaired upper extremity following motor cortex injury. *Exp Brain Res* 202, 529-542.
- DeMers, G., Meurer, W.J., Shih, R., Rosenbaum, S., Vilke, G.M., 2012. Tissue plasminogen activator and stroke: review of the literature for the clinician. *J Emerg Med* 43, 1149-1154.
- Dum, R.P., Strick, P.L., 1991. The origin of corticospinal projections from the premotor areas in the frontal lobe. *The Journal of neuroscience : the official journal of the Society for Neuroscience* 11, 667-689.
- Fulton, J.K.M., 1934. A study of flaccid and spastic paralysis produced by lesions of the cerebral cortex in primates. *Res Publ Assoc Res Nerv Men Dis*, 158-210
- .
- Graham, B.T.S., CS, 1913. Note on the functions of the cortex cerebr. *The Journal of physiology*, xxii.
- Grefkes, C., Fink, G.R., 2011. Reorganization of cerebral networks after stroke: new insights from neuroimaging with connectivity approaches. *Brain : a journal of neurology* 134, 1264-1276.
- Hagemann, G., Redecker, C., Neumann-Haefelin, T., Freund, H.J., Witte, O.W., 1998. Increased long-term potentiation in the surround of experimentally induced focal cortical infarction. *Annals of neurology* 44, 255-258.
- Halsband, U., Matsuzaka, Y., Tanji, J., 1994. Neuronal activity in the primate supplementary, pre-supplementary and premotor cortex during externally and internally instructed sequential movements. *Neurosci Res* 20, 149-155.
- Hira, R., Ohkubo, F., Tanaka, Y.R., Masamizu, Y., Augustine, G.J., Kasai, H., Matsuzaki, M., 2013. In vivo optogenetic tracing of functional corticocortical connections between motor forelimb areas. *Frontiers in neural circuits* 7, 55.
- Holtmaat, A., Svoboda, K., 2009. Experience-dependent structural synaptic plasticity in the mammalian brain. *Nature reviews. Neuroscience* 10, 647-658.

- Hoshi, E., Tanji, J., 2007. Distinctions between dorsal and ventral premotor areas: anatomical connectivity and functional properties. *Current opinion in neurobiology* 17, 234-242.
- Howard, G., Goff, D.C., 2012. Population shifts and the future of stroke: forecasts of the future burden of stroke. *Ann N Y Acad Sci* 1268, 14-20.
- Hulme, S.R., Jones, O.D., Abraham, W.C., 2013. Emerging roles of metaplasticity in behaviour and disease. *Trends in neurosciences* 36, 353-362.
- Ishida, A., Isa, K., Umeda, T., Kobayashi, K., Kobayashi, K., Hida, H., Isa, T., 2016. Causal Link between the Cortico-Rubral Pathway and Functional Recovery through Forced Impaired Limb Use in Rats with Stroke. *The Journal of neuroscience : the official journal of the Society for Neuroscience* 36, 455-467.
- Johansen-Berg, H., Dawes, H., Guy, C., Smith, S.M., Wade, D.T., Matthews, P.M., 2002. Correlation between motor improvements and altered fMRI activity after rehabilitative therapy. *Brain : a journal of neurology* 125, 2731-2742.
- Johansson, I.M., Wester, P., Hakova, M., Gu, W., Seckl, J.R., Olsson, T., 2000. Early and delayed induction of immediate early gene expression in a novel focal cerebral ischemia model in the rat. *The European journal of neuroscience* 12, 3615-3625.
- Kaas, J.H., Qi, H.X., 2004. The reorganization of the motor system in primates after the loss of a limb. *Restor Neurol Neurosci* 22, 145-152.
- Kelly-Hayes, M., Beiser, A., Kase, C.S., Scaramucci, A., D'Agostino, R.B., Wolf, P.A., 2003. The influence of gender and age on disability following ischemic stroke: the Framingham study. *Journal of Stroke and Cerebrovascular Diseases* 12, 119-126.
- Keyvani, K., Witte, O.W., Paulus, W., 2002. Gene expression profiling in perilesional and contralateral areas after ischemia in rat brain. *Journal of cerebral blood flow and metabolism : official journal of the International Society of Cerebral Blood Flow and Metabolism* 22, 153-160.
- Kim, S.Y., Allred, R.P., Adkins, D.L., Tennant, K.A., Donlan, N.A., Kleim, J.A., Jones, T.A., 2015. Experience with the "good" limb induces aberrant synaptic plasticity in the perilesion cortex after stroke. *The Journal of neuroscience : the official journal of the Society for Neuroscience* 35, 8604-8610.
- Kleim, J.A., Jones, T.A., Schallert, T., 2003. Motor enrichment and the induction of plasticity before or after brain injury. *Neurochem Res* 28, 1757-1769.

- Kleiser, R., Wittsack, H.J., Butefisch, C.M., Jorgens, S., Seitz, R.J., 2005. Functional activation within the PI-DWI mismatch region in recovery from ischemic stroke: preliminary observations. *NeuroImage* 24, 515-523.
- Koennecke, H.C., Belz, W., Berfelde, D., Endres, M., Fitzek, S., Hamilton, F., Kreitsch, P., Mackert, B.M., Nabavi, D.G., Nolte, C.H., Pohls, W., Schmehl, I., Schmitz, B., von Brevern, M., Walter, G., Heuschmann, P.U., Berlin Stroke Register, I., 2011. Factors influencing in-hospital mortality and morbidity in patients treated on a stroke unit. *Neurology* 77, 965-972.
- Kogure, K., Kato, H., 1993. Altered gene expression in cerebral ischemia. *Stroke; a journal of cerebral circulation* 24, 2121-2127.
- Kruger, C., Cira, D., Sommer, C., Fischer, A., Schabitz, W.R., Schneider, A., 2006. Long-term gene expression changes in the cortex following cortical ischemia revealed by transcriptional profiling. *Experimental neurology* 200, 135-152.
- Kugler, C.A., T; Lochner, P; Ferbert, A, 2003. Does age influence early recovery from ischemic stroke?
- Leyton, A.S., CS, 1917. Observations on the excitable cortex of the chimpanzee, orangutan and gorilla. *Exp Physiol*, 135-222.
- Li, S., Overman, J.J., Katsman, D., Kozlov, S.V., Donnelly, C.J., Twiss, J.L., Giger, R.J., Coppola, G., Geschwind, D.H., Carmichael, S.T., 2010. An age-related sprouting transcriptome provides molecular control of axonal sprouting after stroke. *Nature neuroscience* 13, 1496-1504.
- Lindau, N.T., Banninger, B.J., Gullo, M., Good, N.A., Bachmann, L.C., Starkey, M.L., Schwab, M.E., 2014. Rewiring of the corticospinal tract in the adult rat after unilateral stroke and anti-Nogo-A therapy. *Brain : a journal of neurology* 137, 739-756.
- Liu, Y., Rouiller, E.M., 1999. Mechanisms of recovery of dexterity following unilateral lesion of the sensorimotor cortex in adult monkeys. *Exp Brain Res* 128, 149-159.
- Mansoori, B.K., Jean-Charles, L., Touvykine, B., Liu, A., Quessy, S., Dancause, N., 2014. Acute inactivation of the contralesional hemisphere for longer durations improves recovery after cortical injury. *Experimental neurology* 254, 18-28.
- McNeal, D.W., Darling, W.G., Ge, J., Stilwell-Morecraft, K.S., Solon, K.M., Hynes, S.M., Pizzimenti, M.A., Rotella, D.L., Vanadurongvan, T., Morecraft, R.J., 2010. Selective long-term reorganization of the corticospinal projection from the supplementary motor cortex

- following recovery from lateral motor cortex injury. *The Journal of comparative neurology* 518, 586-621.
- Meiri, K.F.K.H.P., K.H.; Willard, M.B., 1986. Growth-associated protein, GAP-43, a polypeptide that is induced when neurons extend axons, is a component of growth cones and corresponds to pp46, a major polypeptide of a subcellular fraction enriched in growth cones. *Proceedings of the National Academy of Sciences of the United States of America* 83, 3537-3541.
- Mohapatra, S., Harrington, R., Chan, E., Dromerick, A.W., Breceda, E.Y., Harris-Love, M., 2016. Role of contralesional hemisphere in paretic arm reaching in patients with severe arm paresis due to stroke: A preliminary report. *Neuroscience letters* 617, 52-58.
- Morris, D.M., Crago, J.E., Deluca, S.C., Pidikiti, R.D., Taub, E., 1997. Constraint-induced movement therapy for moter recovery after stroke. *NeuroRehabilitation* 9, 29-43.
- Mostany, R., Anstey, J.E., Crump, K.L., Maco, B., Knott, G., Portera-Cailliau, C., 2013. Altered synaptic dynamics during normal brain aging. *The Journal of neuroscience : the official journal of the Society for Neuroscience* 33, 4094-4104.
- Mostany, R., Chowdhury, T.G., Johnston, D.G., Portonovo, S.A., Carmichael, S.T., Portera-Cailliau, C., 2010. Local hemodynamics dictate long-term dendritic plasticity in peri-infarct cortex. *The Journal of neuroscience : the official journal of the Society for Neuroscience* 30, 14116-14126.
- Mozaffarian, D., Benjamin, E.J., Go, A.S., Arnett, D.K., Blaha, M.J., Cushman, M., Das, S.R., de Ferranti, S., Despres, J.P., Fullerton, H.J., Howard, V.J., Huffman, M.D., Isasi, C.R., Jimenez, M.C., Judd, S.E., Kissela, B.M., Lichtman, J.H., Lisabeth, L.D., Liu, S., Mackey, R.H., Magid, D.J., McGuire, D.K., Mohler, E.R., 3rd, Moy, C.S., Muntner, P., Mussolino, M.E., Nasir, K., Neumar, R.W., Nichol, G., Palaniappan, L., Pandey, D.K., Reeves, M.J., Rodriguez, C.J., Rosamond, W., Sorlie, P.D., Stein, J., Towfighi, A., Turan, T.N., Virani, S.S., Woo, D., Yeh, R.W., Turner, M.B., American Heart Association Statistics, C., Stroke Statistics, S., 2016. Heart Disease and Stroke Statistics-2016 Update: A Report From the American Heart Association. *Circulation* 133, e38-e360.
- Mozaffarian, D., Benjamin, E.J., Go, A.S., Arnett, D.K., Blaha, M.J., Cushman, M., de Ferranti, S., Despres, J.P., Fullerton, H.J., Howard, V.J., Huffman, M.D., Judd, S.E., Kissela, B.M., Lackland, D.T., Lichtman, J.H., Lisabeth, L.D., Liu, S., Mackey, R.H., Matchar, D.B., McGuire, D.K., Mohler, E.R., 3rd, Moy, C.S., Muntner, P., Mussolino, M.E., Nasir, K., Neumar, R.W., Nichol, G., Palaniappan, L., Pandey, D.K., Reeves, M.J., Rodriguez, C.J., Sorlie, P.D., Stein, J., Towfighi, A., Turan, T.N., Virani, S.S., Willey, J.Z., Woo, D., Yeh,

- R.W., Turner, M.B., American Heart Association Statistics, C., Stroke Statistics, S., 2015. Heart disease and stroke statistics--2015 update: a report from the American Heart Association. *Circulation* 131, e29-322.
- Muramatsu, R., Takahashi, C., Miyake, S., Fujimura, H., Mochizuki, H., Yamashita, T., 2012. Angiogenesis induced by CNS inflammation promotes neuronal remodeling through vessel-derived prostacyclin. *Nat Med* 18, 1658-1664.
- Murphy, T.H., Corbett, D., 2009. Plasticity during stroke recovery: from synapse to behaviour. *Nature reviews. Neuroscience* 10, 861-872.
- Neafsey, E.J., Bold, E.L., Haas, G., Hurley-Gius, K.M., Quirk, G., Sievert, C.F., Terreberry, R.R., 1986. The organization of the rat motor cortex: a microstimulation mapping study. *Brain research* 396, 77-96.
- Nudo, R.J., Milliken, G.W., 1996. Reorganization of movement representations in primary motor cortex following focal ischemic infarcts in adult squirrel monkeys. *Journal of neurophysiology* 75, 2144-2149.
- Nudo, R.J., Wise, B.M., SiFuentes, F., Milliken, G.W., 1996. Neural substrates for the effects of rehabilitative training on motor recovery after ischemic infarct. *Science* 272, 1791-1794.
- Ogden, R., Franz, S.I., 1917. On cerebral motor control: The recovery from experimentally produced hemiplegia. . *Psychobiology*, 33-49.
- Ohab, J.J., Fleming, S., Blesch, A., Carmichael, S.T., 2006. A neurovascular niche for neurogenesis after stroke. *The Journal of neuroscience : the official journal of the Society for Neuroscience* 26, 13007-13016.
- Overman, J.J., Clarkson, A.N., Wanner, I.B., Overman, W.T., Eckstein, I., Maguire, J.L., Dinov, I.D., Toga, A.W., Carmichael, S.T., 2012. A role for ephrin-A5 in axonal sprouting, recovery, and activity-dependent plasticity after stroke. *Proceedings of the National Academy of Sciences of the United States of America* 109, E2230-2239.
- Phillips, M., Pozzo-Miller, L., 2015. Dendritic spine dysgenesis in autism related disorders. *Neuroscience letters* 601, 30-40.
- Plow, E.B., Carey, J.R., Nudo, R.J., Pascual-Leone, A., 2009. Invasive cortical stimulation to promote recovery of function after stroke: a critical appraisal. *Stroke; a journal of cerebral circulation* 40, 1926-1931.

- Pons, T.P., Garraghty, P.E., Ommaya, A.K., Kaas, J.H., Taub, E., Mishkin, M., 1991. Massive cortical reorganization after sensory deafferentation in adult macaques. *Science* 252, 1857-1860.
- Raivich, G., Bohatschek, M., Da Costa, C., Iwata, O., Galiano, M., Hristova, M., Nateri, A.S., Makwana, M., Riera-Sans, L., Wolfer, D.P., Lipp, H.P., Aguzzi, A., Wagner, E.F., Behrens, A., 2004. The AP-1 transcription factor c-Jun is required for efficient axonal regeneration. *Neuron* 43, 57-67.
- Rizzolatti, G., Sinigaglia, C., 2010. The functional role of the parieto-frontal mirror circuit: interpretations and misinterpretations. *Nature reviews. Neuroscience* 11, 264-274.
- Schaechter, J.D., van Oers, C.A., Groisser, B.N., Salles, S.S., Vangel, M.G., Moore, C.I., Dijkhuizen, R.M., 2012. Increase in sensorimotor cortex response to somatosensory stimulation over subacute poststroke period correlates with motor recovery in hemiparetic patients. *Neurorehabilitation and neural repair* 26, 325-334.
- Silasi, G., Murphy, T.H., 2014. Stroke and the connectome: how connectivity guides therapeutic intervention. *Neuron* 83, 1354-1368.
- Skene, J.H., Jacobson, R.D., Snipes, G.J., McGuire, C.B., Norden, J.J., Freeman, J.A., 1986. A protein induced during nerve growth (GAP-43) is a major component of growth-cone membranes. *Science* 233, 783-786.
- Sozmen, E.G., Kolekar, A., Havton, L.A., Carmichael, S.T., 2009. A white matter stroke model in the mouse: axonal damage, progenitor responses and MRI correlates. *Journal of neuroscience methods* 180, 261-272.
- Starkey, M.L., Schwab, M.E., 2014. How Plastic Is the Brain after a Stroke? *The Neuroscientist : a review journal bringing neurobiology, neurology and psychiatry* 20, 359-371.
- Taub, E. 1980. Somatosensory deafferentation research with monkeys: implications for rehabilitation medicine. In: *Behavioral Psychology in Rehabilitation Medicine: Clinical Applications*. pp. 371–401. Ed. L.P. Ince. Williams & Wilkins: New York, NY.
- Taub, E., Uswatte, G., Mark, V.W., 2014. The functional significance of cortical reorganization and the parallel development of CI therapy. *Frontiers in human neuroscience* 8, 396.
- Tennant, K.A., Adkins, D.L., Donlan, N.A., Asay, A.L., Thomas, N., Kleim, J.A., Jones, T.A., 2011. The organization of the forelimb representation of the C57BL/6 mouse motor cortex as defined by intracortical microstimulation and cytoarchitecture. *Cerebral cortex* 21, 865-876.

- Thiede-Stan, N.K., Schwab, M.E., 2015. Attractive and repulsive factors act through multi-subunit receptor complexes to regulate nerve fiber growth. *J Cell Sci* 128, 2403-2414.
- Travis, A., 1955. Neurological deficiencies following supplementary motor area lesions in *Macaca mulatta* *Brain : a journal of neurology*, 174-198.
- Tsai, P.T., Ohab, J.J., Kertesz, N., Groszer, M., Matter, C., Gao, J., Liu, X., Wu, H., Carmichael, S.T., 2006. A critical role of erythropoietin receptor in neurogenesis and post-stroke recovery. *The Journal of neuroscience : the official journal of the Society for Neuroscience* 26, 1269-1274.
- Vallone, F., Lai, S., Spalletti, C., Panarese, A., Alia, C., Micera, S., Caleo, M., Di Garbo, A., 2016. Post-Stroke Longitudinal Alterations of Inter-Hemispheric Correlation and Hemispheric Dominance in Mouse Pre-Motor Cortex. *PLoS one* 11, e0146858.
- Von Monakow, C. 1969. Diaschisis. In: *Brain and Behavior I: Mood States and Mind*. pp. 27-36. Ed. K.H. Pribram. Penguin: Baltimore.
- Wahl, A.S., Omlor, W., Rubio, J.C., Chen, J.L., Zheng, H., Schroter, A., Gullo, M., Weinmann, O., Kobayashi, K., Helmchen, F., Ommer, B., Schwab, M.E., 2014. Neuronal repair. Asynchronous therapy restores motor control by rewiring of the rat corticospinal tract after stroke. *Science* 344, 1250-1255.
- Wahl, A.S., Schwab, M.E., 2014. Finding an optimal rehabilitation paradigm after stroke: enhancing fiber growth and training of the brain at the right moment. *Frontiers in human neuroscience* 8, 381.
- Wise, S.P., 1996. Corticospinal efferents of the supplementary sensorimotor area in relation to the primary motor area. *Adv Neurol* 70, 57-69.
- Wittenberg, G.F., Lovelace, C.T., Foster, D.J., Maldjian, J.A., 2012. Functional neuroimaging of dressing-related skills. *Brain imaging and behavior*.
- Wolf, S.L., Winstein, C.J., Miller, J.P., Taub, E., Uswatte, G., Morris, D., Giuliani, C., Light, K.E., Nichols-Larsen, D., Investigators, E., 2006. Effect of constraint-induced movement therapy on upper extremity function 3 to 9 months after stroke: the EXCITE randomized clinical trial. *JAMA : the journal of the American Medical Association* 296, 2095-2104.
- Wolf, S.L., Winstein, C.J., Miller, J.P., Thompson, P.A., Taub, E., Uswatte, G., Morris, D., Blanton, S., Nichols-Larsen, D., Clark, P.C., 2008. Retention of upper limb function in stroke survivors who have received constraint-induced movement therapy: the EXCITE randomised trial. *Lancet neurology* 7, 33-40.

- Wu, C.W., Kaas, J.H., 1999. Reorganization in primary motor cortex of primates with long-standing therapeutic amputations. *The Journal of neuroscience : the official journal of the Society for Neuroscience* 19, 7679-7697.
- Xu, T., Yu, X., Perlik, A.J., Tobin, W.F., Zweig, J.A., Tennant, K., Jones, T., Zuo, Y., 2009. Rapid formation and selective stabilization of synapses for enduring motor memories. *Nature* 462, 915-919.
- Yang, G., Pan, F., Gan, W.B., 2009. Stably maintained dendritic spines are associated with lifelong memories. *Nature* 462, 920-924.
- Zeiler, S.R., Gibson, E.M., Hoesch, R.E., Li, M.Y., Worley, P.F., O'Brien, R.J., Krakauer, J.W., 2013. Medial premotor cortex shows a reduction in inhibitory markers and mediates recovery in a mouse model of focal stroke. *Stroke; a journal of cerebral circulation* 44, 483-489.

CHAPTER 2.

LIMB OVERUSE INDUCES AXONAL SPROUTING BETWEEN RETROSPLLENIAL CORTEX (RSC) AND PREMOTOR CORTEX (PMC)

2.1 Introduction

Previous studies in the field have identified at least one process of brain reorganization after stroke: 1) stroke triggers axonal sprouting in the surviving brain; 2) a specific molecular growth program initiates this process; and 3) increased behavioral activity through limb overuse can promote the formation of new connections (Li *et al.*, 2010; Overman *et al.*, 2012). Moreover, the 2006 clinical trial EXCITE (Extremity Constraint Induced Movement Therapy Evaluation) found that hemiparetic stroke patients who engage in a limb overuse neurorehabilitation demonstrate significant and lasting behavioral improvements (Wolf *et al.*, 2008). The results of the EXCITE clinical trial show that an activity-based strategy of limb overuse after stroke produces improved recovery. This clinical finding links with the pre-clinical studies that increased behavioral activity promotes axonal sprouting (Overman *et al.*, 2012), and suggests that activity-based rehabilitation may also specifically promote the formation of new brain connections during recovery after stroke.

Axonal sprouting in the post-stroke brain has now been established as a true phenomenon across many studies (Carmichael *et al.*, 2001; Dancause *et al.*, 2005; Li *et al.*, 2010; Wahl *et al.*, 2014). However, studies in the field of stroke recovery have left significant gaps in our understanding of the circuit rewiring neurons undergo during repair after injury. Specifically, the exact origins and targets of neuronal connections formed by post-stroke axonal sprouting have not been identified. Furthermore, the role of behavioral activity and the molecular substrates that shape activity-induced circuits after stroke are unknown.

Based on the established role of premotor cortex in functional recovery after stroke, this neuroanatomical study sought to systematically map input connections to premotor cortex formed

upon limb-overuse after stroke using a mouse model of ischemic stroke. This is done by injecting a retrograde neuronal tracer into premotor cortex, and quantitatively mapping and comparing the back-labeled cells across limb overuse and control conditions. Constraint-induced movement therapy is modeled by botulinum toxin (Botox) treatment specifically of the stroke-unaffected limb, which causes the mouse to locomote, feed, and groom by preferentially using its stroke-affected limb (Overman *et al.*, 2012). This is a close approximation of constraint-induced movement therapy, in which patients are forced to use only their stroke-affected limb for all activities during a given period of time (McIntyre *et al.*, 2012; Ostendorf, 1981).

2.2 Results

Limb overuse induces a novel pattern of cortical axonal sprouting

Four weeks after forelimb motor stroke +/- limb overuse, total cortical input to premotor cortex was quantitatively mapped across ipsilesional cortex using Fluorogold (FG), a retrograde neuronal tracer (Fig 2.1a experimental timeline). FG back labels the cells bodies of all neurons projecting to the injection site, in this case the premotor cortex. A four-week recovery period was chosen based on previous rodent studies that prominent post-stroke axonal sprouting during this time (Carmichael *et al.*, 2005; Li *et al.*, 2010). After layer II/III cortical tissue was flattened for tangential preparation (Fig 2.1b), quantitative neuronal mapping revealed significantly different population maps between the limb overuse and stroke only or no stroke control groups (Hotelling's T matrix test $p < 0.05$). In particular, after stroke and limb overuse, a profound increase in premotor input connectivity was seen from three regions: 1) insular cortex 2) lateral S1/S2 cortex and 3) retrosplenial cortex (Fig 2.2). The significance values reported here were performed on whole population maps, due to a lack of ROI statistics on current version of the quantitative cortical mapping program. This means that even given the tremendous amount of overlap between the

connectivity maps, the regions that were uniquely connected in the limb overuse condition were prominent enough to appreciate a statistical effect across whole map statistics. These findings were confirmed in a second independent cohort of animals, in which the same regions exhibited circuit plasticity after limb overuse (Fig 2.3). The population maps between no stroke vs. stroke only conditions were not significantly different using the same statistical criteria Fig2.2a.

In order to further explore spatial distribution of connections, the Cartesian maps were divided into 20 wedge-shaped polar segments. Polar plots were generated to represent both quantity and spatial direction of connections across binned subregions across the entire projection map. Fig 2.3b indicates that the segments oriented toward insula (1), lateral somatosensory areas (2), and retrosplenial cortex (3) are more highly connected to PMC in the limb overuse group compared to stroke only. Weighted vectors in each polar segment of the map represent a normalized number of FG+ cells per direction, which also indicates that the three regions of interest had a higher number of cells connected to PMC in the limb overuse condition.

A unique connection is formed from retrosplenial cortex (RSC) to premotor cortex (PMC)

Next, we wanted to know if the connections formed from the retrosplenial/posterior-medial region of interest in fact mapped outside of known forelimb and hindlimb motor regions. One straightforward approach to this question is to label layer V corticospinal motor neurons for co-registration of these maps to those generated via premotor FG tracer studies after limb overuse. Spinal cord retrograde tracing was performed from cervical and thoracic levels to back-label the regions of cortex that sent direct corticospinal motor projections to the vertebral levels C5 and L2. Forelimb and hindlimb layer V corticospinal motor neurons were mapped and projected onto the tangential section flat maps of premotor afferents (Fig 2.4). The co-registered maps confirmed that the increase in cortical afferents originate from a parietal area distinct from hardwired corticospinal

motor regions (Fig 2.4b, inset). Next, we matched stereotaxic coordinates between tangential and coronal orientations to carefully register the maps anatomically to a reference atlas (Fig 2.5). These analyses map the distinct area of increased cortical afferents to PMC to the retrosplenial cortex (Lein *et al.*, 2007; Paxinos and Watson, 2001).

2.3 Discussion

In the present study, we find that limb overuse after stroke drives prominent axonal sprouting from retrosplenial to premotor cortex (RSC-PMC), insula to premotor cortex, and lateral somatosensory areas to PMC (Fig 2.2b). Among the three main regions uniquely mapped after limb overuse, the retrosplenial cortex, or RSC, became the main focus for further studies for two main reasons. First, a previous study using voltage sensitive-dye imaging had reported that retrosplenial cortex is uniquely active in mice that had recovered from somatosensory stroke (Brown *et al.*, 2009). This finding from a tissue-level network activity data provides a potential functional correlate to the neuronal tracing data in a related but distinct stroke model. Second, the increase in retrosplenial connections was found in a relatively distinct pattern as compared to the more intermixed populations in somatosensory cortex and insula (Fig 2.5). Therefore, the RSC connection would also be a practical target to microdissect for the downstream cell isolation and circuit transcriptome studies.

Two separate cohorts of connectivity tracing experiments find that limb overuse after stroke drives prominent axonal sprouting from retrosplenial to premotor cortex (RSC-PMC) (Fig 2.2 and 2.3). In the stroke only condition, this connection also exists and is mapped, but to a much lesser extent as seen by a consistently lower number of FG+ cell bodies in RSC (Fig 2.2a). The number of connections is markedly increased after limb overuse. If the limb overuse treatment is only applied for 10 days before FG tracer is injected into PMC, the enhanced RSC-PMC connection is not found

(data not shown). This finding suggests that the post-stroke sprouting process may need several weeks to complete pathfinding to the premotor cortex target. The retrosplenial cortex normally sends anterior projections toward the frontal cortex, and we posit that limb overuse causes these projection collaterals to sprout new branches to innervate the premotor cortex. This hypothesis is attractive because if an existing projection is partially axotomized due to stroke, retrograde signaling back to the RSC may already have initiated repair/regrowth mechanisms at the same time limb overuse is applied. An alternative mechanism is that a de-novo axon grows long distance from RSC to frontal cortex, though this is perhaps less energetically favorable, particularly in adult CNS tissue.

The retrosplenial cortex

In these neuronal tracing studies, we identified a high density of FG+ cells in a region posterior and medial to forelimb motor cortex after limb overuse. The cell counting and population maps were generated on tangentially cut sections, an orientation advantageous for layer specific and long-distance connection studies. By carefully aligning these maps back to conventional coronal views, we were able to pinpoint the region of interest as retrosplenial cortex (RSC) (Fig 2.5). These anatomical data were especially encouraging in light of a previous study that mapped functional activity to RSC after stroke (Brown *et al.*, 2009).

The retrosplenial cortex (RSC) is still an understudied part of the neocortex (Vann *et al.*, 2009), so much that in 2001 Vogt and colleagues state “nothing is known about its function.” Located in the parietal cortex, the RSC comprises a large part of higher order “association cortex,” or the evolutionarily newer and perhaps less hardwired regions of the neocortex. In recent years, lesion studies of the RSC have resulted in defects in spatial memory and navigation (Harker and Whishaw, 2004). As a brain region specialized for multimodal integration, RSC is structurally connected to sensorimotor cortex, parietal cortex, and the occipital lobe (Lein *et al.*, 2007; Vann *et al.*, 2009). We

hypothesize that the RSC, as a hub region that coordinates spatial, visual, and sensorimotor function, might be especially well-poised for post-injury plasticity when more hardwired regions nearby, such as FL and HL motor cortex, are damaged by stroke. Again, previous studies bolster this idea; Brown et al. identified RSC as a key cortical region activated after recovery from sensorimotor stroke (Brown *et al.*, 2009). Moreover, RSC is a relay station for neural circuits intimately involved in sensorimotor function, so establishing a connection to PMC after stroke may provide an efficient path to bypass and the damaged motor cortex and promote functional recovery.

Implications, limitations, and prospective questions

One limitation of introducing a retrograde tracer to the PMC target for neuronal back-labeling is that it results in a time-stamped snapshot of the PMC connectivity map. The FG tracer is notable for its high fidelity for axon terminals and usually does not permeate fibers of passage (Schmued and Fallon, 1986). That is, a neuronal cell body is labeled FG+ if and only if its axon terminal has reached the site of injection at the time of tracing, in this case the PMC. One complimentary approach to further map axon outgrowth is to perform anterograde neuronal tracing from RSC across the same conditions. We have used AAV9 to do this (data not shown here). Indeed, we see anteriorly projecting neurons from RSC to PMC after limb overuse, but analyses of collateral sprouting cannot be easily done in these samples because of the same “snapshot connectivity” problem. To date, we have not developed a way of uniquely labeling pre- and post- stroke projection patterns at a cell-by-cell resolution. In an ideal experiment, we would be able to reconstruct brain volumes to chart individual axons from RSC, to identify any neurons sending a collateral to PMC, and finally to determine if that projection existed before stroke. We are working on developing multi-colored synaptic labeling tools to enable this type of research in the future. At the moment, without chronic in-vivo imaging of axonal sprouting (or a priori knowledge of the axon’s path for a

time-series anatomical study with serial tracer injection sites), it is challenging to map the trajectory the RSC projection takes to understand how it sprouts before terminating in PMC.

Despite technical limitations to parallel interpretation of RSC pathfinding, our discovery that sprouting occurs from RSC to PMC is consistent with decades of work on the highly dynamic peri-infarct cortex—that sprouting axons populate this surviving tissue. One might surmise that a sprouting RSC neuron is partially guided by cues of the post-stroke tissue to route to a functionally related neighboring region. In this case, when primary motor cortex suffers stroke and can no longer process input, PMC is next in the motor hierarchy and has been functionally correlated with stroke recovery (Cramer *et al.*, 1997; Zeiler *et al.*, 2013). There is also precedent for intricate post-stroke guidance of axonal sprouting: in squirrel monkeys after M1 stroke, premotor sprouting axons through the peri-infarct tissue sharply repel from the infarct border and instead synapse in neighboring somatosensory cortex (Dancause *et al.*, 2005). Similarly, regenerating retinal ganglion cells (RGCs) and spinal cord axons can also make sharp turns or “U-turns” to avoid scarring or dead ends while en-route to its eventual target (Hollis, 2015; Luo *et al.*, 2013; Pernet *et al.*, 2013). However, across all models, the jury is still out on how guidance cues dictate sprouting cells to correctly route to a target that facilitates functional recovery versus an aberrant target.

We shall propose one possible mechanism for RSC-PMC axonal sprouting here. First, stroke injury to an axon or neighboring cell induces retrograde signaling to RSC (Abe and Cavalli, 2008). Like in peri-infarct neurons (Li *et al.*, 2010), the injury activates a limited intrinsic growth or repair program for the RSC neuron. The growing axon may avert the infarct core and courses through the peri-infarct tissue, whose ECM is permissive for growth during this time frame (Carmichael *et al.*, 2005). Finally, the sprouting RSC projection synapses in the PMC, a functionally relevant brain region previously linked to motor recovery after stroke. To date, the molecular players that drive this coordinated process of cortical reorganization during post-stroke rehabilitation and behavioral

shaping remain unknown. This avenue of investigation will become the next focus of the study.

2.4. Methods

Photothrombotic stroke and forelimb overuse model

Forelimb cortical stroke was induced in young adult (3 month old) C57BL/6 mice using stereotaxic surgery. This technique is well established in the field to generate focal cortical ischemic stroke in the rodent model. Anesthesia induction was performed at 5% isoflurane supplied with 100% O₂ and then maintained at 2% for the duration of the operation. Body temperature was maintained at 37.0 °C +/-0.5°C by homeothermic heating pads. Rose Bengal, a photosensitive chemical was introduced systemically via intraperitoneal injection, and light activated for 15 minutes (using a cold light source KL1500 LCD, Zeiss) the forelimb motor cortex (coordinates ML 1.5mm, AP 0.0mm). After 15 minutes, the wound is closed and the animal is returned to its home cage for recovery. Photothrombotic stroke causes microthromboses that reproducibly generate targeted infarcts of 2.0 mm diameter to the cortical area of interest, which in these studies is the forelimb motor cortex located at 1.5mm lateral to Bregma (Carmichael, 2005; Clarkson *et al.*, 2011).

Forelimb motor cortex stroke was chosen as the model system for these studies for three key reasons. First, it reliably induces forelimb motor deficits that have been quantitated by specific behavioral tests (Clarkson *et al.*, 2011). Second, previous studies using the forelimb motor cortex stroke model have established a critical role of peri-infarct cortex in recovery from ischemic infarct (Clarkson *et al.*, 2010; Clarkson *et al.*, 2011). Third, motor cortical activity is directly correlated with the amount of limb usage by the animal, which is a parameter that can be independently manipulated for these proposed studies of activity-dependent recovery. Constraint-induced movement therapy was modeled by intramuscular botulinum toxin (Botox) treatment specifically of the stroke-unaffected limb. This causes the animal to locomote, feed, and groom by preferentially using its stroke-affected limb. Previous work has shown that forced limb overuse leads to improved functional recovery after stroke (Biernaskie *et al.*, 2005; Schneider *et al.*, 2014).

Neuroanatomical tracing of premotor cortex

After stroke, animals enter a four-week recovery phase in their home cages, a critical period during which new neural connections form after stroke (Carmichael *et al.*, 2005). During this time, half of the animals from each condition group will receive Botox to induce stroke-affected limb overuse. The other half was returned to their home cages with no rehabilitative treatment. Each animal then received 280nL of Fluorogold (Fluorochrome, Denver), retrograde neuronal tracer, by pressure microinjection into the premotor cortex to back-label the somas of all neurons connected to the premotor cortex after stroke. Cortex is then isolated, flattened, PFA fixed, and tangentially sectioned at 40um for layer-specific quantitative analyses.

Spinal cord injections:

Layer V corticospinal motor neurons were labeled by stereotaxic injection of CTB, a retrograde neuronal tracer, into the cervical enlargement at C5 of 5 month-old CD1 mice. Surgeries were performed on a stereotaxic apparatus (David Kopf) interfaced with a microinfusion syringe pump (Harvard Instruments) as previously described (Song *et al.*, Biomaterials, 2012). Animals were anesthetized with general isoflurane in oxygen-enriched air. Single vertebra laminectomy at C5 revealed the cord, and 500nL of CTB tracer (6.67 ug/uL, List Biological Labs) was injected into the right dorsal corticospinal tract (dCST). CTB infusion progressed at 0.2mL/min through a glass micropipette connected by special adapters and high-pressure tubing to a 10 mL Hamilton syringe. All animals were given analgesic prior to suture wound closure. 10 days after tracer delivery, animals were anesthetized with pentobarbital and transcardially perfused with 4% PFA. Brain and spinal cord were isolated and prepared via tangential and coronal cryosectioning, respectively. Tissue preparation and stereological cortical mapping were performed as previously described (Overman *et*

al., 2012). Cervical cord was cryosectioned at 40 μ m and for dCST injection site verification by CTB immunofluorescence (Goat anti-CTB 1:10,000, List Biological Labs).

Statistical analyses of anatomical cortical mapping

The total number and pattern of connections were be mapped and quantified across groups using quantitative cortical mapping. Quantitative cortical mapping digitally plots cell body locations in tangential flattened cortex and converts each cell location into Cartesian coordinates in relation to the injections, with spatial connections statistically compared across groups (Hotelling's inverse T-matrix test and polar plots). More specifically, three statistical analysis paradigms were used. First, scatter plots were analyzed using Hotelling's T^2 test for spatial correlation. For data with a common covariance matrix, such as the map of axonal position in tangential cortical sections, Hotelling's T^2 method tests the hypothesis of multivariate mean equality: that the means for the set outcome variable (axonal location for each individual, averaged by experimental condition) are equivalent across groups. The T statistic is the analog of Student's two-group t-statistic for testing equality of group means for a single outcome variable. P-values were computed without Gaussian assumptions by means of a bootstrap 250 μ m was applied around the injection site to account for the uniformity of the injection site itself and immediately adjacent FG labeling across groups, regardless of projection pattern. Second, polar statistics tested for differences in distribution of axonal projection patterns across treatment groups. For each treatment condition, the x, y coordinate of every FG-positive cell body was converted to an equivalent polar coordinate (r) relative to the tracer injection site as center (Li *et al.*, 2010; Overman *et al.*, 2012). The location of each cell body was transferred to common polar space and a mean projection vector was computed for each treatment group. Differences in mean projection vectors between groups were analyzed using Watson's nonparametric two-sample U^2 test for polar observations. Polygons represent the 70th percentile of the distances of FG+ cell bodies from the reference site (medial edge of section) in each segment of

the graph. Weighted polar vectors represent the median vector multiplied by the median of the normal distribution of the number of points in a given segment of the graph. The normal distribution is the projection pattern that would occur if neurons projected equally and radially from the injection site. Third, total cell numbers in the linear construct across ipsilateral cortex were analyzed using one-way analysis of variance (ANOVA) with *post hoc* Tukey-Kramer test. In addition, differences between two means were assessed by unpaired two-tailed Student's *t* test. Differences among multiple means were assessed by one-way ANOVA followed by Tukey-Kramer's *post hoc* tests. All statistical analyses were performed in R-statistics based custom software (Li *et al.*, 2010; Overman *et al.*, 2012).

Figure 2.1

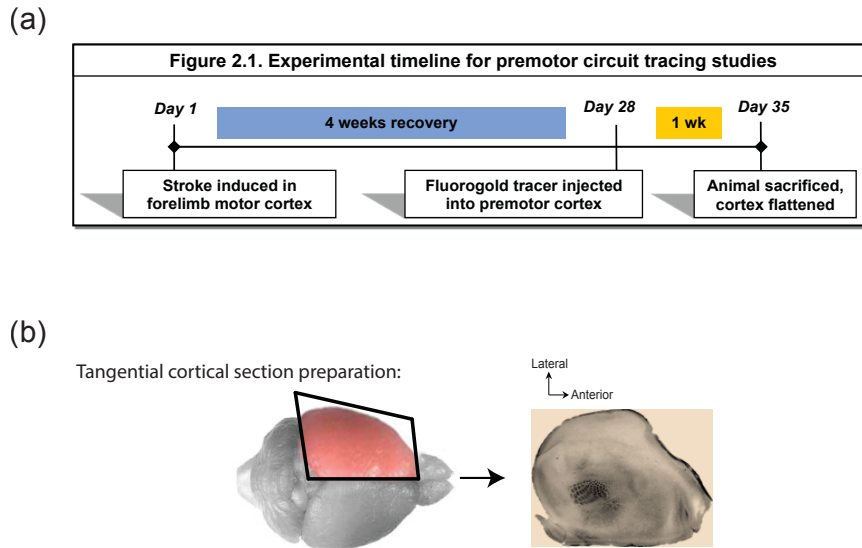
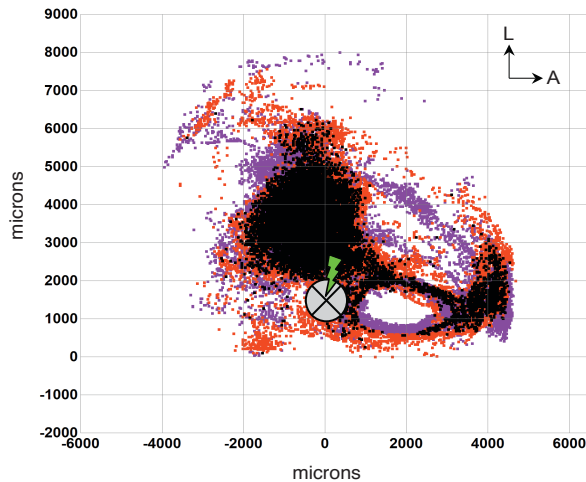


Figure 2.1 Experimental timeline of neuroanatomical mapping studies

a) Premotor circuit mapping studies are performed on a 5-week timeline. Animals undergo a 4-week recovery period after receiving PT stroke, during which time half of the animals receive limb overuse treatment. At day 28, FG retrograde tracer is injected in premotor cortex and given a 1 week uptake period before tissue processing **b)** Tangential sections are prepared from ipsilesional cortex. Left: cortical surface view with Right: A tangential flattened section preparation of the highlighted cortex in adjacent panel.

Figure 2.2

(a) Stroke vs. WT (no injury)

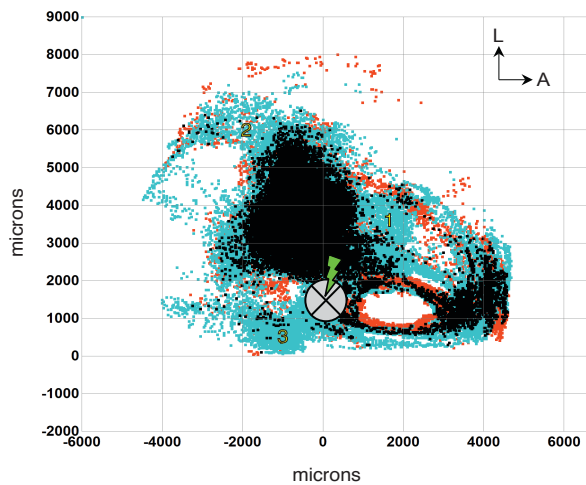


 Stroke Site in FMC




 WT No stroke
 Stroke only
 Overlap

$p > 0.05$
 $n = 5$ per group

(b) Stroke only vs. Stroke+limb overuse



 Stroke Site in FMC

 Stroke + limb overuse
 Stroke only
 Overlap

$p < 0.05$
 $n = 5$ per group

Figure 2.2 Limb overuse produces novel pattern of premotor connections

a) Quantitative cortical connectional maps compare premotor cortex retrograde tracer labeling between WT vs. stroke only overuse conditions ($n=5$ per group). There was no statistically significant premotor connectivity difference between WT versus stroke only groups **b)** Quantitative cortical connectional maps between stroke only vs. stroke + limb overuse conditions ($n=5$ per group). Forced limb overuse produces a novel and statistically significant pattern of premotor cortex connections $p=0.021$.

Figure 2.3

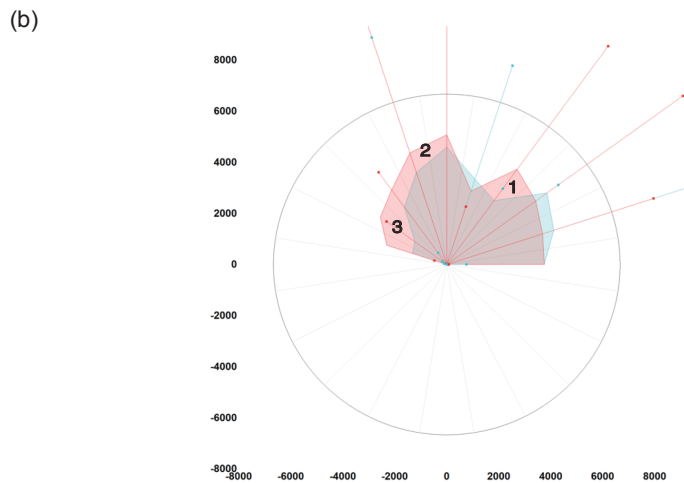
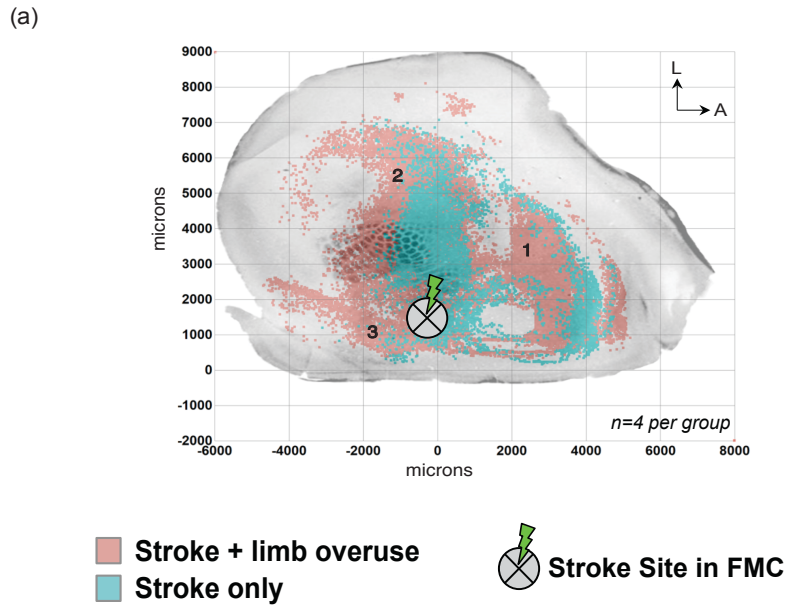
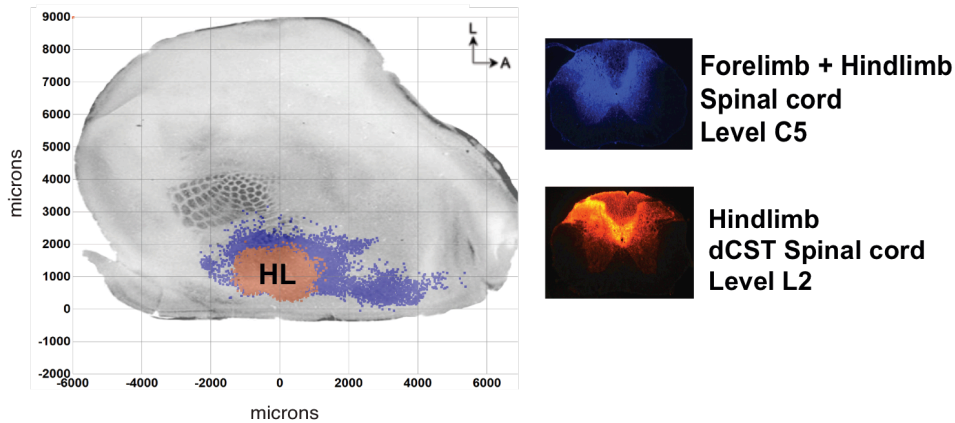


Figure 2.3 A second study reproduces PMC-RSC connectivity maps after limb overuse

- a)** Quantitative population maps generated from a second cohort of neuroanatomical tracing studies indicate three regions of increased connectivity to PMC after limb overuse: (1) insular cortex (2) lateral S1/S2 (3) retrosplenial cortex. Limb overuse PMC connectivity is labeled in pink. Teal represents stroke only condition. **b)** Polar distribution plots of cortical maps generated from this cohort. Shaded polygons represent the 70th percentile of the distances of FG+ somas from a reference point origin. Weighed polar vectors represent the normalized distribution of the number of cell bodies in a given wedge-shaped polar segment of the graph. The three regions of increased connectivity to PMC stand out within the polar distribution and weighed vectors: (1) insular cortex (2) lateral S1/S2 (3) retrosplenial cortex again emerge as regions of unique connectivity.

Figure 2.4

(a) FL and HL Corticospinal Motor Neurons (CSMN)



(b) Posteromedial region distinct from FL/HL CSMN

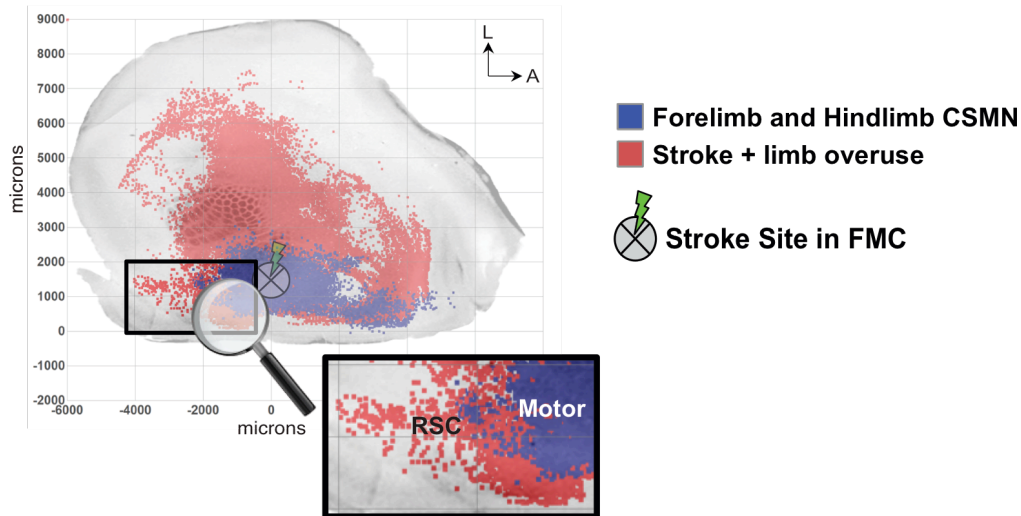


Figure 2.4 Corticospinal motor regions are distinct from RSC origin of PMC connection

a) Tangential flat map with barrel cortex immunostained for anatomical reference. Forelimb (blue) and hindlimb (orange) corticospinal motor neuron CSMN regions. Insets: C5 and L2 spinal cord tracer injection sites targeting the dorsal corticospinal tract (dCST) **b)** Overlay of CSMN projection maps with premotor connectivity map of stroke+limb overuse condition (projection map is from the same condition group presented in Fig 2.2b). Inset: zoomed view of posterior-medial region of interest of FG+ cells that lie outside of motor areas and within the retrosplenial cortex (RSC).

Figure 2.5

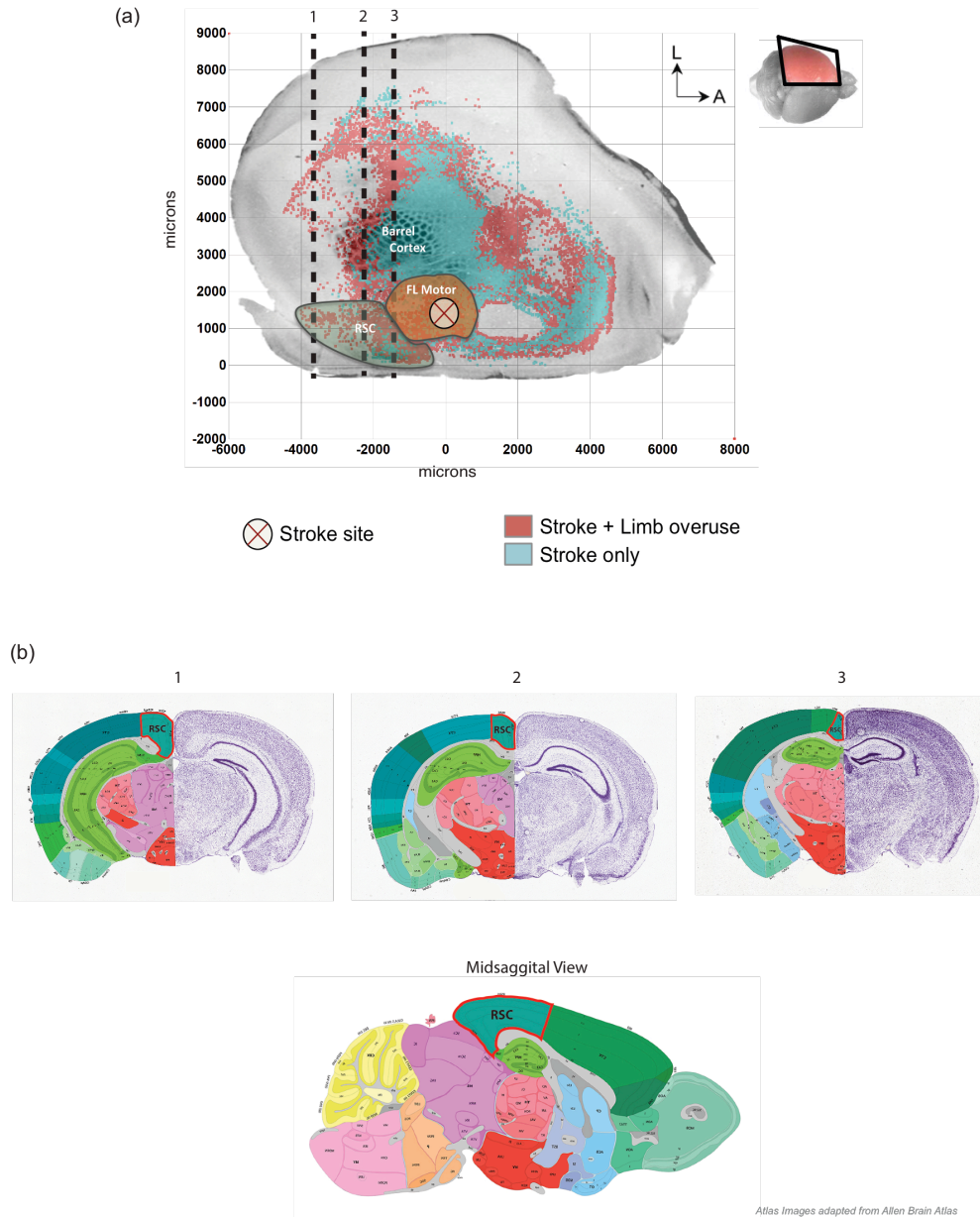


Figure 2.5 Mapping the posterior medial region of interest to retrosplenial cortex

a) Cortical tangential section view of RSC-PMC population maps generated by retrograde tracing. Several neuroanatomical regions are schematized on cortical tangential section. The barrel cortex overlies immunostained cytochrome oxidase; FL motor: forelimb primary motor cortex, RSC: retrosplenial cortex. The three dotted lines mark the anterior posterior (A-P) distances for the brain atlas views in coronal orientation. **b)** Top: three virtual coronal slices are taken at AP-distances of (1)-3.80mm (2)-2.30mm and (3)-1.70mm. RSC spans each of the coronal sections and from anterior (3) to posterior (1). Bottom: sagittal view along the midline reveals that RSC territory extends into the most medial edge, and curls along this edge as seen in coronal slice (1). This midline area maps to the far-most medial edge on tangential sections as seen in panel (a).

2.6 References:

- Abe, N., Cavalli, V., 2008. Nerve injury signaling. *Current opinion in neurobiology* 18, 276-283.
- Biernaskie, J., Szymanska, A., Windle, V., Corbett, D., 2005. Bi-hemispheric contribution to functional motor recovery of the affected forelimb following focal ischemic brain injury in rats. *The European journal of neuroscience* 21, 989-999.
- Brown, C.E., Aminoltejari, K., Erb, H., Winship, I.R., Murphy, T.H., 2009. In vivo voltage-sensitive dye imaging in adult mice reveals that somatosensory maps lost to stroke are replaced over weeks by new structural and functional circuits with prolonged modes of activation within both the peri-infarct zone and distant sites. *The Journal of neuroscience : the official journal of the Society for Neuroscience* 29, 1719-1734.
- Carmichael, S.T., 2005. Rodent models of focal stroke: size, mechanism, and purpose. *NeuroRx : the journal of the American Society for Experimental NeuroTherapeutics* 2, 396-409.
- Carmichael, S.T., Archibeque, I., Luke, L., Nolan, T., Momiy, J., Li, S., 2005. Growth-associated gene expression after stroke: evidence for a growth-promoting region in peri-infarct cortex. *Experimental neurology* 193, 291-311.
- Carmichael, S.T., Wei, L., Rovainen, C.M., Woolsey, T.A., 2001. New patterns of intracortical projections after focal cortical stroke. *Neurobiology of disease* 8, 910-922.
- Clarkson, A.N., Huang, B.S., Macisaac, S.E., Mody, I., Carmichael, S.T., 2010. Reducing excessive GABA-mediated tonic inhibition promotes functional recovery after stroke. *Nature* 468, 305-309.
- Clarkson, A.N., Overman, J.J., Zhong, S., Mueller, R., Lynch, G., Carmichael, S.T., 2011. AMPA receptor-induced local brain-derived neurotrophic factor signaling mediates motor recovery after stroke. *The Journal of neuroscience : the official journal of the Society for Neuroscience* 31, 3766-3775.

- Cramer, S.C., Nelles, G., Benson, R.R., Kaplan, J.D., Parker, R.A., Kwong, K.K., Kennedy, D.N., Finklestein, S.P., Rosen, B.R., 1997. A functional MRI study of subjects recovered from hemiparetic stroke. *Stroke; a journal of cerebral circulation* 28, 2518-2527.
- Dancause, N., Barbay, S., Frost, S.B., Plautz, E.J., Chen, D., Zoubina, E.V., Stowe, A.M., Nudo, R.J., 2005. Extensive cortical rewiring after brain injury. *The Journal of neuroscience : the official journal of the Society for Neuroscience* 25, 10167-10179.
- Harker, K.T., Whishaw, I.Q., 2004. A reaffirmation of the retrosplenial contribution to rodent navigation: reviewing the influences of lesion, strain, and task. *Neuroscience and biobehavioral reviews* 28, 485-496.
- Hollis, E.R., 2nd, 2015. Axon Guidance Molecules and Neural Circuit Remodeling After Spinal Cord Injury. *Neurotherapeutics : the journal of the American Society for Experimental NeuroTherapeutics*.
- Lein, E.S., Hawrylycz, M.J., Ao, N., Ayres, M., Bensinger, A., Bernard, A., Boe, A.F., Boguski, M.S., Brockway, K.S., Byrnes, E.J., Chen, L., Chen, L., Chen, T.M., Chin, M.C., Chong, J., Crook, B.E., Czaplinska, A., Dang, C.N., Datta, S., Dee, N.R., Desaki, A.L., Desta, T., Diep, E., Dolbeare, T.A., Donelan, M.J., Dong, H.W., Dougherty, J.G., Duncan, B.J., Ebbert, A.J., Eichele, G., Estin, L.K., Faber, C., Facer, B.A., Fields, R., Fischer, S.R., Fliss, T.P., Frensley, C., Gates, S.N., Glattfelder, K.J., Halverson, K.R., Hart, M.R., Hohmann, J.G., Howell, M.P., Jeung, D.P., Johnson, R.A., Karr, P.T., Kawal, R., Kidney, J.M., Knapik, R.H., Kuan, C.L., Lake, J.H., Laramée, A.R., Larsen, K.D., Lau, C., Lemon, T.A., Liang, A.J., Liu, Y., Luong, L.T., Michaels, J., Morgan, J.J., Morgan, R.J., Mortrud, M.T., Mosqueda, N.F., Ng, L.L., Ng, R., Orta, G.J., Overly, C.C., Pak, T.H., Parry, S.E., Pathak, S.D., Pearson, O.C., Puchalski, R.B., Riley, Z.L., Rockett, H.R., Rowland, S.A., Royall, J.J., Ruiz, M.J., Sarno, N.R., Schaffnit, K., Shapovalova, N.V., Sivisay, T., Slaughterbeck, C.R., Smith, S.C., Smith, K.A., Smith, B.I., Sodt, A.J., Stewart, N.N., Stumpf, K.R., Sunkin, S.M., Sutram, M., Tam, A., Teemer, C.D.,

- Thaller, C., Thompson, C.L., Varnam, L.R., Visel, A., Whitlock, R.M., Wohnoutka, P.E., Wolkey, C.K., Wong, V.Y., Wood, M., Yaylaoglu, M.B., Young, R.C., Youngstrom, B.L., Yuan, X.F., Zhang, B., Zwingman, T.A., Jones, A.R., 2007. Genome-wide atlas of gene expression in the adult mouse brain. *Nature* 445, 168-176.
- Li, S., Overman, J.J., Katsman, D., Kozlov, S.V., Donnelly, C.J., Twiss, J.L., Giger, R.J., Coppola, G., Geschwind, D.H., Carmichael, S.T., 2010. An age-related sprouting transcriptome provides molecular control of axonal sprouting after stroke. *Nature neuroscience* 13, 1496-1504.
- Luo, X., Salgueiro, Y., Beckerman, S.R., Lemmon, V.P., Tsoulfas, P., Park, K.K., 2013. Three-dimensional evaluation of retinal ganglion cell axon regeneration and pathfinding in whole mouse tissue after injury. *Experimental neurology* 247, 653-662.
- McIntyre, A., Viana, R., Janzen, S., Mehta, S., Pereira, S., Teasell, R., 2012. Systematic review and meta-analysis of constraint-induced movement therapy in the hemiparetic upper extremity more than six months post stroke. *Topics in stroke rehabilitation* 19, 499-513.
- Ostendorf, C.G.a.W., S.L., 1981. Effect of Forced Use of the Upper Extremity of a Hemiplegic Patient on Changes in Function: A Single-Case Design. *Physical Therapy* 61, 1022-1028.
- Overman, J.J., Clarkson, A.N., Wanner, I.B., Overman, W.T., Eckstein, I., Maguire, J.L., Dinov, I.D., Toga, A.W., Carmichael, S.T., 2012. A role for ephrin-A5 in axonal sprouting, recovery, and activity-dependent plasticity after stroke. *Proceedings of the National Academy of Sciences of the United States of America* 109, E2230-2239.
- Paxinos, G., Watson, K.B.J., 2001. *The Mouse Brain in Stereotaxic Coordinates 2nd ed.* . Academic Press: San Diego.
- Pernet, V., Joly, S., Dalkara, D., Jordi, N., Schwarz, O., Christ, F., Schaffer, D.V., Flannery, J.G., Schwab, M.E., 2013. Long-distance axonal regeneration induced by CNTF gene transfer is

- impaired by axonal misguidance in the injured adult optic nerve. *Neurobiology of disease* 51, 202-213.
- Schmued, L.C., Fallon, J.H., 1986. Fluoro-Gold: a new fluorescent retrograde axonal tracer with numerous unique properties. *Brain research* 377, 147-154.
- Schneider, A., Rogalewski, A., Wafzig, O., Kirsch, F., Gretz, N., Krüger, C., Diederich, K., Pitzer, C., Laage, R., Plaas, C., Vogt, G., Minnerup, J.S., W, 2014. Forced arm use is superior to voluntary training for motor recovery and brain plasticity after cortical ischemia in rats. *Experimental & Translational Stroke Medicine* 6, 1-12.
- Vann, S.D., Aggleton, J.P., Maguire, E.A., 2009. What does the retrosplenial cortex do? *Nature reviews. Neuroscience* 10, 792-802.
- Wahl, A.S., Omlor, W., Rubio, J.C., Chen, J.L., Zheng, H., Schroter, A., Gullo, M., Weinmann, O., Kobayashi, K., Helmchen, F., Ommer, B., Schwab, M.E., 2014. Neuronal repair. Asynchronous therapy restores motor control by rewiring of the rat corticospinal tract after stroke. *Science* 344, 1250-1255.
- Wolf, S.L., Winstein, C.J., Miller, J.P., Thompson, P.A., Taub, E., Uswatte, G., Morris, D., Blanton, S., Nichols-Larsen, D., Clark, P.C., 2008. Retention of upper limb function in stroke survivors who have received constraint-induced movement therapy: the EXCITE randomised trial. *Lancet neurology* 7, 33-40.
- Zeiler, S.R., Gibson, E.M., Hoesch, R.E., Li, M.Y., Worley, P.F., O'Brien, R.J., Krakauer, J.W., 2013. Medial premotor cortex shows a reduction in inhibitory markers and mediates recovery in a mouse model of focal stroke. *Stroke; a journal of cerebral circulation* 44, 483-489.

CHAPTER 3.

AN ACTIVITY-DEPENDENT AND CONNECTION-SPECIFIC TRANSCRIPTOME AFTER STROKE AND LIMB OVERUSE

3.1 Introduction

The neuroanatomical studies described in Ch. 2 demonstrated that limb overuse induces axonal sprouting from retrosplenial (RSC) to premotor cortex (PMC). The next goal was to specifically isolate the neurons that project from RSC to PMC to identify a connection-specific molecular transcriptome after a post-stroke rehabilitative behavioral paradigm. We hypothesize that such a transcriptome would capture both injury-induced and learning-activated genes. Ultimately, we want to understand how activity-dependent cues from limb overuse shape neural remodeling and recovery after injury. Figure 3.1 schematizes the experimental approach, in which RSC cells labeled with FG+ are purified using FACS (Fluorescence Activated Cell Sorting) for RNA isolation and transcriptome analyses. To this end, we opted to use RNA deep sequencing to capture the molecular transcriptome of a CIMT-driven circuit between RSC and PMC. In contrast to microarray hybridization techniques, RNA-Seq has superior dynamic range for transcript quantification and also identifies splice variants within the transcriptional profile (Wang *et al.*, 2009). This second advantage of RNA-Seq will offer key insights into the isoform-specific roles of activity-dependent molecules in post stroke plasticity. For example, Homer1, which is an activity-induced postsynaptic protein upregulated in sprouting neurons (Li *et al.*, 2010), has a truncated isoform with a short intracellular tail that prevents glutamate receptor clustering to mediate homeostatic plasticity (Leslie and Nedivi, 2011). This added resolution for splice variation in RNA-Seq expression data will help guide the subsequent gain or loss-of-function mechanistic studies.

Prior to RNA-Seq transcriptome profiling, there were several cell purification technical hurdles in to overcome. Previously, our lab and others have used laser capture microdissection to isolate cells of interest for molecular studies (Cahoy *et al.*, 2008; Li *et al.*, 2010), but this technique necessitates macroscopic laser-guided cutting of tissue, so it is difficult to truly obtain a single pure cell type (Okaty *et al.*, 2011). Other labs have also used Fluorescence Activated Cell Sorting (FACS) to isolate pure cell populations of interest, but usually this is done in the more easily dissociable pup brain (Arlotta *et al.*, 2005), non-cortical regions such as striatum (Lobo *et al.*, 2006), or transgenic animal lines where there is an overabundance of collectable cells. Our specific needs were to purify cortical cells from the adult brain, a relatively small population of cells from a distinctly mapped region of the brain. However, since the population of cells we wanted to collect had been labeled by a fluorescent neuron-specific tracer and we had detailed maps for their expected location in RSC, we set out to optimize this next tier of studies for FACS purification.

3.2 Results

FACS purification of adult cortical neurons

In a set of initial proof-of-concept experiments, Fluorogold (FG) tracer-labeled neurons were successfully dissociated from adult cortex, FACS purified, and high quality startup RNA extracted for transcriptome profiling. Because adult cortical neurons are morphologically complex and physically enmeshed within dense networks, a specific cell isolation protocol using a density-gradient column was adapted for careful cell release from tissue (Brewer and Torricelli, 2007). A pH stabilizing buffer Hibernate and excitotoxicity blockers were used for FACS cell isolation and suspension (details and references in Methods section). This unique protocol overcomes the anticipated hurdles of low cell yield from tissue digestion, shearing injury during cell release, and low neuronal viability. Optimized papain tissue digests of both naïve and stroke brains yielded 120,000-

150,000 cells per cortical sample, yields that are well suited for FACS analyses. After isolating neurons from fresh tissue, a subpopulation of FG positive cells was visually confirmed by fluorescent microscopy, and positive FACS cell. FG sorting was fluorescently distinct from and equally efficient as a positive control sorting of CTB-488, a control retrograde tracer conjugated to a conventional fluorophore. Gates were defined by negative controls in unlabeled animals (Fig 3.2). In total, these experiments demonstrate a successful and reproducible approach to dissociate and isolate FG labeled adult cortical neurons for molecular characterization of the identified activity-induced recovery circuit.

Next, we used FACS to collect RSC FG+ cells from multiple replicates of stroke (n=8) and stroke + limb overuse (n=7) animals. An additional control group of RSC neurons not connected to PMC (FG-) but labeled with neuronal surface marker NCAM was included (n=7). This final control group represents RSC neurons adjacent to FG+ cells but not labeled with tracer—essentially a cell-type specific control from the same cortical region. Fig 3.3 diagrams representative FACS collection plots from each experimental group. Total numbers of cells isolated from each condition are summarized in Table 3.1. On average, between 500-1000 FG+ cells were collected per sample. The experimental timeline for stroke and premotor FG tracing were identical to that used for the first phase of neuroanatomical mapping studies (mapped in Fig 2.1), and fresh tissue dissections were performed for all FACS experiments.

The RSC-PMC circuit transcriptome includes activity-dependent and growth-related genes

High quality RNA was purified from FACS-isolated FG positive RSC neurons and NCAM+ RSC neurons for cDNA library generation and RNA-Seq. The first comparison we performed was a ranked analysis across all three groups, which indicated that premotor projecting RSC cells isolated from stroke were most different from their neighboring RSC cells (FDR <0.1 across any

comparison) (Fig3.4). In a second comparison, RSC+ cells from stroke+limb overuse were tested against stroke alone, and the overuse group is statistically different from stroke alone and differentially regulates a unique set of genes.

In this first comparison, among the top 100 differentially regulated genes were activity-dependent genes such as FosB and KCNJ10, and neuronal outgrowth genes RhoB, Sparc, and Egr1. Immune molecules that are differentially regulated include MHCI-related Beta-2 microglobulin, HLA proteins like H2-K1, and C1q. Many of these have been implicated in developmental and adult plasticity mechanisms in recent years (Adelson *et al.*, 2012; Bialas and Stevens, 2013; Shatz, 2009).

Within the second comparison, a unique set of 160 genes is differentially regulated in the retrosplenial to premotor cortex circuit upon limb overuse after stroke ($p < 0.005$, FDR < 0.1) (Table 3.2). Several novel candidates emerge from this analysis. SOSTDC1, a BMP antagonist upregulated 64 fold, belongs to a class of activity-dependent proteins involved in Wnt signaling and tissue patterning during development (Cho *et al.*, 2011; Clausen *et al.*, 2011). Nat8l (+28X) produces a brain-specific metabolite that regulates TNF-alpha expression, a signal that can increase AMPA receptor insertion into the membrane (Pickering *et al.*, 2005; Santello and Volterra, 2012). Nat8l also induces axonal outgrowth in primary neurons in-vitro via energy regulation and microtubule stabilization (Sumi *et al.*, 2015; Toriumi *et al.*, 2013). Two molecules involved in the ubiquitin protease system are also significantly upregulated: MARCH3, an E3 ubiquitin ligase, and UBE2c, a ubiquitin conjugating enzyme implicated in the hypoxia inducible factor pathway. There is a precedent in the field for ubiquitination-induced axonal sprouting. For example, NEDD4 ubiquitinates PTEN to increase axonal sprouting during development of hippocampal neurons (Drinjakovic *et al.*, 2010). Limb overuse after stroke differentially regulates a unique list of genes; many candidate genes are novel, but also have promising relevance supported through the literature.

Bioinformatic Analyses of functional network signaling, gene co-regulation, and transcriptomic relationship to other learning and memory paradigms

Next, we strived for a more comprehensive analysis of the identified genes by studying their network connectivity, relationship to each other, and broadly to other plasticity transcriptomes. Ingenuity Pathway Analysis (IPA) categorized the gene differentially regulated by limb overuse into canonical pathways that include 1) CREB signaling in neurons 2) Ephrin Signaling, and 3) Calcium Signaling. Top network hits include 1) cellular development, cell death and survival, gene expression 2) cellular growth and proliferation, and 3) embryonic and organ development (Fig3.5). Next, an IPA upstream analysis was also run to identify potential transcription factors or master regulators of the identified differentially regulated genes. This resulted in the identification of 6 transcriptional regulators: Otx2, YY1, CREBBP, NeuroD1, NeuroG3, and Crx. Otx2 is a secreted protein that establishes the end of the critical period of dominance column plasticity. Blocking Otx2 in the mature brain can reestablish this plasticity in the adult visual system (Miyata *et al.*, 2012). YY1 (named Yin-Yang 1 for its activation/repression bipotential activity) is a Kruppel class transcription factor previously found to play a role in TNF- α mediated neuronal protection (Karki *et al.*, 2016) as well as liver and muscle regeneration (Du *et al.*, 1998). YY1 also represses brain MMP9, an enzyme that degrades extracellular matrix and may therefore permit sprouting (Deryugina and Quigley, 2006). In the PNS, YY1 regulates myelination (He Ye, 2010), a mechanism that can potentially contribute to increased integrity of circuits after cortical reorganization. Finally, a closely related homolog YY2 has been found to critically regulate neuronal outgrowth of hippocampal neurons (Klar *et al.*, 2015). NeuroD1, which is a developmental transcription factor downregulated in the limb overuse condition, is controlled by upstream regulator NeuroG3. CREBBP is a modulator of the widely known activity-dependent gene, CREB, which been shown to be involved in axonal outgrowth of DRG spinal neurons after injury (Gao *et al.*, 2004) and in peri-infarct neurons after stroke

(unpublished data from our group). Finally, Crx is a transcription factor important to the visual system development, and has been reported to interact with Otx2 (Li *et al.*, 2015a) These upstream regulators, their associated genes, and basic known roles are summarized in Table 3.3.

In a next tier of analysis, we used weighted gene co-expression network analysis (WGCNA), to identify candidate genes that are coordinately regulated. WGCNA analyzes and groups genes that exhibit similar expression patterns across samples and places them into gene modules (Zhang and Horvath, 2005). The main advantage of this analysis is that it overcomes many of the limitations of conventional single gene studies by looking for co-expression patterns of candidate genes without using a database of pre-curated functional networks (Langfelder and Horvath, 2008). Unbiased modules were generated across samples from the three conditions: RSC FG+ cells from stroke and stroke + limb overuse, and NCAM+ cells from RSC (Fig 3.6a). In RSC FG+ neurons versus RSC NCAM+ neurons, three upregulated gene modules (turquoise, purple, yellow modules) were identified with Gene Ontology (GO) specifications: growth factor receptor, brain and CNS development, and c4b innate immunity. There were also 8 downregulated modules (bisque4, maroon, plum2, brown4, tan, brown, light green, black modules) in RSC-PMC groups. These modules included ontologies from KRAB domain (transcriptional repressor) signaling, negative regulators of tissue development (i.e. BMP4 and HDAC5), epigenetic modifiers, action potential synaptic transmission genes, axonal guidance factors, and regulators of microtubule polymerization. When comparing RSC-PMC neurons from limb overuse groups with those from stroke alone, there were three upregulated modules (thistle, floral white, and white modules) upon limb overuse. GO analysis maps many of these genes to CNS development, cell cycle, and neuronal projection morphogenesis. One downregulated module (honeydew module) was ontologically related to homophilic cell adhesion, which may play a permissive role for axonal sprouting. The significance criterion for selecting these gene modules was at a p -value between 1×10^{-6} and 0.0456, a range consistent with

other published WGCNA analyses (Chandran *et al.*, 2016; Saris *et al.*, 2009).

Finally, we also performed a transcriptome overlap analysis to compare the retrosplenial-premotor transcriptome to previously published gene expression datasets from various other activity-dependent and plasticity paradigms. We asked the question: How is the molecular transcriptome of limb training after stroke related to the genetic signature of other learning and memory or injury-induced circuits? Principle component analyses reveal that the post-stroke limb overuse behavioral paradigm induces genes also implicated in hippocampal learning, environmental enrichment, and calmodulin-regulated plasticity (Fig3.7). On the other hand, the RSC-PMC limb overuse transcriptome after stroke lies distant from developmental profiles entered into this analysis, including developmental expression profiles from visual cortex. These data help relate molecular programs after injury to other paradigms of plasticity using unbiased comparisons between entire transcriptomes.

3.3 Discussion

Previous studies in rodents, primates, and humans have demonstrated that premotor cortex is often responsible for motor functional recovery after stroke (Cramer *et al.*, 1997; Dancause *et al.*, 2005; Johansen-Berg *et al.*, 2002; Overman *et al.*, 2012; Seitz *et al.*, 1998). The first phase of this work identified that limb overuse after stroke induces a unique connection from retrosplenial cortex to premotor cortex. The present RNA-Seq study captures the molecular transcriptome underlying this activity-driven premotor circuit. These analyses reveal that limb overuse after stroke induces an RSC-PMC circuit that is molecularly distinct from other injury-induced and plasticity paradigms and raises significant molecular targets for further investigation.

In general, RSC neurons connected to PMC were transcriptionally more similar to each other than to adjacent RSC neurons not projecting to PMC. Highly significant genes seen in the

RSC-PMC connection include activity-dependent genes such as FosB and KCNJ10, and neuronal outgrowth genes including RhoB, Sparc, and Egr1. Some of these genes have also been previously associated with ischemic injury and nerve regeneration. We interpret this first finding as molecular evidence for a specific endogenous premotor repair strategy activated after stroke. Next, a closer investigation of the limb overuse group reveals highly novel genes that are differentially regulated only in the stroke + limb overuse condition. We believe these genes are responsible for the striking and vast enrichment of RSC-PMC connections seen after limb overuse treatment that mimics clinical CIMT (Fig2.2).

Each of these two categories of differentially regulated genes contributes valuable insight for understanding different facets of the underlying biology of the RSC-PMC connection after stroke. If the brain initiates an endogenous program for RSC-PMC reorganization after stroke, one possible (the favorable and ideal) outcome is that injury alone initiates axonal sprouting, route finding, and synapse formation at a functionally useful target in PMC. The alternative is that the endogenous response in RSC is in itself not enough for ample or functionally meaningful circuit rewiring, but is facilitated by behavioral activity akin to CIMT. Based on several lines of evidence, that 1) neuroanatomical mapping and FACS data show the stroke alone condition has substantially fewer RSC-PMC connections than the limb overuse condition (Fig2.2) that 2) CNS regeneration is rarely unencumbered and relatively inefficient (Abe and Cavalli, 2008; Chandran *et al.*, 2016), and that 3) limb overuse improves functional recovery and is linked to premotor input (Livingston-Thomas *et al.*, 2014; Seitz *et al.*, 1998), the second interpretation favoring CIMT molecular shaping of the RSC-PMC circuit is much more likely. The relatively few FG+ cells in the stroke group without limb overuse may represent neurons that managed to reach PMC in the absence of focused limb overuse therapy, though in total comprises a small subset of all possible sprouting neurons.

The present analyses find that limb overuse after stroke induces an RSC-PMC circuit that is molecularly distinct. A unique set of 160 genes is differentially regulated in the retrosplenial to premotor cortex circuit upon post-injury limb overuse ($p < 0.005$, $FDR < 0.1$). Among the most significantly upregulated genes are *NeuroD1* (11 fold), *NGFR* (14 fold), *EphA10* (5 fold), and *ZbtB32* (36 fold). *NeuroD1* is a transcriptional activator of genes involved in neurogenesis, insulin signaling, and associates with the p300/CBP transcriptional co-activator (Kuwabara *et al.*, 2009). *NGFR* mediates cell survival and GLUT4 insulin response (Chaldakov *et al.*, 2009). These two genes, both linked to insulin and growth signaling, recall to a previous finding that sprouting neurons after stroke are uniquely sensitive to IGF-1 (Li *et al.*, 2010), and may depend on growth factor titration for survival. In fact, a rich literature connecting NGF and IGF-1 can be found in the neuroendocrine field and may provide overlapping mechanisms to CNS function of the two post-stroke candidate genes. *EphA10* is a developmental molecule that cues growth cone avoidance, and whose differential regulation seen after limb overuse may guide targeted axonal sprouting (Dickson, 2002). *Zbtb32* is a novel zinc finger transcription factor that has bipotential activator and repressor function of downstream genes. *Zbtb32* also represses MHCII function (Yoon *et al.*, 2012), possibly drawing a link to neuroimmune mediators of plasticity including MHCI and B2m, which have both been shown to play a role in restriction of plasticity in the developing and mature brain (Goddard *et al.*, 2007; Shatz, 2009; Syken *et al.*, 2006). Additionally, another complement pathway protein, C4, has also been shown to direct synapse elimination (Sekar *et al.*, 2016), and C4 gain of function is positively associated with risk of schizophrenia, a disease pathologically characterized by dramatic gray matter and synapse loss (Cannon *et al.*, 2002; Glantz and Lewis, 2000). In the limb overuse dataset, C4 binding protein is downregulated, which would result in higher C4 availability and perhaps increased synaptic pruning. This may represent a potential mechanism for synapse formation and stabilization after axonal sprouting.

Other significantly regulated genes include Nat8l, Ube2C, and SOSTDC1. Nat8l is a brain specific metabolite that regulates AMPA receptor expression and regulates neuronal outgrowth through ATP regulation and microtubule stabilization (Toriumi *et al.*, 2013). Ube2c is a hypoxia-inducible ubiquitin-conjugating enzyme. Precedent in the field for ubiquitination as a mechanism for neuronal outgrowth is seen with molecules like NEDD4 (Drinjakovic *et al.*, 2010). We are also interested in control point, second messenger types of molecules because they may help orchestrate the complex cascade of events during post-stroke neural repair. SOSTDC1 is a BMP antagonist expressed in cortex and hippocampus that regulates BMPs 2,4,6,7 during cell proliferation, differentiation, and apoptosis (Clausen *et al.*, 2011; Yanagita, 2005). As a potential TGF- β antagonist, this molecule may also regulate astrocyte response after stroke and growth factor pathways during neural repair (Bialas and Stevens, 2013; Li *et al.*, 2015b; Rustenhoven *et al.*, 2016).

Timing of RNA-Seq study and its implications

The RNA-Seq study captures the transcriptomic landscape of a sprouting neuron 4 weeks after stroke. This time point was chosen for two key reasons. First, previous studies have shown that one month is sufficient for substantial axonal sprouting to occur after stroke (Li *et al.*, 2010; Overman *et al.*, 2012). Moreover, since retrograde tracer was introduced to premotor cortex, we chose a time point in which sprouting axons could reach premotor cortex in order to be traced. Because the RNA-Seq studies are performed at this subacute time point after stroke, the identified candidate genes most likely involved in ongoing axonal sprouting, target finding, and synapse formation and maintenance. This transcriptomic snapshot will not necessarily capture the foremost molecular cues that initiated axonal sprouting upon stroke and limb overuse. In fact, the timing of this study is one of the key variables that sets this work apart from previous molecular profiles of stroke and sprouting (Li *et al.*, 2010), but this boon also comes along with caveats in interpretation.

The most ideal (but technically demanding) approach to mapping time-dependent molecular cascades during this process would be to perform serial time course studies to trace the RSC projection as it grows toward PMC, and RNA-Seq at each time point. However, this approach assumes we can predict the position and trajectory of the growing axon projection, which is difficult given our current biological understanding of the process and chronic-imaging technology. Instead, we tracer-labeled neurons that successfully reach PMC, molecularly profile them, and then used a bioinformatics approach within IPA to generate hypotheses of the key molecules that were activated or turned off upstream. IPA's upstream analysis is based off of prior database and literature knowledge of gene-to-gene relationships within molecular pathways (Kramer *et al.*, 2014). The differentially regulated genes at 4 weeks after limb overuse were queried for common upstream regulators such as transcription factors. We find several fascinating candidates for upstream control. The results (Table 3.3) draw attention to several developmental and/or activity-dependent plasticity genes that may coordinately regulate several DEGs found through RNA-Seq study of the RSC-PMC circuit. One example is the transcription factor *Otx2*, which is involved in opening and closing of plasticity period both in development and adulthood (Beurdeley *et al.*, 2012; Miyata *et al.*, 2012; Sugiyama *et al.*, 2008). These upstream regulators will comprise a portion of the focused mechanistic studies.

The current study finds that RSC-PMC cortical reorganization after stroke is in part molecularly related to those of other learning and memory paradigms, but is more distant from developmental transcriptional profiles. There is a semi-dogmatic statement in the field that “neural regeneration recapitulates development.” This belief is grounded in some basic similarities between the two processes, such as growth cone pathfinding, but even in early work in the field hinted that gene regulation of adult axonal sprouting was unique (Carmichael *et al.*, 2005; Li and Carmichael, 2006). The present study provides further evidence to support this by comparing various molecular

transcriptomes to each other and showing that developmental and injury-induced transcriptomes are in fact quite distinct from each other.

The first phase of this project suggested that one strategy for neural repair after forelimb motor stroke is RSC axonal sprouting to the premotor cortex. The present RNA-Seq study of the RSC-PMC connection points towards a molecularly distinct connection that is vastly enhanced upon behavioral activity of the stroke-affected limb. We combined IPA network and upstream regulator analyses, gene co-expression analyses, and unbiased transcriptome comparisons to complete a deep bioinformatics analysis of candidate genes to prioritize for further study. In the next chapter of studies, we want to further investigate how candidate genes from both statistical comparisons contribute to axonal sprouting and functional rewiring. We hope this line of investigation may lead to molecular or pharmacological entry points of a tunable endogenous mechanism of brain repair after stroke.

Figure 3.1

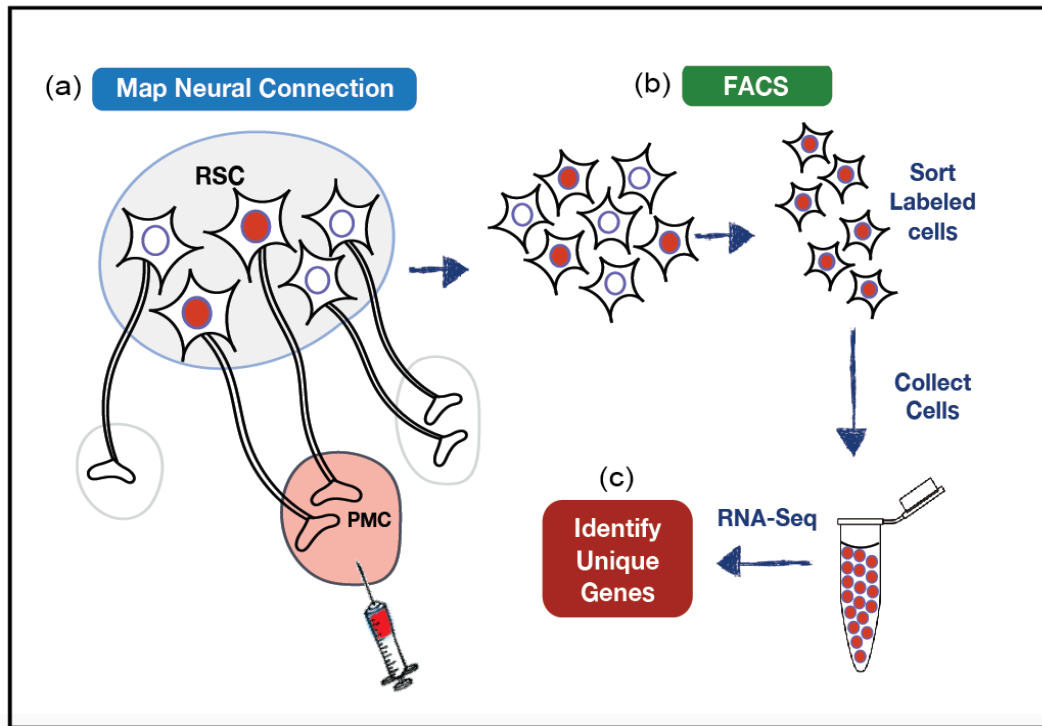


Figure 3.1 Workflow from cell tracing to RNA-sequencing

Following retrograde neuroanatomical tracing from PMC (demarcated in pink oval with injection site), the FG+ neurons (red cell bodies) from RSC are FACS purified for RNA isolation and cDNA library construction. Each treatment group undergoes RNA-sequencing and bioinformatics analysis.

Figure 3.2

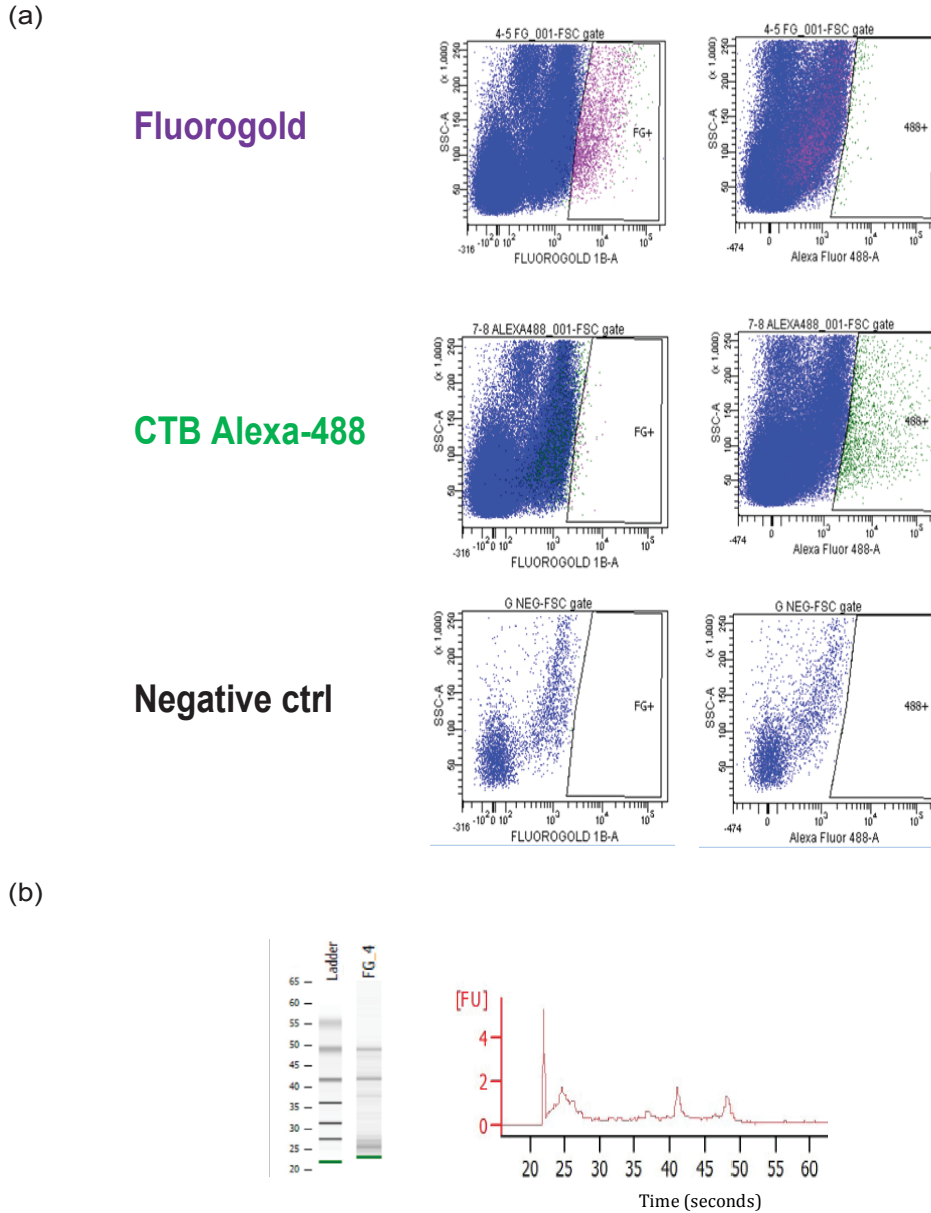


Figure 3.2 FACS purification of Fluorogold-labeled neurons

Fluorogold labeled sensorimotor cortical neurons were isolated and sorted using fluorescence activated cell sorting (FACS). **a)** FG+ cells were collected at a total cell yield similar to that of CTB-Alexa488, a tracer conjugated to a fluorophore commonly used in FACS. Top: FG+ cell collected from 2 pooled animals after 3 weeks of FG uptake. Middle: 2 pooled animals after 3 weeks of CTB-Alexa488 uptake Bottom: FG and Alex 488 gates shown from negative control animals. **b)** RNA integrity from FACS collected cells analyzed with BioAnalyzer 2100. 18S and 28S peaks seen at ~40s and 50s RIN=7.

Figure 3.3

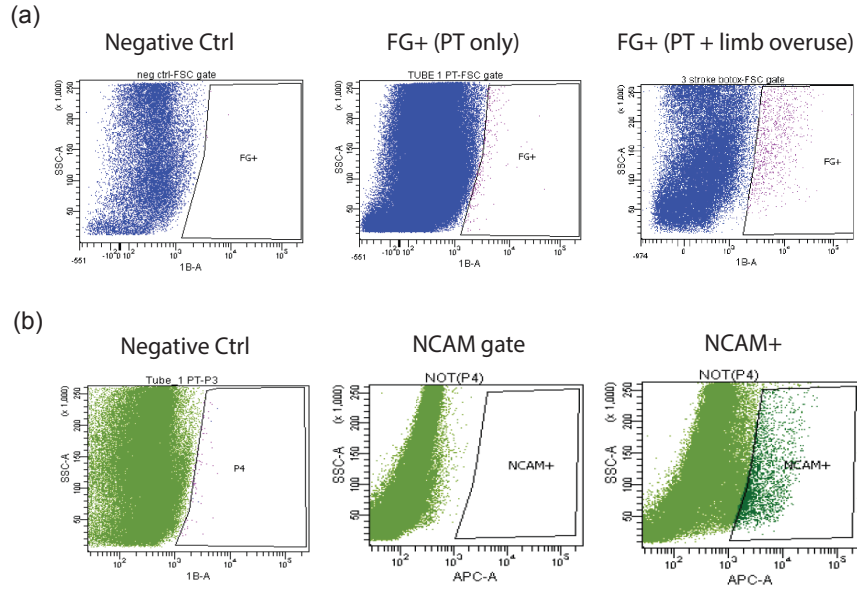


Figure 3.3 FACS purification of RSC FG+ and NCAM+ neurons for RNA-Sequencing

a) FG+ and control NCAM+ groups from retrosplenial cortex were isolated by microdissection and sorted by Fluorescence Activated Cell Sorting (FACS) Top row indicates negative control gate, FG+ neurons in RSC in stroke and stroke + limb overuse groups **b)** RSC control neurons were sorted from RSC FG- cells (left) labeled with neuronal surface marker NCAM conjugated to APC fluorophore. Middle: APC negative control gate and APC+ cell sort for RNA isolation

Table 3.1

Stroke + Limb overuse RSC FG+ cells (n=7)	Stroke only RSC FG+ cells (n=8)	NCAM+ FG- cells in RSC (n=7)
497 (PTBtx1)	1208 (PT1)	14567 NCAM APC (NCAM1)*
1575 (PTBtx2)	2518 (PT2)	20940 NCAM APC (NCAM2)*
1374 (PTBtx3)	4122 (PT3)*	11790 NCAM APC (NCAM3)
654 (PTBtx4)	1108 (PT4)	3539 NCAM APC (NCAM4)
335 (PTBtx5)	168 (PT5)	37345 NCAM APC (NCAM5)
650 (PTBtx6)	614 (PT6)	80814 NCAM APC (NCAM6)
279 (PTBtx7)	406 (PT7)	80814 NCAM APC (NCAM7)
-	580 (PT8)*	-

Table 3.1 Samples collected by FACS purification for RNA-Sequencing

FACS purified cells were collected along into three conditions: FG+ stroke only (n=8) and stroke+limb overuse (n=7), and RSC FG- NCAM+ cells (n=7). *denotes samples that were excluded from bioinformatics analyses due to outlier status on quality control tests or number of uniquely mapped reads. All input material for sequencing samples was quantified and normalized for transcript differential expression analyses.

Figure 3.4

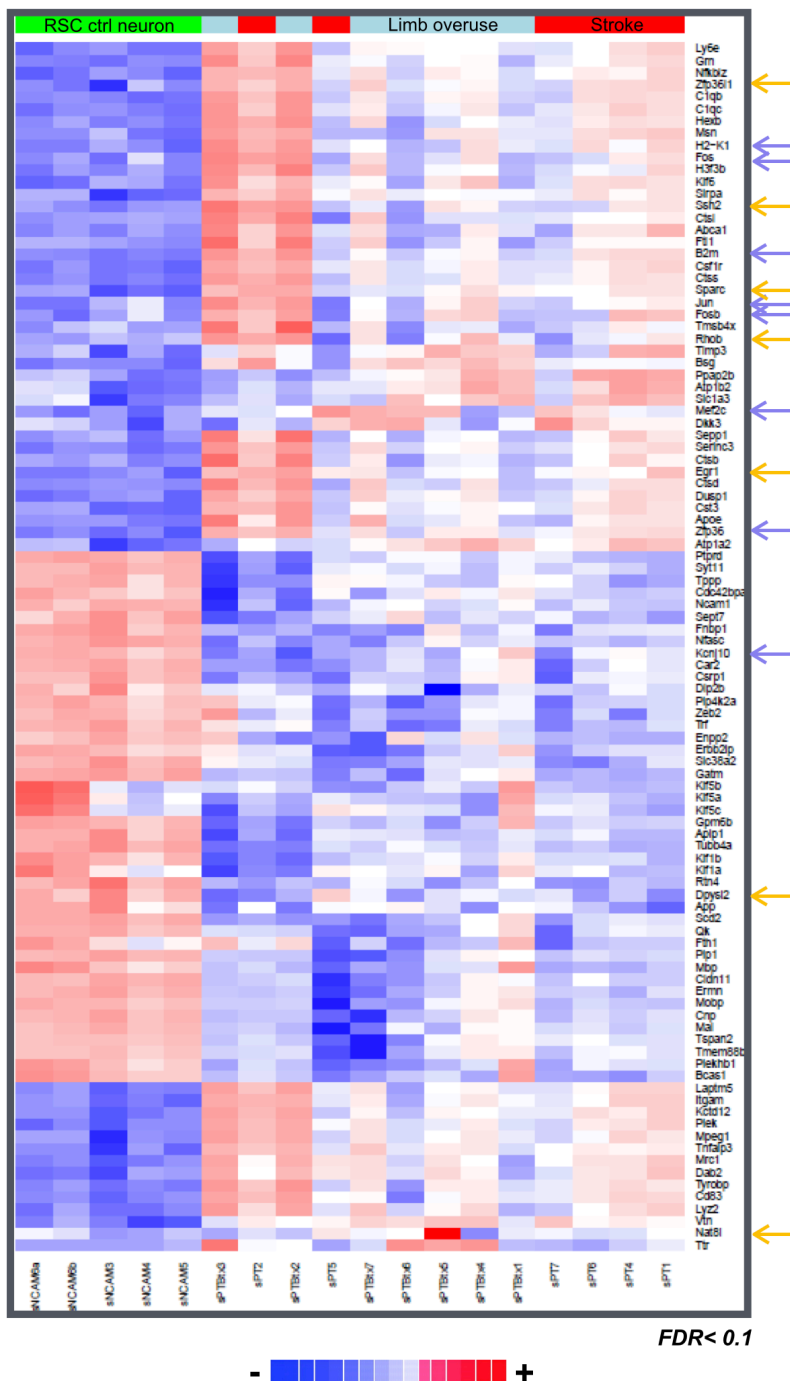


Figure 3.4 Top 100 differentially expressed genes ranked across all comparisons

A ranked clustered display of top differentially regulated genes across FG+ stroke only (green) and stroke+limb overuse (blue), and RSC FG- NCAM+ cells (red). A subset of candidates identified as activity-induced (purple arrow) for neuronal growth-related (gold arrow) genes. Hierarchical clustering across all RNA-Seq samples performed at FDR <0.1.

Table 3.2 160 genes differentially regulated by limb overuse after stroke

Gene	Refseq	entrez	Chromosome	Description	StrokesStroke+overuse_logFC	P-value
Olfir191	NM_001011807	258035	chr16	olfactory receptor 191	-1.442769487.5	0.001079666
4933427E11RIK	NR_033197	66769	chr15	RIKEN cDNA 4933427E11 gene	-1.44269486	0.000833775
Pad16	NM_153106	242726	chr4	peptidyl arginine deiminase, type VI	-1.44269485.6	0.000834944
A330050F15RIK	NM_001145192	320722	chr17	RIKEN cDNA A330050F15 gene	-1.44269485.4	0.002749637
Tr	NM_013697	22139	chr18	transthyretin	-8.46326949	1.05E-08
Olfir394	NM_147007	259009	chr11	olfactory receptor 394	-7.857542154	0.0033866217
4921539E11RIK	NM_027612	70941	chr4	RIKEN cDNA 4921539E11 gene	-7.693447396	0.004459806
Slc35d3	NM_029529	76157	chr10	solute carrier family 35, member D3	-7.622299097	0.002415928
Sostdc1	NM_025312	66042	chr12	scrostin domain containing 1	-5.912508415	0.001040435
Gfof2	NM_027469	70575	chr8	glucose-fructose oxidoreductase domain containing 2	-5.40996039	0.00319749
41336	NM_177115	320253	chr18	membrane-associated ring finger (C3HC4) 3	-5.001532496	0.004295512
Nat8l	NM_001001985	269642	chr5	N-acetyltransferase 8-like	-4.097708127	0.0000347
Ube2c	NM_026785	68612	chr2	ubiquitin-conjugating enzyme E2C	-3.962358245	0.001612134
Fcna	NM_007995	14133	chr2	ficollin A	-3.670104932	0.004525755
4930478L05RIK	NA	NA	NA	NA	-3.549176119	0.001821229
Zfp503	NM_145459	218820	chr14	zinc finger protein 503	-3.474229412	0.000234491
Gjrc2	NM_175452	118454	chr11	gap junction protein, gamma 2	-3.463530471	0.000243175
Gdpgp1	NA	NA	NA	NA	-3.421595556	0.001269985
Top2a	NM_011623	21973	chr11	topoisomerase (DNA) II alpha	-3.343318855	0.001970863
Lrfd4	NM_153388	225875	chr19	leucine rich repeat and fibronectin type III domain containing 4	-3.05602757	0.001923828
LOC100642166	NA	NA	NA	NA	-2.897612752	0.003672824
Polce2	NM_029620	76477	chr9	procollagen C-endopeptidase enhancer 2	-2.895499055	0.001946413
Eme2	NM_001163102	193838	chr17	essential meiotic endonuclease 1 homolog 2 (s. pombe)	-2.886416291	0.000395842
Snta1	NM_009228	20648	chr2	synthrophin, acidic 1	-2.792393067	0.001052504
Trim59	NM_025863	66949	chr3	tripartite motif-containing 59	-2.745620051	0.000603
Zfp52	NM_144515	22710	chr17	zinc finger protein 52	-2.716162276	0.003627301
Bcas1	NM_029815	76960	chr2	breast carcinoma amplified sequence 1	-2.694884277	0.000258388
Col9a3	NM_009936	12841	chr2	collagen, type IX, alpha 3	-2.443037001	0.002452595
Adssl1	NM_007421	11565	chr12	adenylosuccinate synthetase like 1	-2.423980023	0.002405582
Tmem98	NM_029537	103743	chr11	transmembrane protein 98	-2.423371004	0.002844103
Fbx19	NM_172748	233902	chr7	F-box and leucine-rich repeat protein 19	-2.291692312	0.003707339
Mbp	NM_010777	17196	chr18	myelin basic protein	-2.250308291	0.001109213
Slc35c2	NR_045544	228875	chr2	solute carrier family 35, member C2	-2.033653091	0.004831504
Blvrb	NM_144923	233016	chr7	biliverdin reductase B (flavin reductase (NADPH))	-1.951520711	0.003529416
Wdfy2	NM_175546	268752	chr14	WD repeat and FYVE domain containing 2	-1.908772916	0.002633506
Pagr1a	NA	NA	NA	NA	-1.867094705	0.004670354
Rpap2	NM_144911	231571	chr5	RNA polymerase II associated protein 2	-1.844765827	0.002630621
BC003965	NM_183150	214489	chr17	cDNA sequence BC003965	-1.768065987	0.001009181
Fbxw5	NM_013908	30839	chr2	F-box and WD-40 domain protein 5	-1.653537528	0.003710955
Enpp2	NM_015744	18606	chr15	ectonucleotide pyrophosphatase/phosphodiesterase 2	-1.599503459	0.001463046
Pim3	NM_145478	223775	chr15	proviral integration site 3	-1.534311417	0.004818908
Nup62	NM_053074	18226	chr7	nucleoporin 62	-1.53007621	0.003079011
Adipor2	NM_197985	68465	chr6	adiponectin receptor 2	-1.302541808	0.000985398
TuH5	NM_001081423	320244	chr12	tubulin tyrosine ligase-like family, member 5	-1.257836255	0.003788239
Spcc2	NM_025668	66624	chr7	signal peptidase complex subunit 2 homolog (s. cerevisiae)	-1.175476323	0.004558388
061003106RIK	NM_020003	56700	chr3	RIKEN cDNA 061003106 gene	-1.166369491	0.00398978
Lsm14a	NM_025948	67070	chr7	LSM14 homolog A (SCD6, S. cerevisiae)	-1.001254701	0.003095939
Trim32	NM_053084	69807	chr4	tripartite motif-containing 32	1.26793944	0.002334432
Gri1	NM_008169	14810	chr2	glutamate receptor, ionotropic, NMDA1 (zeta 1)	1.352006556	0.00374562
Bai2	NM_173071	230775	chr4	brain-specific angiogenesis inhibitor 2	1.462188124	0.002877077
Zfp597	NM_001033159	71063	chr16	zinc finger protein 597	1.832175452	0.004894082
Atg16l1	NM_029846	77040	chr1	autophagy-related 16-like 1 (yeast)	1.85904119	0.004149477
Hectd2	NM_172637	226098	chr19	HECT domain containing 2	1.889503758	0.002191568
Cttn	NM_007803	13043	chr7	contactin	1.994087379	0.001131758

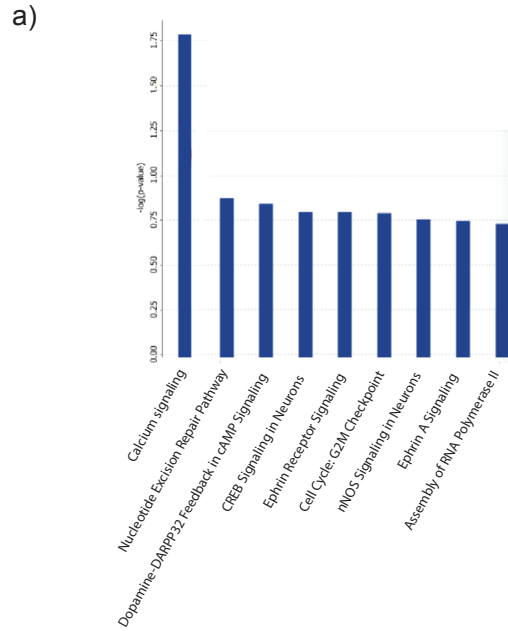
Table 3.2 (cont'd)

Ppp1r26	NA	NA	NA	NA	NA	2.042909954	0.003946908
Camk1g	NM_144817	215303	chr1	calcium/calmodulin-dependent protein kinase I gamma	2.16759078	0.004074568	
Ralgps1	NM_175211	241308	chr2	Ral GEF with PH domain and SH3 binding motif 1	2.40034737	0.000276219	
A730017C20Rik	NR_033765	225583	chr18	RIKEN cDNA A730017C20 gene	2.43871376	0.000502251	
Ysk4	NM_0111737	22625	chr1	Yeast Sps1/Ste20-related kinase 4 (S. cerevisiae)	2.354394419	0.004388897	
Cone5	NM_153166	240058	chr17	copine V	2.371759789	0.000668679	
Epha10	NM_177671	230735	chr4	Eph receptor A10	2.410729403	0.00301389	
Synpo2	NM_080451	118449	chr3	synaptopodin 2	2.483895245	0.001963509	
Synpr	NM_028052	72003	chr14	synaptoporin	2.48414468	0.003807823	
Adamts3	NM_177872	330119	chr5	a disintegrin-like and metalloproteinase (reprolysin type) with thrombospondin type 1 motif, 3	2.547165951	0.003917297	
Cmya5	NM_023821	76469	chr13	cardiomyopathy associated 5	2.73269499	0.001632848	
Lsm11	NM_028185	72290	chr11	U7 snRNP-specific Sm-like protein LSM11	2.860102944	0.000992397	
Zfp61	NM_009561	22719	chr7	zinc finger protein 61	2.86681317	0.003929809	
Stc1	NM_009285	20855	chr14	stanniocalcin 1	2.897793032	0.004139338	
Wdr85	NM_026044	67228	chr2	WD repeat domain 85	2.929356437	0.000502541	
Lrrc55	NM_001033346	241528	chr2	leucine rich repeat containing 55	2.998949099	0.001236361	
Polr1j	NM_0111293	20022	chr5	polymerase (RNA) II (DNA directed) polypeptide J	3.12070645	0.000141911	
4921531C2Rik	NA	NA	NA	NA	3.254215407	0.002130541	
Inpp5j	NM_172439	170835	chr11	inositol polyphosphate 5-phosphatase J	3.369617398	0.000308665	
Neurod1	NM_010894	18012	chr2	neurogenic differentiation 1	3.495986342	0.004067563	
Adamts17	NM_001033877	233332	chr7	a disintegrin-like and metalloproteinase (reprolysin type) with thrombospondin type 1 motif, 17	3.653336853	0.001637849	
Dach1	NM_007826	13134	chr14	dachshund 1 (Drosophila)	3.75568692	0.0000874	
Radil	NM_178702	231858	chr5	Ras association and DIL domains	3.859259905	0.002121058	
4922501L14Rik	NM_175176	209601	chr3	RIKEN cDNA 4922501L14 gene	3.878474093	0.000478264	
Nvap1	NA	NA	NA	NA	4.061143455	0.000295942	
Tnc	NM_011607	21923	chr4	tenascin C	4.132541706	0.001053378	
Myo15	NM_182698	17910	chr11	myosin XV	4.207652524	0.003860166	
Imp22	NM_174876	224224	chr16	interphotoreceptor matrix proteoglycan 2	4.36940237	0.001833476	
Pcdh9	NM_138661	192161	chr18	protocadherin alpha 9	4.429753714	0.001779592	
Mir1933	NA	NA	NA	NA	4.633483703	0.002971929	
Gm5177	NA	NA	NA	NA	4.756157201	0.002759478	
Zfp618	NM_028326	72701	chr4	zinc fingerprotein 618	4.775996696	0.00299254	
Kazalid1	NM_178929	107250	chr19	Kazal-type serine peptidase inhibitor domain 1	4.95876115	0.002202695	
Rsc1a1	NM_023544	69994	chr4	regulatory solute carrier protein, family 1, member 1	5.040086674	0.001334864	
C130036L24Rik	NR_015507	319336	chr1	RIKEN cDNA C130036L24 gene	5.045266635	0.002727875	
Zbtb32	NM_021397	58206	chr7	zinc finger and BTB domain containing 32	5.15769153	0.003460749	
1700034H15Rik	NR_030669	98736	chr1	RIKEN cDNA 1700034H15 gene	5.370646507	0.002046694	
D330050G23Rik	NA	NA	NA	NA	5.428677947	0.000388762	
2010002M12Rik	NM_053217	112419	chr19	RIKEN cDNA 2010002M12 gene	5.457335621	0.004004555	
Kcnj5	NM_010605	16521	chr9	potassium inwardly-rectifying channel, subfamily J, member 5	5.687508492	0.00282544	
6820408C15Rik	NM_177656	228778	chr2	RIKEN cDNA 6820408C15 gene	5.811647882	0.002583177	
Atp6ap1l	NM_001145879	435376	chr13	ATPase, H+ transporting, lysosomal accessory protein 1-like	6.063566277	0.002552204	
Ostb	NM_178933	330962	chr9	organic solute transporter beta	6.256983705	0.002832435	
Gm6150	NA	NA	NA	NA	6.405373426	0.002187098	
Lrrd1	NA	NA	NA	NA	6.785846889	0.003625186	
Rad51ap1	NM_009013	19362	chr6	RAD51 associated protein 1	6.792044548	0.003194039	
Bfsp1	NM_109751	12075	chr2	beaded filament structural protein 1, in lens-CP94	7.039153108	0.000793467	
Al661453	NM_145489	224833	chr17	expressed sequence Al661453	7.068187406	0.001908054	
Gm9839	NA	NA	NA	NA	7.430355865	0.002557467	
Tmem171	NM_001025606	380863	chr13	transmembrane protein 171	7.525075373	0.001834815	
Atp8b3	NM_026094	67331	chr10	ATPase, class I, type 8B, member 3	7.578085496	0.000970488	
Tnnc2	NM_009394	21925	chr2	troponin C2, fast	7.669449269	0.002686018	
Rtp1	NM_001004151	239766	chr16	receptor transporter protein 1	7.721787237	0.001309642	
Lipk	NM_172837	240633	chr19	lipase, family member K	7.897119807	0.002207287	
Insm2	NM_020287	56856	chr12	insulinoma-associated 2	8.016306606	0.001623842	

Table 3.2 (cont'd)

Sprze	NM_011471	20759	chr3	small proline-rich protein 2E	8.116218341	0.002781569
1700092M07Rik	NA	NA	NA	NA	8.185156534	0.003773701
Gm5766	NR_003628	436332	chr16	ribosomal protein L7a pseudogene	8.198924506	0.000274397
4930526D03Rik	NM_199023	277496	chr2	RIKEN cDNA 4930526D03 gene	8.223880652	0.003656489
Fam169b	NM_001013811	434197	chr7	family with sequence similarity 169, member B	8.349771393	0.001326556
C4bp	NM_007576	12269	chr1	complement component 4 binding protein	8.400674518	0.001105087
F630042J09Rik	NA	NA	NA	NA	144269483.3	0.00286824
Cyp4f39	NM_177307	320997	chr17	cytochrome P450, family 4, subfamily f, polypeptide 39	144269483.3	0.003859366
9430069I07Rik	NA	NA	NA	NA	144269483.3	0.004776829
Chst5	NM_019950	56773	chr8	carbohydrate (N-acetyl)glucosamine 6-O) sulfotransferase 5	144269483.5	0.004893121
220002D01Rik	NM_028179	72275	chr7	RIKEN cDNA 220002D01 gene	144269483.7	0.004653997
Gnat1	NM_008140	14685	chr9	guanine nucleotide binding protein, alpha transducing 1	144269483.7	0.003991312
1700015E13Rik	NM_001039593	76925	chr1	RIKEN cDNA 1700015E13 gene	144269483.7	0.004206809
Tpo	NM_009417	22018	chr12	thyroid peroxidase	144269483.9	0.004488155
Ktbd13	NA	NA	NA	NA	144269484.1	0.004213706
1810020O05Rik	NA	NA	NA	NA	144269484.3	0.00246315
Gm10731	NR_045392	1E+08	chr3	predicted gene 10731	144269484.3	0.003306954
Gm6642	NA	NA	NA	NA	144269484.4	0.001945099
4930565D16Rik	NA	NA	NA	NA	144269484.5	0.004699131
Oas1h	NM_145228	246729	chr5	2'-5' oligoadenylate synthetase 1H	144269484.6	0.001997667
Nimbr	NM_008703	18101	chr10	neurexin B receptor	144269484.6	0.001726999
Vsig8	NR_027644	240916	chr1	V-set and immunoglobulin domain containing 8	144269484.7	0.004565813
Olf495	NM_146364	258361	chr7	olfactory receptor 495	144269484.7	0.003537683
Rpl11	NM_146246	271209	chr14	retinitis pigmentosa 1 homolog (human)-like 1	144269484.7	0.00151907
Lrrc43	NM_001033461	381741	chr5	leucine rich repeat containing 43	144269484.8	0.004172545
Gm6260	NA	NA	NA	NA	144269484.8	0.003733512
9430018G01Rik	NA	NA	NA	NA	144269485.1	0.000218137
Olf658	NM_147049	259051	chr7	olfactory receptor 658	144269485.2	0.002053691
Sic36a3	NM_172258	215332	chr11	solute carrier family 36 (proton/amino acid symporter), member 3	144269485.3	0.002134895
Olf330	NM_146879	258879	chr11	olfactory receptor 330	144269485.3	0.00401317
4930543E12Rik	NA	NA	NA	NA	144269485.3	0.001520434
Hoxb1	NM_008266	15407	chr11	homeobox B1	144269485.3	0.00056371
Btnl4	NA	NA	NA	NA	144269485.5	0.000265755
4930547E14Rik	NA	NA	NA	NA	144269485.5	0.000833347
Mir695	NR_030475	735287	chr2	microRNA 695	144269485.6	0.000489159
Olf786	NM_146549	258542	chr10	olfactory receptor 786	144269485.6	0.003507331
Wap	NM_011709	22373	chr11	whey acidic protein	144269485.6	0.004677216
Gm5136	NM_203660	368203	chr10	predicted gene 5136	144269485.7	0.000776623
Ferd3l	NM_033522	114712	chr12	Fer3-like (Drosophila)	144269485.7	0.001407268
4930442L01Rik	NR_015596	67583	chr3	RIKEN cDNA 4930442L01 gene	144269485.8	0.000541528
Lg1	NM_029796	76905	chr17	leucine-rich alpha-2-glycoprotein 1	144269485.9	0.000165391
Gm5925	NA	NA	NA	NA	144269485.9	0.002497241
Trim2	NM_001160412	622117	chr8	tripartite motif family-like 2	144269485.9	0.003011427
Olf517	NM_001011846	258136	chr7	olfactory receptor 517	144269486	0.002425243
Nrl	NM_008736	18185	chr14	neural retina leucine zipper gene	144269486.1	0.000893404
Zfp663	NA	NA	NA	NA	144269486.2	0.000852544
Olf883	NM_146419	258414	chr9	olfactory receptor 883	144269486.3	0.001197032
Olf148	NM_146505	258498	chr9	olfactory receptor 148	144269486.6	0.000123966
Syce3	NA	NA	NA	NA	144269486.7	0.001041826
Casp14	NM_009809	12365	chr10	caspase 14	144269487.2	0.000214112
Gm19990	NA	NA	NA	NA	144269488.2	0.00000564

Figure 3.5



b)

Canonical Pathways	
CREB signaling in neurons	CAMK1G +2.168, GRIN1 +1.352, TNNC2 +7.669 UA: CREBBP (8.46E-03)
Ephrin Receptor signaling	EPHA10 +2.4, GNAT1 +20, GRIN1 +1.352
Calcium signaling	CAMK1G +2.168, GRIN1 +1.352, TNNC2 +7.669
Top Associated Networks	
1. Cellular development, cell death and survival, cancer	
2. Gene Expression, Cellular Growth and Proliferation, DNA Replication, Recombination and Repair	
3. Embryonic Development, organ development, organismal development	

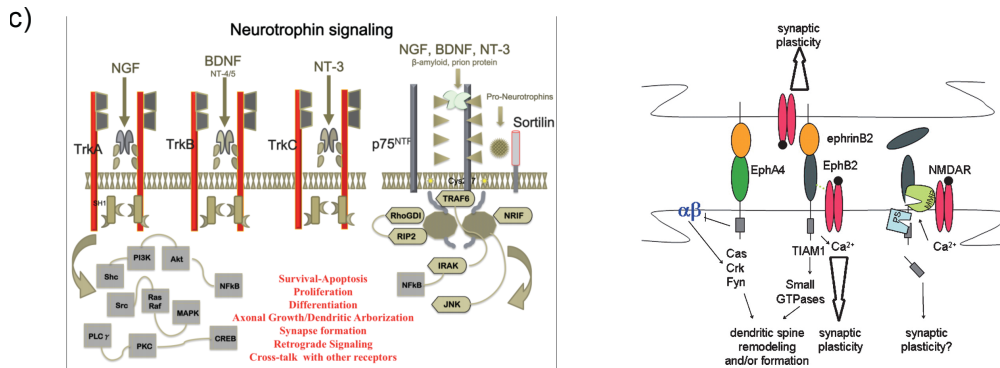


Figure 3.5 Ingenuity Pathway Analysis (IPA) of differentially regulated genes in RSC-PMC

a) Canonical pathways of differentially regulated gene comparison between stroke vs. stroke + botox (160 genes, $p < 0.005$). The Ephrin, CREB, and Calcium signaling pathways are of particular relevance as they signal toward growth-related and activity-dependent processes associated with limb overuse **b)** Three canonical pathways of interest and the associated genes that were differentially regulated **c)** Left: one of the growth-related pathways includes nerve growth factor (NGF) signaling, which acts upstream of neuronal outgrowth and other cell-cycle promoting genes Right: Ephrin signaling, another canonical pathway associated with limb overuse, occurs through tyrosine kinase bidirectional signaling. Interaction of ligand and receptor can lead to a variety of pre- and post-synaptic changes in growth and plasticity.

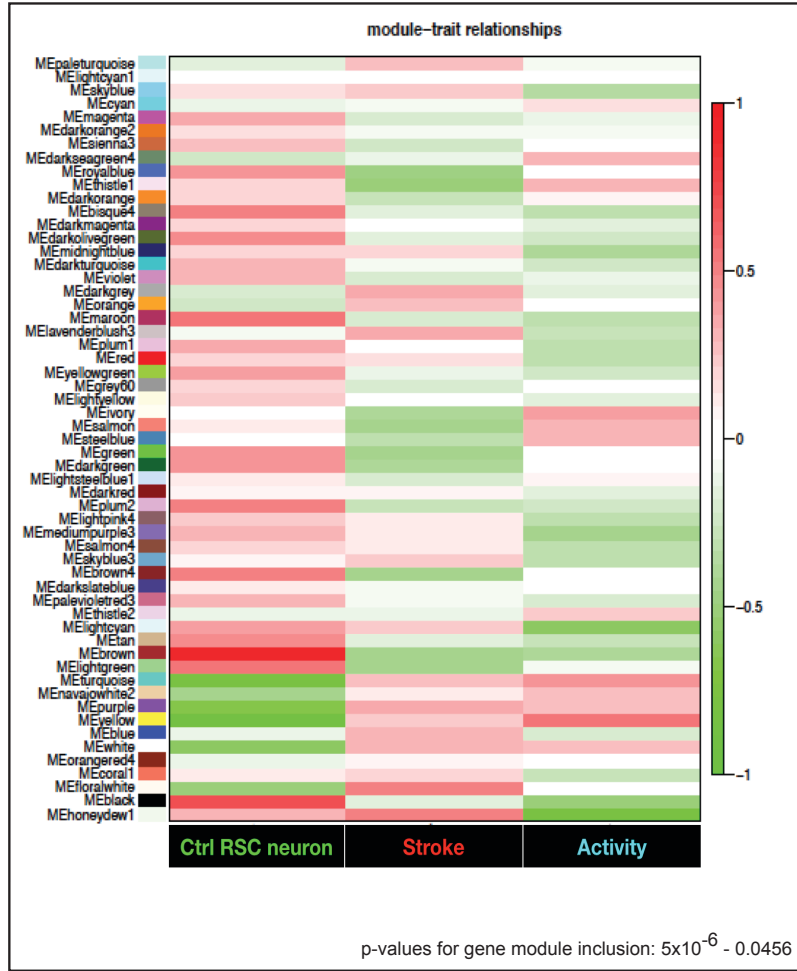
Table 3.3

Upstream Regulator	Downstream genes regulated by limb overuse	Known roles
NeuroG3	INSM2, NEUROD1	<ul style="list-style-type: none"> Initiates transcriptional activation of NEUROD1 Works together with Nkx2.2 to promote neurogenesis
NeuroD1	INSM2, NEUROD1	<ul style="list-style-type: none"> Associates w/ chromatin to enhancer regulatory elements in genes encoding transcriptional regulators of neurogenesis Basic HLH TF, transcriptional activator of genes with DNA sequence E-box Regulates expression of insulin gene; associates with p300/CBP txn coactivator
YY1	COL9A3, TOP2A, RAD51AP1, TNNC2	<ul style="list-style-type: none"> TF of the GLI-Kruppel class of zinc finger proteins: transcriptional repression and activation (“Yin-Yang 1”) Direct HDACs and HATS for histone modification Smad/YY1-recognized by BMP2, acts as transcriptional regulatory module in GAT promotor Critical repressor of brain MMP-9 Regulates peripheral myelination in Schwann cells YY2 is a related TF and increases neurite outgrowth in hippocampal neurons
CREBBP	CAMK1G, GRIN1, NEUROD1	<ul style="list-style-type: none"> Binds to phosphorylated CREB activating cAMP-responsive genes downstream CREB signaling in neurons important for learning and memory, increases axonal sprouting in spinal neurons
Otx2	ENPP2, NRL	<ul style="list-style-type: none"> TF in brain, craniofacial, sensory organ development Constrains developmental and adult cortical plasticity Choroid plexus derived and remains active in GABA cells in mature forebrain
Crx	GNAT1, NEUROD1, NRL	<ul style="list-style-type: none"> Differentiation of photoreceptor cells Regulation of immediate early genes in suprachiasmatic nucleus
Key: DOWN UP ; TF= Transcription Factor		

Table 3.3 Upstream analysis of genes differentially regulated by limb overuse

Figure 3.6

(a)



(b)

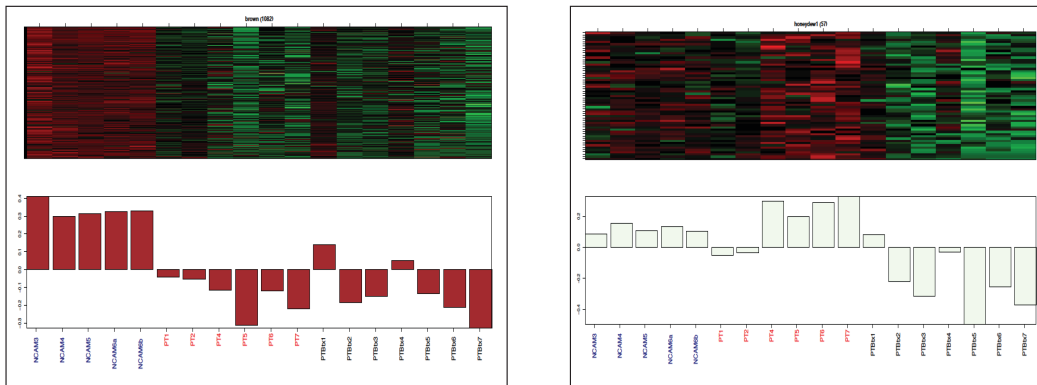


Figure 3.6 WGCNA gene modules

a) Gene modules were generated across samples from the three conditions: Ctrl RSC neuron, FG+ cells from stroke and stroke + limb overuse group. Each module represents coordinated gene expression along condition lines. 11 modules, turquoise, purple, yellow, bisque4, maroon, plum2, brown4, tan, brown, light green, and black were significantly differentially regulated between RSC FG+ neurons versus RSC NCAM+ neurons. When comparing RSC-PMC neurons from limb overuse groups with those from stroke alone, four additional modules were significant: thistle, floral white, and white. Module *p*-values were between 1×10^{-6} and 0.0456. **b)** Example modules brown and honeydew1 are shown by individual replicates (Blue text IDs= RSC NCAM+ samples; Red text IDs= RSC FG+ neurons from stroke only; Black text ID= RSC FG+ neurons from stroke+limb overuse. In the brown module, RSC FG+ neurons from stroke and stroke+limb overuse groups significantly upregulated genes within this module when compared to the control NCAM+ neurons. In contrast, honeydew 1 is a module in which the stroke only group upregulated module genes relative to the other two conditions, though this comparison did not reach statistical significance and was not further considered.

Figure 3.7

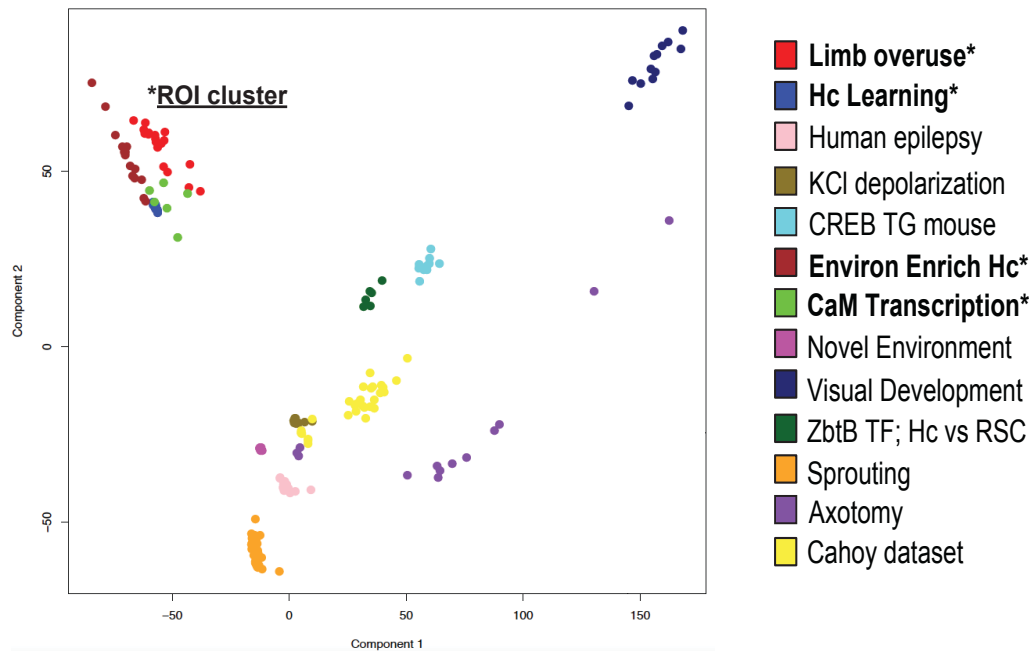


Figure 3.7 Transcriptome overlay analysis

Transcriptomes representing different activity-dependent, injury-related, and developmental states were compared against genes differentially regulated by limb overuse after stroke. The upper left corner indicates a statistical clustering of three other gene sets with genes from the post-stroke limb overuse RSC-PMC connection. These include a hippocampal learning task, calcium calmodulin transcription, and environmental enrichment. Full descriptions of the various plasticity paradigms are found in Table 3.4

Table 3.4

Study	GSE number	Method	Species	Publication	Keyword Identifier
Synaptic plasticity and memory (hc) after learned task	GSE44229	RNA-seq	Mouse	Vogel-Ciernia A et al., <i>Nat Neurosci</i> , 2013	Hc learning
Mesial Temporal Lobe Epilepsy: humans	GSE25453	Microarray	Human	Venugopal et al., <i>J Proteomics Bioinform</i> , 2012	Human Epilepsy
KCl depol 4hrs DIV7 primary neuronal culture	GSE11256	Microarray	Mouse	Lin Y et al., <i>Nature</i> , 2008	KCl depolarization
VP16-CREB TG mouse, constitutively active CREB	GSE3965	Microarray	Mouse	Barco A et al., <i>Neuron</i> , 2005	Const CREB TG Mouse
Environmental Enrichment Hippocampus 2wks	GSE30880	Microarray	Mouse	Lopez, Atalaya et al., <i>EMBO J</i> , 2011	Environ Enrich Hc 2wks
CaM regulated transcriptome	GSE23796	Microarray	Mouse	Pang et al., <i>J Biol Chem</i> , 2010	CaM Transcription
Novel Environment Rat Forebrain 3hrs	GSE13539	Microarray	Rat	Flavell et al., <i>Neuron</i> , 2008	Novel Env Forebrain
Mouse V1 transcriptome after deprivation DR or MD	GSE4537	Microarray	Mouse	Tropea et al., <i>Nat Neurosci</i> , 2006	Visual Development
ZBtb20 repression of genes that specifies Hc CA1 from RSC/subiculum	GSE38837	Microarray	Mouse	Nielsen JV et al., <i>Cereb Cortex</i> 2014	Zbtb20 TF; Hc vs RSC
Sprouting Transcriptome after stroke; young and aged rat	GSE24442	Microarray	Rat	Li et al., <i>Nat Neurosci</i> , 2010	Sprouting
mRNAs in uninjured and injured rat cortical axons isolated at DIV13	GSE11730	Microarray	Rat	Taylor et al., <i>J Neurosci</i> , 2009	Axotomy
purified cell types astrocytes, neurons, oligodendrocytes from mature and developing brain	GSE11764	Microarray	Mouse	Cahoy et al., <i>J Neurosci</i> , 2008	Cahoy

Table 3.4 Expression profile sources used for transcriptome overlap analyses

3.5 Methods

FACS

Tissue and cell preparation:

Male C57BL/6 mice age 4 months were anesthetized with isoflurane, decapitated, and cortical tissue removed from underlying white matter over ice. Neuroanatomical retrosplenial cortex (RSC) microdissection was guided by cortical flat maps and performed using a #11 surgical scalpel and tissue punch to remove the posteromedial 8mm³ of tissue from the ipsilesional hemisphere. Cortical tissue was enzymatically digested and triturated based on a published protocol (Brewer and Torricelli, 2007). Briefly, cortical tissue was equilibrated for 8 minutes and digested for 30 min at 30°C and 190 rpm in 6mL papain solution (12mg/mL). Complete Hibernate buffer (BrainBits) was used to maintain neural metabolites and pH during tissue dissection and digestion. Glutamate antagonists kynurenic acid and AP5 were added to minimize excitotoxicity, as previously described in (Ozdinler and Macklis, 2006). Tissue was triturated into 6mL suspension and loaded onto density gradient column (4mL of 12.4% OptiPrep in Hibernate), and centrifuged for 15min at 900g at 22°C. The bottom 5 mL was collected and washed 2x at 400g for 5 min each before antibody staining. Two cortices were pooled for each FACS sample. 44 animals were coupled for a total of 22 samples across the 3 experimental groups for FACS analysis: 1) Stroke only FG+ ($n=8$) 2) Stroke+limb overuse FG+ ($n=7$) and 3) FG- NCAM+ RSC neurons ($n=7$).

Cell sorting and RNA extraction:

Prior to flow cytometry, cell suspensions for group 3 animals were immunostained for neuronal surface marker NCAM (Mouse; NCAM-1/CD56 Allophycocyanin MAb, 10uL antibody/10⁶ cells, FAB7820A R&D Systems,) for 20 min at 25°C, and washed twice with HABG. Samples were maintained on ice during FACS isolation. APC sort gates were set using positive and

negative controls prior to neuron sorting. Neurons were collected via FACS (FACsARIA, Becton Dickinson, UCLA FACS Core) directly into 400uL lysis buffer for RNA isolation. Total RNA was extracted using RNA-Microprep kit (Zymo-Research) and eluted into 7uL ddH₂O. RNA-quality was verified (RIN>7) on an Agilent Bioanalyzer. RNA libraries were prepared using a NuGen Ovation Ultra Low Mass kit for paired-end 2x50 RNA-sequencing (HiSeq2000, UCLA UNGC core).

RNA-Seq and Bioinformatics of other neuronal transcriptomes

Total RNA was purified (Quick RNA Microprep, Zymo Research, Irvine, CA) from 22 samples of FACS-isolated cells from the following conditions: RSC FG+ cells from stroke+limb overuse (n=7), RSC FG+ cells from stroke only (n=8) and RSC FG- NCAM+ cells (n=7). Each sample consisted of two pooled cortices from the same condition. An RNA Integrity Number (RIN) reading of >7 ensured high quality input RNA (Agilent, Santa Rosa, CA). Total RNA was amplified and converted into double-stranded DNA, which is typically between 200 and 300 bp (Ovation RNA-Seq System v2, Nugen, San Carlos, CA) that was then processed with the Ovation UltraLow kit (NuGen). RNA libraries were prepared using a NuGen Ovation Ultra Low Mass kit for paired-end 2x50 RNA-sequencing (HiSeq2000, UCLA ICNN core). After cDNA library preparation (Encore NGS Library System I, NuGen), amplified double-stranded cDNA was fragmented into 300 bp (Covaris-S2, Woburn, MA). DNA fragments (200 ng) were end-repaired to generate blunt ends with 5' phosphate and 3' hydroxyls and adapters ligated. The purified cDNA library products were evaluated using the Agilent Bioanalyzer (Santa Rosa, CA) and diluted to 10 nM for cluster generation in situ on the HiSeq paired-end flow cell using the CBot automated cluster generation system.

All libraries were sequenced using an Illumina HiSeq 2000 sequencer across 8 lanes of 50 bp-paired-end sequencing, corresponding to 3 samples per HiSeq 2000 lane. After demultiplexing, we

obtained between 52 and 75 million reads per sample. Quality control was performed on base qualities and nucleotide composition of sequences. Alignment to the *M. musculus* (mm9) refSeq (refFlat) reference gene annotation was performed using the STAR spliced read aligner with default parameters. Additional QC was performed after the alignment to examine: the level of mismatch rate, mapping rate to the whole genome, repeats, chromosomes, and key transcriptomic regions (exons, introns, UTRs, genes). Four samples (NCAM1, PT8, NCAM2, PT3) did not meet threshold for quality and were excluded from downstream analysis. Total counts of read-fragments aligned to candidate gene regions were derived using HTSeq program (www.huber.embl.de/users/anders/HTSeq/doc/overview.html) and used as a basis for the quantification of gene expression. Only uniquely mapped reads were used for subsequent analyses. Across the samples >25% of the annotated genes have been detected by at least 50 reads. Following alignment and read quantification, we performed quality control using a variety of indices, including sample clustering, consistency of replicates, and average gene coverage.

Differential expression analysis was performed using the EdgeR Bioconductor package (Robinson et al., '10), and differentially expressed genes were selected based on False Discovery Rate (FDR Benjamini Hochberg-adjusted p values) estimated at ≤ 0.1 (or 10% FDR). 5 pooled samples each from PT and NCAM, and 8 samples PTBtx were compared for all downstream statistical analyses. Clustering and overlap analyses were performed using Bioconductor packages within the statistical environment R (www.r-project.org/).

Genes that were differentially expressed false discovery rate (FDR) < 10% were submitted to Cluster 3.0 for hierarchical clustering analysis (Euclidian distance, centroid linkage clustering) and visualized using Java TreeView. Differentially expressed genes were further analyzed by molecular pathway analysis and canonical signaling systems (IPA, Redwood City, CA). Briefly, for IPA analyses the genes regulated in each specific category, filtered to only include genes $\leq 10\%$ FDR, where

compared to all genes known to be involved in a given molecular pathway or canonical signaling system in a large curated database of molecular interactions. Fisher's exact p value was calculated by IPA to determine a statistically different relationship of a data set in the NCAM and stroke+/-limb overuse cortical transcriptomes to chance representation of these genes. For the upstream analysis there are 4 values that go into the Fisher's exact p-value calculation with Benjamini Hochberg correction for multiple comparisons.

For genome-wide association testing in transcriptome overlay studies, individual data from .cell, SRA or Excel files was obtained for each experiment (Table 3.4). The gene symbol was located for each probe and average expression computed for duplicated genes. The data was combined with RNA-Seq data from this study and variance stabilization transformation normalization performed.

Weighted Gene Co-expression Network Analysis

Gene co-expression analyses were performed using the R package WGCNA (Langfelder and Horvath, 2008) to construct coordinated gene expression networks, as previously described (Oldham *et al.*, 2006; Zhang and Horvath, 2005). Modules were identified based on coordinated changes in expression of genes across the three conditions: FG+ cells from stroke only and stroke+limb overuse, as well as NCAM+ RSC neurons. As previously described, modules and connectivity networks were created by using scale-free topology criterion (Zhang and Horvath, 2005). To identify hub genes and modules shared across independent conditions and datasets, consensus network analysis was applied (Langfelder and Horvath, 2007). GO and pathway enrichment analysis was performed using the Database for Annotation, Visualization and Integrated Discovery (DAVID) platform (<https://david.ncifcrf.gov/>). All network plots were constructed using the Cytoscape software (Saito *et al.*, 2012).

3.6 References:

- Abe, N., Cavalli, V., 2008. Nerve injury signaling. *Current opinion in neurobiology* 18, 276-283.
- Adelson, J.D., Barreto, G.E., Xu, L., Kim, T., Brott, B.K., Ouyang, Y.B., Naserke, T., Djurusic, M., Xiong, X., Shatz, C.J., Giffard, R.G., 2012. Neuroprotection from stroke in the absence of MHCI or PirB. *Neuron* 73, 1100-1107.
- Arlotta, P., Molyneaux, B.J., Chen, J., Inoue, J., Kominami, R., Macklis, J.D., 2005. Neuronal subtype-specific genes that control corticospinal motor neuron development in vivo. *Neuron* 45, 207-221.
- Beurdeley, M., Spatzza, J., Lee, H.H., Sugiyama, S., Bernard, C., Di Nardo, A.A., Hensch, T.K., Prochiantz, A., 2012. Otx2 binding to perineuronal nets persistently regulates plasticity in the mature visual cortex. *The Journal of neuroscience : the official journal of the Society for Neuroscience* 32, 9429-9437.
- Bialas, A.R., Stevens, B., 2013. TGF-beta signaling regulates neuronal C1q expression and developmental synaptic refinement. *Nature neuroscience* 16, 1773-1782.
- Brewer, G.J., Torricelli, J.R., 2007. Isolation and culture of adult neurons and neurospheres. *Nature protocols* 2, 1490-1498.
- Cahoy, J.D., Emery, B., Kaushal, A., Foo, L.C., Zamanian, J.L., Christopherson, K.S., Xing, Y., Lubischer, J.L., Krieg, P.A., Krupenko, S.A., Thompson, W.J., Barres, B.A., 2008. A transcriptome database for astrocytes, neurons, and oligodendrocytes: a new resource for understanding brain development and function. *The Journal of neuroscience : the official journal of the Society for Neuroscience* 28, 264-278.
- Cannon, T.D., Thompson, P.M., van Erp, T.G., Toga, A.W., Poutanen, V.P., Huttunen, M., Lonnqvist, J., Standerskjold-Nordenstam, C.G., Narr, K.L., Khaledy, M., Zoumalan, C.I., Dail, R., Kaprio, J., 2002. Cortex mapping reveals regionally specific patterns of genetic and

- disease-specific gray-matter deficits in twins discordant for schizophrenia. *Proceedings of the National Academy of Sciences of the United States of America* 99, 3228-3233.
- Carmichael, S.T., Archibeque, I., Luke, L., Nolan, T., Momiy, J., Li, S., 2005. Growth-associated gene expression after stroke: evidence for a growth-promoting region in peri-infarct cortex. *Experimental neurology* 193, 291-311.
- Chaldakov, G.N., Tonchev, A.B., Aloe, L., 2009. NGF and BDNF: from nerves to adipose tissue, from neurokines to metabokines. *Riv Psichiatr* 44, 79-87.
- Chandran, V., Coppola, G., Nawabi, H., Omura, T., Versano, R., Huebner, E.A., Zhang, A., Costigan, M., Yekkirala, A., Barrett, L., Blesch, A., Michaelovski, I., Davis-Turak, J., Gao, F., Langfelder, P., Horvath, S., He, Z., Benowitz, L., Fainzilber, M., Tuszynski, M., Woolf, C.J., Geschwind, D.H., 2016. A Systems-Level Analysis of the Peripheral Nerve Intrinsic Axonal Growth Program. *Neuron* 89, 956-970.
- Cho, S.W., Kwak, S., Woolley, T.E., Lee, M.J., Kim, E.J., Baker, R.E., Kim, H.J., Shin, J.S., Tickle, C., Maini, P.K., Jung, H.S., 2011. Interactions between Shh, Sostdc1 and Wnt signaling and a new feedback loop for spatial patterning of the teeth. *Development* 138, 1807-1816.
- Clausen, K.A., Blish, K.R., Birse, C.E., Triplette, M.A., Kute, T.E., Russell, G.B., D'Agostino, R.B., Jr., Miller, L.D., Torti, F.M., Torti, S.V., 2011. SOSTDC1 differentially modulates Smad and beta-catenin activation and is down-regulated in breast cancer. *Breast Cancer Res Treat* 129, 737-746.
- Cramer, S.C., Nelles, G., Benson, R.R., Kaplan, J.D., Parker, R.A., Kwong, K.K., Kennedy, D.N., Finklestein, S.P., Rosen, B.R., 1997. A functional MRI study of subjects recovered from hemiparetic stroke. *Stroke; a journal of cerebral circulation* 28, 2518-2527.

- Dancause, N., Barbay, S., Frost, S.B., Plautz, E.J., Chen, D., Zoubina, E.V., Stowe, A.M., Nudo, R.J., 2005. Extensive cortical rewiring after brain injury. *The Journal of neuroscience : the official journal of the Society for Neuroscience* 25, 10167-10179.
- Deryugina, E.I., Quigley, J.P., 2006. Matrix metalloproteinases and tumor metastasis. *Cancer Metastasis Rev* 25, 9-34.
- Dickson, B.J., 2002. Molecular mechanisms of axon guidance. *Science* 298, 1959-1964.
- Drinjakovic, J., Jung, H., Campbell, D.S., Strohlic, L., Dwivedy, A., Holt, C.E., 2010. E3 ligase Nedd4 promotes axon branching by downregulating PTEN. *Neuron* 65, 341-357.
- Du, K., Leu, J.I., Peng, Y., Taub, R., 1998. Transcriptional up-regulation of the delayed early gene HRS/SRp40 during liver regeneration. Interactions among YY1, GA-binding proteins, and mitogenic signals. *The Journal of biological chemistry* 273, 35208-35215.
- Gao, Y., Deng, K., Hou, J., Bryson, J.B., Barco, A., Nikulina, E., Spencer, T., Mellado, W., Kandel, E.R., Filbin, M.T., 2004. Activated CREB is sufficient to overcome inhibitors in myelin and promote spinal axon regeneration in vivo. *Neuron* 44, 609-621.
- Glantz, L.A., Lewis, D.A., 2000. Decreased dendritic spine density on prefrontal cortical pyramidal neurons in schizophrenia. *Arch Gen Psychiatry* 57, 65-73.
- Goddard, C.A., Butts, D.A., Shatz, C.J., 2007. Regulation of CNS synapses by neuronal MHC class I. *Proceedings of the National Academy of Sciences of the United States of America* 104, 6828-6833.
- He Ye, K.J., Dupree J, Tewari A, Melendez-Vasquez C, Svaren J, Casaccia P., 2010. Yy1 as a molecular link between neuregulin and transcriptional modulation of peripheral myelination. *Nat Neurosci.*, 1472-1480.
- Johansen-Berg, H., Rushworth, M.F., Bogdanovic, M.D., Kischka, U., Wimalaratna, S., Matthews, P.M., 2002. The role of ipsilateral premotor cortex in hand movement after stroke. *Proceedings of the National Academy of Sciences of the United States of America* 99, 14518-14523.

- Karki, P., Johnson, J., Jr., Son, D.S., Aschner, M., Lee, E., 2016. Transcriptional Regulation of Human Transforming Growth Factor-alpha in Astrocytes. *Mol Neurobiol*.
- Klar, M., Fenske, P., Vega, F.R., Dame, C., Brauer, A.U., 2015. Transcription factor Yin-Yang 2 alters neuronal outgrowth in vitro. *Cell and tissue research* 362, 453-460.
- Kramer, A., Green, J., Pollard, J., Jr., Tugendreich, S., 2014. Causal analysis approaches in Ingenuity Pathway Analysis. *Bioinformatics* 30, 523-530.
- Kuwabara, T., Hsieh, J., Muotri, A., Yeo, G., Warashina, M., Lie, D.C., Moore, L., Nakashima, K., Asashima, M., Gage, F.H., 2009. Wnt-mediated activation of NeuroD1 and retro-elements during adult neurogenesis. *Nature neuroscience* 12, 1097-1105.
- Langfelder, P., Horvath, S., 2007. Eigengene networks for studying the relationships between co-expression modules. *BMC Syst Biol* 1, 54.
- Langfelder, P., Horvath, S., 2008. WGCNA: an R package for weighted correlation network analysis. *BMC Bioinformatics* 9, 559.
- Leslie, J.H., Nedivi, E., 2011. Activity-regulated genes as mediators of neural circuit plasticity. *Progress in neurobiology* 94, 223-237.
- Li, J., Di, C., Jing, J., Di, Q., Nakhla, J., Adamson, D.C., 2015a. OTX2 is a therapeutic target for retinoblastoma and may function as a common factor between C-MYC, CRX, and phosphorylated RB pathways. *Int J Oncol* 47, 1703-1710.
- Li, S., Carmichael, S.T., 2006. Growth-associated gene and protein expression in the region of axonal sprouting in the aged brain after stroke. *Neurobiology of disease* 23, 362-373.
- Li, S., Nie, E.H., Yin, Y., Benowitz, L.I., Tung, S., Vinters, H.V., Bahjat, F.R., Stenzel-Poore, M.P., Kawaguchi, R., Coppola, G., Carmichael, S.T., 2015b. GDF10 is a signal for axonal sprouting and functional recovery after stroke. *Nature neuroscience* 18, 1737-1745.

- Li, S., Overman, J.J., Katsman, D., Kozlov, S.V., Donnelly, C.J., Twiss, J.L., Giger, R.J., Coppola, G., Geschwind, D.H., Carmichael, S.T., 2010. An age-related sprouting transcriptome provides molecular control of axonal sprouting after stroke. *Nature neuroscience* 13, 1496-1504.
- Livingston-Thomas, J.M., McGuire, E.P., Doucette, T.A., Tasker, R.A., 2014. Voluntary forced use of the impaired limb following stroke facilitates functional recovery in the rat. *Behavioural brain research* 261, 210-219.
- Lobo, M.K., Karsten, S.L., Gray, M., Geschwind, D.H., Yang, X.W., 2006. FACS-array profiling of striatal projection neuron subtypes in juvenile and adult mouse brains. *Nature neuroscience* 9, 443-452.
- Miyata, S., Komatsu, Y., Yoshimura, Y., Taya, C., Kitagawa, H., 2012. Persistent cortical plasticity by upregulation of chondroitin 6-sulfation. *Nature neuroscience* 15, 414-422, S411-412.
- Okaty, B.W., Sugino, K., Nelson, S.B., 2011. A quantitative comparison of cell-type-specific microarray gene expression profiling methods in the mouse brain. *PLoS one* 6, e16493.
- Oldham, M.C., Horvath, S., Geschwind, D.H., 2006. Conservation and evolution of gene coexpression networks in human and chimpanzee brains. *Proceedings of the National Academy of Sciences of the United States of America* 103, 17973-17978.
- Overman, J.J., Clarkson, A.N., Wanner, I.B., Overman, W.T., Eckstein, I., Maguire, J.L., Dinov, I.D., Toga, A.W., Carmichael, S.T., 2012. A role for ephrin-A5 in axonal sprouting, recovery, and activity-dependent plasticity after stroke. *Proceedings of the National Academy of Sciences of the United States of America* 109, E2230-2239.
- Ozdinler, P.H., Macklis, J.D., 2006. IGF-I specifically enhances axon outgrowth of corticospinal motor neurons. *Nature neuroscience* 9, 1371-1381.
- Pickering, M., Cumiskey, D., O'Connor, J.J., 2005. Actions of TNF-alpha on glutamatergic synaptic transmission in the central nervous system. *Exp Physiol* 90, 663-670.

- Rustenhoven, J., Aalderink, M., Scotter, E.L., Oldfield, R.L., Bergin, P.S., Mee, E.W., Graham, E.S., Faull, R.L., Curtis, M.A., Park, T.I., Dragunow, M., 2016. TGF-beta1 regulates human brain pericyte inflammatory processes involved in neurovasculature function. *J Neuroinflammation* 13, 37.
- Saito, R., Smoot, M.E., Ono, K., Ruschinski, J., Wang, P.L., Lotia, S., Pico, A.R., Bader, G.D., Ideker, T., 2012. A travel guide to Cytoscape plugins. *Nat Methods* 9, 1069-1076.
- Santello, M., Volterra, A., 2012. TNFalpha in synaptic function: switching gears. *Trends in neurosciences* 35, 638-647.
- Saris, C.G., Horvath, S., van Vught, P.W., van Es, M.A., Blauw, H.M., Fuller, T.F., Langfelder, P., DeYoung, J., Wokke, J.H., Veldink, J.H., van den Berg, L.H., Ophoff, R.A., 2009. Weighted gene co-expression network analysis of the peripheral blood from Amyotrophic Lateral Sclerosis patients. *BMC Genomics* 10, 405.
- Seitz, R.J., Hoflich, P., Binkofski, F., Tellmann, L., Herzog, H., Freund, H.J., 1998. Role of the premotor cortex in recovery from middle cerebral artery infarction. *Archives of neurology* 55, 1081-1088.
- Sekar, A., Bialas, A.R., de Rivera, H., Davis, A., Hammond, T.R., Kamitaki, N., Tooley, K., Presumey, J., Baum, M., Van Doren, V., Genovese, G., Rose, S.A., Handsaker, R.E., Schizophrenia Working Group of the Psychiatric Genomics, C., Daly, M.J., Carroll, M.C., Stevens, B., McCarroll, S.A., 2016. Schizophrenia risk from complex variation of complement component 4. *Nature* 530, 177-183.
- Shatz, C.J., 2009. MHC class I: an unexpected role in neuronal plasticity. *Neuron* 64, 40-45.
- Sugiyama, S., Di Nardo, A.A., Aizawa, S., Matsuo, I., Volovitch, M., Prochiantz, A., Hensch, T.K., 2008. Experience-dependent transfer of Otx2 homeoprotein into the visual cortex activates postnatal plasticity. *Cell* 134, 508-520.

- Sumi, K., Uno, K., Matsumura, S., Miyamoto, Y., Furukawa-Hibi, Y., Muramatsu, S., Nabeshima, T., Nitta, A., 2015. Induction of neuronal axon outgrowth by Shati/Nat8l by energy metabolism in mice cultured neurons. *Neuroreport* 26, 740-746.
- Syken, J., Grandpre, T., Kanold, P.O., Shatz, C.J., 2006. PirB restricts ocular-dominance plasticity in visual cortex. *Science* 313, 1795-1800.
- Toriumi, K., Ikami, M., Kondo, M., Mouri, A., Koseki, T., Ibi, D., Furukawa-Hibi, Y., Nagai, T., Mamiya, T., Nitta, A., Yamada, K., Nabeshima, T., 2013. SHATI/NAT8L regulates neurite outgrowth via microtubule stabilization. *Journal of neuroscience research* 91, 1525-1532.
- Wang, Z., Gerstein, M., Snyder, M., 2009. RNA-Seq: a revolutionary tool for transcriptomics. *Nature reviews. Genetics* 10, 57-63.
- Yanagita, M., 2005. BMP antagonists: their roles in development and involvement in pathophysiology. *Cytokine Growth Factor Rev* 16, 309-317.
- Yoon, H.S., Scharer, C.D., Majumder, P., Davis, C.W., Butler, R., Zinzow-Kramer, W., Skountzou, I., Koutsonanos, D.G., Ahmed, R., Boss, J.M., 2012. ZBTB32 is an early repressor of the CIITA and MHC class II gene expression during B cell differentiation to plasma cells. *Journal of immunology* 189, 2393-2403.
- Zhang, B., Horvath, S., 2005. A general framework for weighted gene co-expression network analysis. *Statistical applications in genetics and molecular biology* 4, Article17.

CHAPTER 4.

CRISPR/CAS9 IN-VITRO SCREENING OF CANDIDATE GENES

4.1 Introduction

The next arm of studies sought to validate candidate genes and functionally characterize the gene systems identified through RNA-Seq of the retrosplenial-premotor cortical neurons. Candidate gene exploration and mechanistic studies were planned to occur in two phases: first an in-vitro phenotype screen of 10-15 candidates, and then 2-3 candidates will be taken in-vivo in a second phase. The present study describes the first phase of this work, as in-vivo investigations are ongoing. To prioritize and screen top RNA-Seq gene candidates for potential roles in neurite outgrowth, we engineered a CRISPR/cas9 platform to generate a medium throughput knockout screen in primary neurons. Cas9 is a powerful tool at the forefront of the genome-editing field, and importantly, may facilitate multiplexed gene manipulations. This is a critical technical advantage in the field because it is becoming increasingly clear that a single gene effect can only account for a limited facet of the complex process of post-stroke brain repair.

CRISPR/cas9 is a uniquely tractable RNA-guided DNA editing technique. Cas9 is a DNA nuclease derived from the bacterial immune system and only recently appropriated for eukaryotic genome editing (Cong *et al.*, 2013; Mali *et al.*, 2013). The term “CRISPR” or clustered regularly interspersed palindromic repeats, emerged as a descriptive reference to patterned prokaryotic DNA sequences originally discovered by bacteriologists in the 1980s (Ishino *et al.*, 1987). As it turned out, these bacterial CRISPR sequences matched pieces of viral genome sequences introduced from previous infections, and essentially serve as a memory of the infection. A CRISPR associated nuclease, later named “cas,” is a nuclease that cuts recognizable viral DNA upon a repeat infection,

and thus provides immune defense for the host bacteria. Surprisingly, the prokaryotic cas nuclease could be functionally expressed in eukaryotic models, thereby forging a new method of genome editing in eukaryotic and mammalian systems (Cong *et al.*, 2013; Mali *et al.*, 2013). In the last three years, the CRISPR/cas revolution has taken biological research by storm and thousands of unique studies continue to be published, with applications ranging from advances in plant biology to cas9 directed gene therapy (Doudna and Charpentier, 2014; Nelson *et al.*, 2016; Tabebordbar *et al.*, 2016). The story of solving the CRISPR/cas9 mechanism in yogurt bacteria is one great example of how basic science research can ignite new fields of inquiry, tool development, and translational applications.

In mammalian cells, one can design a short 20-22 bp guide RNA (gRNA) that is complementary to a gene targeted for mutation. The gRNA directs cas-9 to the targeted gene of interest, where it creates a DNA double-strand break and triggers cellular repair. Mutation generation occurs when either of two endogenous mechanisms of DNA repair is initiated: nonhomologous end joining (NHEJ) or homology directed repair (HDR) (Hsu *et al.*, 2014; Ran *et al.*, 2013). NHEJ creates random insertions and deletions, usually of 1-8 bp, at the targeted genomic region, and gene knockout is produced upon translation of a premature stop codon. HDR can be used to insert specific mutations at a given genomic site (further reviewed in Hsu *et al.*, 2014; Ran *et al.*, 2013). For the present in-vitro candidate screen, we design gRNAs targeted against 15 top candidate genes and confirm NHEJ directed gene knockout for a loss-of-function screen.

4.2 Results

Fluidigm qPCR validation of gene targets

After collating data from the bioinformatics analyses, a list of top candidate genes was used for multiplexed gene expression qPCR validation. The samples were collected from an independent

cohort of animals generated (n=6 animals per group) to represent each RNA-Seq group: stroke only, stroke+limb overuse, and RSC control neurons. Initially, a group of 40 genes were picked after statistical cutoffs (FDR <0.1, p<0.005) based on direction and degree of fold change (>±4x), network connectedness, IPA upstream regulation, and WGCNA/transcriptome overlay analyses. This list (Table 4.1) included genes that had previously been implicated in activity-dependent plasticity (i.e. MEF2c, CaMKIIg), neuronal growth (i.e. EphA10, RhoB), development (i.e. NeuroD1, Zbtb32), and ones that were more biologically novel in this context (ie. SOSTDC1, NMBR). The amount of input RNA for FG+ cells from RSC was low, on the order of pg/uL. We were able to validate 10 of 13 of the targets from the RSC FG+ vs. NCAM+ groups but several of the stroke+limb overuse samples were lacking ample signal or reported a missed calls. The following targets were validated: RhoB, KCNJ10, Sparc, FosB, Ssh(3), Zfp11, Dpysl2, B2m, Jun, Ssh2(2) (Fig 4.1). However, due to a lack of sensitivity from the stroke + limb overuse samples, we ultimately decided not to exclude these negative calls from the next phase of validation studies in the axonal sprouting screen.

Generation and validation of CRISPR/cas9 constructs for in-vitro screen

To assemble a tractable group of genes for CRISPR/cas9 gRNA design and phenotype screening, the initial list of 40 candidate genes used in qPCR validation was further narrowed down to 15 genes. Selection was based on degree of fold change, overlap with WGCNA/transcriptome PCA studies, hypothesized upstream regulator effects, and biological novelty. Candidates were chosen from both statistical comparisons: FG+ versus NCAM+ cells, as well as RSC FG+ cells from stroke and stroke + limb overuse. The candidates in Table 4.2 were used for CRISPR gRNA generation. For each target gene, I designed two gRNAs, performed mutation testing, and packaged targeting gRNAs into CRISPR lentiviruses for the axonal outgrowth screen. gRNAs were typically

designed to target the first coding exon of the candidate gene. Guides were then cloned into the LentiCRISPRV2 DNA backbone (gift from Feng Zhang) and sequence verified for insertion. In order to confirm that the gRNA and cas9 were in fact targeting and working, a mutation detection assay was performed using the SURVEYOR Cel-I nuclease assay (Fig4.3a). In a mixture of mutated and control DNA, Cel-I nuclease is able to detect DNA mismatches and cleave double stranded DNA at the site of mutation. One can then detect cleaved products on a gel. A representative SURVEYOR assay is shown in Fig 4.3b; gRNA targets cas9 to MEF2C, a candidate gene, whereby the cas9 cleavage generates insertions and deletions (indels) that lead to Cel-I recognition and confirmatory mutation detection.

CRISPR/cas9 lentiviral packaging and validation

Primary neurons are not amenable to chemical transfection (Ding and Kilpatrick, 2013; Geraerts *et al.*, 2006). Therefore, we packaged the tested cas9 constructs with integrated gRNAs into lentivirus, a gene delivery vehicle that we and others have used to transduce neurons at a high efficiency. We used LentiCRISPRV2 (Fig 4.4a), a lenti-ready DNA backbone with Spcas9 and U6 promoter driving gRNA (Sanjana *et al.*, 2014). LentiCRISPRV2 does not have a fluorescent reporter, so packaging was always done alongside a lentivirus CMV-GFP for transfection control. In order to confirm LentiCRISPRV2 particles were functional, all collected virus samples were tested by HEK293 transduction and subsequent cas9 and target gene antibody staining (Figure 4.4b). CMV-EGFP lentivirus packaged in parallel was also used as transduction controls to help verify positive viral packaging for all batches of lentivirus synthesis. qPCR was also performed to confirm transcriptional decrease for targeted genes.

In-vitro neuronal outgrowth phenotype screen

After the panel of gRNAs were generated and packaged into lentivirus, we ran the primary neuronal outgrowth phenotype screen using an ImageXpress system (Molecular Devices). This platform allows for automated multi-field image acquisition and systematic neurite outgrowth quantification. Neurite outgrowth was measured in primary cortical mouse neurons across all conditions. Tau, MAP2, and NeuN were used to immunostain axons, dendrites, and neuronal cell bodies, respectively. (Figure 4.5). Average neurite outgrowth was normalized to number of neurons per imaging field.

The CRISPR screen resulted in 8 candidate genes that significantly alters neurite outgrowth after knockout in primary cortical neurons. 4 genes were identified by quantification of the Tau axonal marker. These genes were: YY1 ($p=0.0329$), WAP ($p=0.003$), NeuroG3 ($p=0.0002$), Otx2 ($p=0.0469$), Otx2 gRNA #2 ($p=0.0077$). From MAP2 dendrite analyses, each of these genes was revalidated with increased significance: YY1 ($p=0.0012$), WAP ($p=0.0312$), NeuroG3 ($p<0.0001$), Otx2 ($p=0.0001$). Additionally, 4 more significant genes were discovered: NGFR ($p=0.0206$), EphA10 ($p=0.0002$), SOSTDC1 ($p<0.0001$), and Zbtb32 ($p<0.0001$), totaling to 8 genes for prioritized follow-up study. 6 of the 8 genes increased neurite (axonal or dendritic) sprouting after knockout: YY1, WAP, EphA10, SOSTDC1, Otx2, and Zbtb32. On the other hand, knockout of NeuroG3 or NGFR resulted in decreased neuronal outgrowth. Interestingly, 3 of the 8 significant genes were transcription factors generated through the upstream regulator analyses (Table 3.3). Candidate genes significant in both Tau and MAP2 analyses always affected outgrowth in the same direction. That is, a gene that significantly increased axonal outgrowth would never simultaneously decrease dendritic length. The three upstream regulators tested, YY1, Otx2 and NeuroG3 were validated using both Tau and MAP2 markers in the screen.

4.3 Discussion

After validation of a subset of candidate genes using Fluidigm qPCR, we decided to approach a smaller curated list of candidate genes in a phenotype screen for neurite outgrowth. Here, we generated CRISPR/cas9 tools for neuronal application in-vitro and performed a medium throughput loss-of-function phenotype screen for neurite outgrowth using 15 candidates. Since we were most interested in axonal sprouting, we focused selection of candidate genes whose knockout would potentially improve neuronal outgrowth. One interesting trend from the RNA-Seq analyses was that many more candidate genes were downregulated than upregulated in the sprouting RSC-PMC circuit (Table 3.2). Therefore, we chose to pursue a loss-of-function screen first and did not initially include gain-of-function studies for upregulated sprouting candidates. These studies are now ongoing.

The data from the CRISPR/cas9 screen confirmed 8 candidate genes that significantly alter axonal sprouting after knockout in primary cortical neurons. We had chosen the gRNA list mostly for candidates whose knockout we hypothesized (from the RNA-Seq data) would increase axonal sprouting, as this is the phenotype we want to enhance. Therefore, it was encouraging to see that 6 of the 8 significant genes increased axonal sprouting after knockout by cas9. These were YY1, WAP, EphA10, SOSTDC1, Otx2, and Zbtb32. YY1 was an upstream regulator that differentially activated and repressed various candidates identified by RNA-Seq of the RSC-PMC connection (Table 3.3). WAP was one of the most downregulated genes in sprouting neurons from RSC-PMC; it was essentially turned off in sprouting cells (Table 3.2). WAP is a protein that has not been studied in CNS injury, but is expressed in the cortex (Wen *et al.*, 1995), inhibits cell cycle (Ikeda *et al.*, 2004), and regulated by the extracellular matrix through TGF-alpha suppression (Lin *et al.*, 1995). These are all potentially favorable mechanisms for the sprouting axon. A WAP protein homolog regulates immune response to injury (Karlstetter *et al.*, 2010), and may link to some of the other neuroimmune

molecules differentially regulated in the RSC-PMC. EphA10 is a molecule known for its growth cone chemorepellant roles in neurodevelopment (Dickson, 2002; Sperry, 1963). The current in-vitro screen data demonstrate that cas9 knockout of EphA10 promotes neurite sprouting, a result that is consistent with previous findings in the literature (Overman *et al.*, 2012). SOSTDC1, a BMP antagonist, has developmental roles (Cho *et al.*, 2011) but is novel to CNS injury. Otx2, one of the upstream regulators screened, has an incredibly fascinating and complex biology. Briefly, during development the protein is transported across synapses from the retina to the visual cortex upon sensory experience, where it regulates the critical period by association with parvalbumin neurons (Sugiyama *et al.*, 2008). Otx2 binds to peri-neuronal nets and stabilizes circuits in the adult brain; conversely, loss of Otx2 can reestablish ocular dominance plasticity in the adult (Beurdeley *et al.*, 2012). Since Otx2 inhibits plasticity by closing the critical period, its knockout-induced axonal sprouting is also consistent with our hypotheses from the study's outset. Since Otx2 is associated with activity-dependent induction during development, it is an especially interesting candidate for us during behavioral overuse after injury. Zbtb32 is a novel zinc finger transcription factor that has bipotential activator and repressor functions, and was significantly downregulated in sprouting RSC cells. Although Zbtb32 has not been studied much in the adult brain, Zbtb20 is a related transcription factor that is frequently co-expressed with Zbtb32, that has been shown to repress many plasticity and growth-related genes in the hippocampus during developmental specification from retrosplenial cortex and subiculum (Nielsen *et al.*, 2014).

Additionally, knockout of two genes, NGFR and NeuroG3, decreased axonal sprouting. Nerve growth factor receptor (NGFR) regulates nerve trophic support through BDNF and insulin signaling, (Chaldakov *et al.*, 2009), so this loss-of-function result is consistent with its known biological roles. NeuroG3 is a transcription factor that is involved in neurogenesis (Ma *et al.*, 2009) and dendritic development in hippocampal neurons (Simon-Areces *et al.*, 2011). It entered the screen

as an upstream regulator candidate gene that induces NeuroD1, a proneural gene associated with NGF and insulin signaling in neuronal growth (Sharma *et al.*, 1999). It is worth noting that 3 of the 4 upstream candidate genes tested significantly altered neuronal outgrowth in this screen. This result is promising because these genes are transcriptional regulators that we can potentially manipulate early in the recovery period.

We use CRISPR/cas 9 for candidate gene screening because of several advantages over siRNA or shRNA for our studies. First, cas9 editing of candidate genes allows for knockout (instead of knockdown) screening. While such an approach would not be appropriate for all applications, creating gene knockouts works well in this screening platform because we wanted to mimic highly differentially regulated genes after stroke, some of which are switched on or off after stroke based on the RNA-Seq data and screen for large effect sizes on neuronal outgrowth. Second, RNA can be fickle to downregulate, while editing at the genome level is reliable and indelible after cas9 takes effect. This helps ensure we efficiently generate loss-of-function in screened candidates. Additionally, the long-lasting time course of gene editing is advantageous for in-vivo experiments planned after the screen. We want to produce the same genetic manipulations after stroke, during a period of axonal sprouting that can last 3-4 weeks in the mouse (Carmichael *et al.*, 2005) and months in primates (Dancause *et al.*, 2005). This overcomes traditional short-term efficacy of siRNA. Furthermore, CRISPR/cas9 is a technique with high tractability, requiring only 20bp gRNAs for target design. Finally, and perhaps most importantly, gRNAs can be multiplexed for simultaneous targeting of multiple candidates (Cheng *et al.*, 2013; Cong *et al.*, 2013). Because targets are a mere 20bp, multiple guides could also be packaged into viral vectors for generating mutations in hard to transfect cells such as neurons, and these studies are planned for upcoming experiments. Neuronal sprouting after stroke is a complex biological process that is ultimately dependent on coordinated arrays of plasticity and injury-related molecules (Overman and Carmichael, 2014). Technologies are

beginning to emerge in which various forms of cas9 and gRNA combinations can simultaneously facilitate knockout, activation, and repression to different targets all in one cell (Dahlman *et al.*, 2015; Gilbert *et al.*, 2014).

Advantages and limitations of the in-vitro screen

The in-vitro screen utilized in these studies was designed to measure neuronal outgrowth as the central phenotypic outcome. Since limb overuse enhanced the sprouting of retrosplenial cells to premotor cortex, we hypothesized that a subset of the differentially regulated genes must be essential to neuronal outgrowth after injury. The advantage of using a phenotypic screen over qPCR validation is that it provides a mechanistic readout for each candidate gene modification, rather than only relative transcript expression levels. However, the disadvantage is that this one screen may overlook candidate genes important to RSC-PMC cortical reorganization that affect processes other than physical neuronal outgrowth. For example, genes that alter neuronal excitability or other mechanisms of functional plasticity may be induced by limb overuse but do not directly lead to axonal outgrowth. Genes involved in synaptic pathfinding, synaptogenesis, and synapse maintenance are likely just as important to functional recovery. In fact, genes of this sort are expected to appear on the differentially regulated gene list from this 4-week time point after stroke, since axonal sprouting has been ongoing and others have reported functional recovery at this time point (Overman *et al.*, 2012; Wahl *et al.*, 2014). However, we focus candidate selection to genes that promote axonal sprouting for two key reasons. First, neuronal outgrowth is a relatively easily quantifiable phenotype that we could scale up into a screen. Second, neuronal outgrowth must at least be initiated or ongoing before synaptogenesis and other downstream processes come into play, and has traditionally been the bottleneck in CNS repair after injury (Abe and Cavalli, 2008; Chandran *et al.*, 2016). Thus we want to identify molecules that facilitate sprouting. Additionally, we surmised that several of the upstream regulators may drive neuronal outgrowth, since they are

activated earlier than 4 weeks and map to a period of robust axonal sprouting seen in other studies (Carmichael *et al.*, 2005). Nonetheless, this discussion does reemphasize the multitude of mechanisms in the post-stroke brain that must all work in concert (and sequentially) to promote recovery after injury.

4.4 Figures

Table 4.1

	1	2	3	4	5
A	SOSTDC1	NMBR	SLC35D3	RhoB	NRLS1
B	NeuroD1	PADI6	c4bp	KCNJ10	NRLS2
C	NGFR	TNNC2	LRG1	Sparc	PADI6
D	HOXB1	ZBTB32	FosB	TNFaip3	Ssh
E	INSM2	TOP2A	MEF2c	Kctd12	Hprt
F	EphA10	Ube2c (3)	ZfpL1	Dpysl2	sdha
G	CASP14	CamKlg	B2m	Jun	Ywhaz
H	MARCH3	TTR	EGR1	Ssh2	GAPDH

Table 4.1 Candidate genes for Fluidigm qPCR validation

Candidate genes are in aqua; housekeeping genes in grey

Figure 4.1

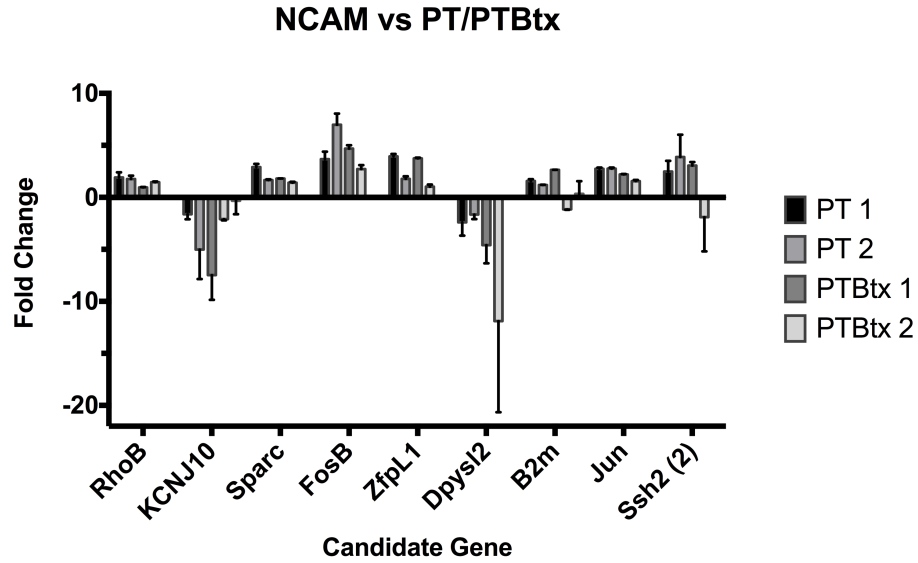


Figure 4.1 Fluidigm qPCR candidate gene validation

Fold change mapped for RSC FG+ neurons from stroke groups (PT) and stroke+limb overuse (PTBtx) relative to NCAM+ controls. 2 of 9 validated genes (KCNJ10 and Dpysl2) from this comparison were downregulated in FG+ neurons, and the rest (RhoB, Sparc, FosB, ZfpL1, B2m, Jun, Ssh2) were upregulated.

Figure 4.2

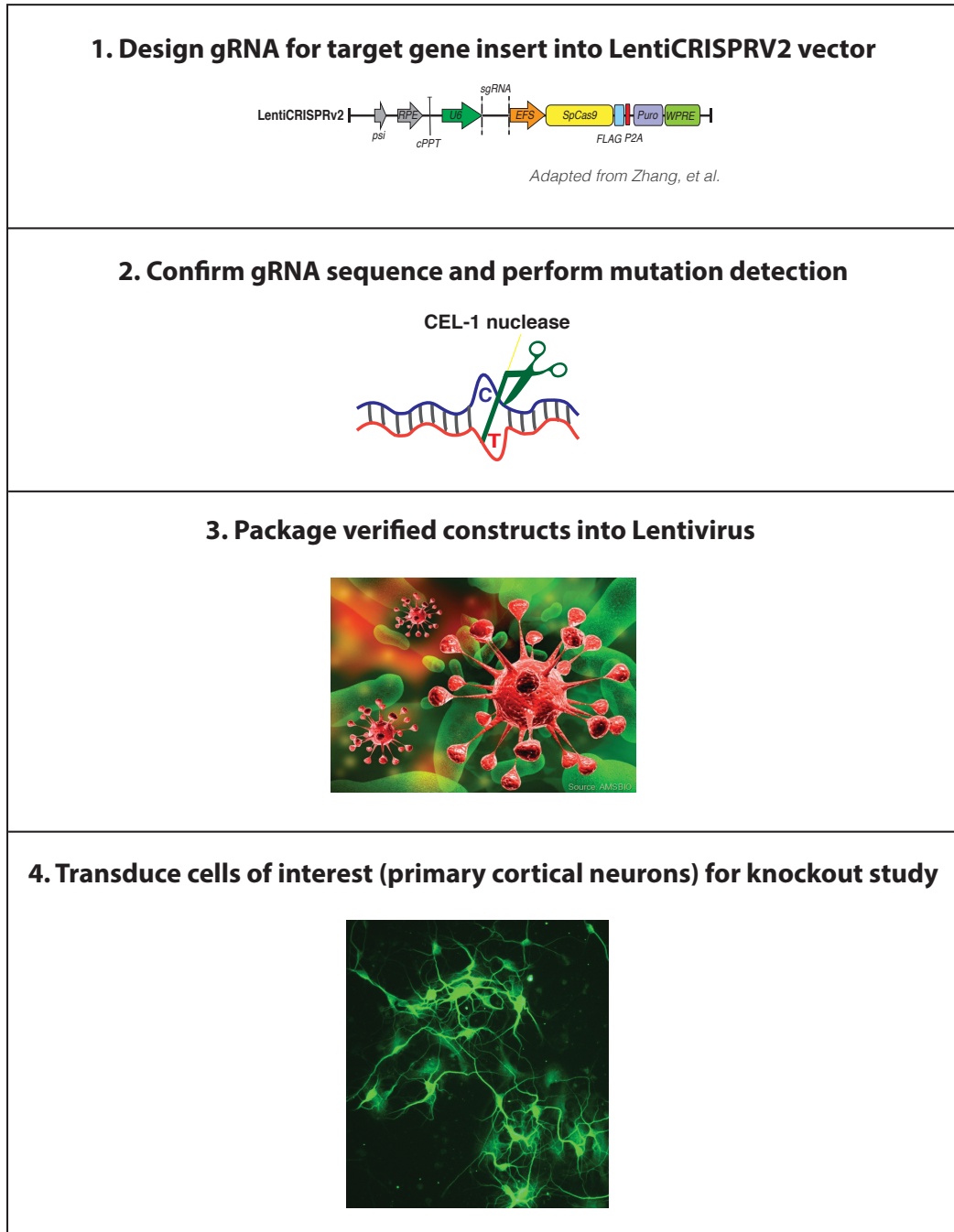


Figure 4.2 CRISPR/cas9 gRNA and lentivirus workflow

1) Guide-RNA (20-22bp) is designed against candidate genes and inserted into the LentiCRISPRV2 backbone, which contains SpCas9 for gRNA-directed. **2)** Once gRNA insertions are sequenced and verified, the construct is tested in cell line for mutation generation using a Cel-I nuclease assay. This platform is able to recognize mutations and cleaves. **3)** Constructs that pass mutation detection are packaged into functional lentiviral particles and **4)** delivered to primary mouse cortical neurons for gene knockout screening of neuronal outgrowth

Table 4.2

Target	CHOPCHOP#	CRISPR/cas9 gRNA	Genomic Location	gRNA Oligos F&R
MEF2c	1	GAAGAAACACGGGGACTATGGGG	chr13:835756 60	F:5'CACCGAAGAAACACGGGGACTATG3' R:5'AAACCATAGTCCCGTGTTCCTTC3'
MEF2c	2	GAAGAAGGAAACGTGTTGAAGG	chr13:835755 79	F:5'CACCGAAGAAGGAAACGTGTTGA3' R:5'AAACTCAAACACGTTTCCTTCCTTC3'
YY1	1	GCAGCGTAACGCCGGCCCGGAGG	chr12:108793 071	F:5'CACCGCAGCGTAACGCCGGCCCGG3' R:5'AAACCCGGGCCGGCGTTACGCTGC3'
YY1	2	GGTATTTGTGTGGAAGGAGGCGG	chr12:108793 030	F:5'CACCGGTATTTGTGTGGAAGGAGG3' R:5'AAACCTCCTTCCACACAAATACC3'
EphA10	1	GCTCCAGCTGAACCTTCGGAGG	chr4:1248809 01	F:5'CACCCTCCAGCTGAACCTTCGG3' R:5'AAACCCGAAGAGTTTCAGCTGGAGC3'
EphA10	4	TGCTCCAAGGCTAGCTAAGAGG	chr4:1248814 25	F:5'CACCTGCTCCAAGGCTAGCTAAG3' R:5'AAACCTTAGCTAGCCTTGGGAGCA3'
Zbtb32	1	TGGGGATCCATGATTGAAGTGG	chr7:3059191 9	F:5'CACCTGGGGATCCATGATTGAAG3' R:5'AAACCTTCAATCATGGATCCCCCA3'
Zbtb32	3	TGGGCTGATTAGTCTTGTGGGGG	chr7:3059183 6	F:5'CACCTGGGCTGATTAGTCTTGTGG3' R:5'AAACCCACAAGACTAATCAGCCCA3'
Wap	2	CGCAAACCTCTGTCAACATTGG	chr11:663548 2:6638637:-1	F:5'CACC CGCAAACCTCTGTCAACATT3' R:5'AAACATGTTGACAGGAGTTTTGCG3'
Wap	3	GAAGGGTTACTACTGGCACTGGG		F:5'CACC GAAGGGTTACTACTGGCACT3' R:5'AAACAGTGCCAGTGATAACCCCTTC3'
Casp14	1	GTGTGTACCAAAGCCCGGGAGG	chr10:787153 47	F:5'CACC GTGTGTACCAAAGCCCGGG3' R:5'AAACCCCGGGCTTTGGTGACACAC3'
Casp14	1	GCCTGTGAGCTGTGCCTTTGTGG	chr10:787150 85	F:5'CACC GCCTGTGAGCTGTGCCTTTG3' R:5'AAACCAAAGGCACAGCTGACAGGC3'
Nmbr	1	TGAGAGCGAGCTGGTACCCGAGG	chr10:147603 36	F:5'CACC TGAGAGCGAGCTGGTACCCG3' R:5'AAACCGGGTACCAGCTCGCTCTCA3'
Nmbr	5	AGAGGGATGGTATCACACAGCGG	chr10:147604 14	F:5'CACC AGAGGGATGGTATCACACAG3' R:5'AAACCTGTGTGATACCATCCCTCT3'
Nat8l	2	GGTCGGGTGTCAGATTGGAGTGG	chr5:3399604 5	F:5'CACC GGTCGGGTGTCAGATTGGAG3' R:5'AAACCTCCAATCTGACACCCGACC3'
Nat8l	5	GTGAGGACGCGGCTGAAATGTGG	chr5:3399610 4	F:5'CACC GTGAGGACGCGGCTGAAATG3' R:5'AAACATTTGAGCCGGCTCCTCAC3'
Crx	1	TGATGGCATATATGAACCCGGGG	chr7:1587122 0	F:5'CACC TGATGGCATATATGAACCCG3' R:5'AAACCGGGTTTATATATGCCATCA3'
Crx	6	TGGTGCATCAGTCCACATTGGG	chr7:1587116 1	F:5'CACCTGGTGCATCAGTCCACATT3' R:5'AAACATGTGGACCTGATGCACCA3'
NeuroG3	1	GTGAGCGCATCCAAGGGATGAGG	chr10:621334 69	F:5'CACC GTGAGCGCATCCAAGGGATG3' R:5'AAACCATCCCTGGATGCGCTCAC3'
NeuroG3	2	AGTCCCTAGGTATGAGAGTGGGG	chr10:621335 76	F:5'CACC AGTCCCTAGGTATGAGAGT3' R:5'AAACCACTCTCATACCTAGGGACT3'
Otx2	2	TGGGACTGAGGTACTAGAGGGGG	chr14:486591 56	F:5'CACCTGGGACTGAGGTACTAGAGG3' R:5'AAACCTCTAGTACCTCAGTCCCA3'
Otx2	5	GCTGGCAATGTTGGGACTGAGG	chr14:486591 44	F:5'CACC GCTGGCAATGTTGGGACTG3' R:5'AAACAGTCCCAACCATTGCCAGC3'
Sostdc1	2	GCCGTCGAAATGATTTGGTGG	chr12:363170 65	F:5'CACC GCCGTCGAAATGATTTGGG3' R:5'AAACCCAATACATTTGCGACGGC3'
Sostdc1	5	GAACAAAGTACTGGAGCCGGAGG	chr12:363171 82	F:5'CACC GAACAAAGTACTGGAGCCGG3' R:5'AAACCCGGCTCCAGTACTTTGTTTC3'
Ngfr	7	GAGTATGCCGCTCCCTGTGTGG	chr11:955782 41	F:5'CACC GAGTATGCCGCTCCCTGTG3' R:5'AAACACAGGGAGCGGCATACTC3'
Ngfr	1	GCCGAATGCGAGGAGATCCCTGG	*:0	F:5'CACC GCCGAATGCGAGGAGATCCC3' R:5'AAACGGGATCTCCTCGCATTCGGCC3'
NeuroD1	2	CGAGTTGCTGATGCTGAGCGCGG	chr2:7945667 0	F:5'CACC CGAGTTGCTGATGCTGAGCG3' R:5'AAACCGCTCAGCATCAGCAACTCG3'
NeuroD1	5	GCTTGAAGCCATGAATGCAGAGG	chr2:7945489 0	F:5'CACC GCTTGAAGCCATGAATGCAG3' R:5'AAACCTGCATCATGGCTTCAAGC3'

Figure 4.3

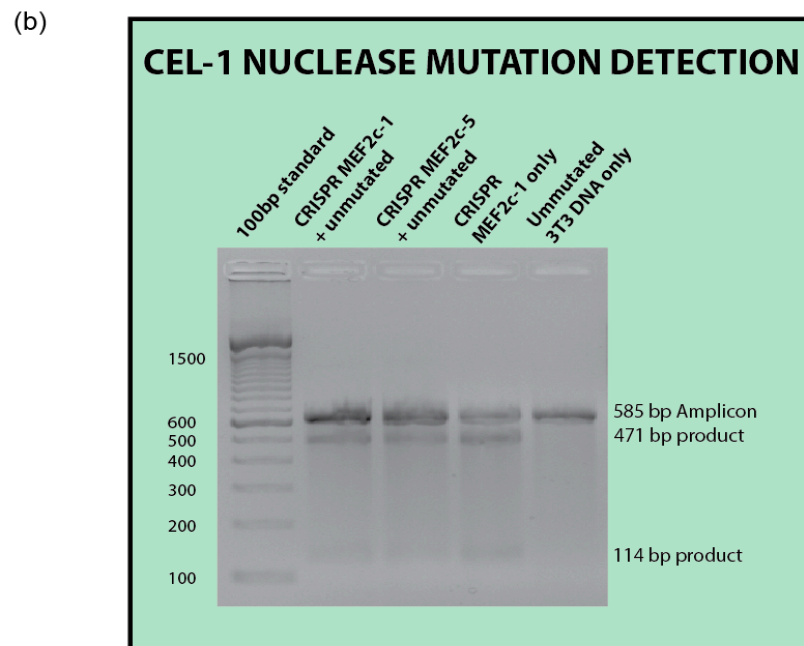
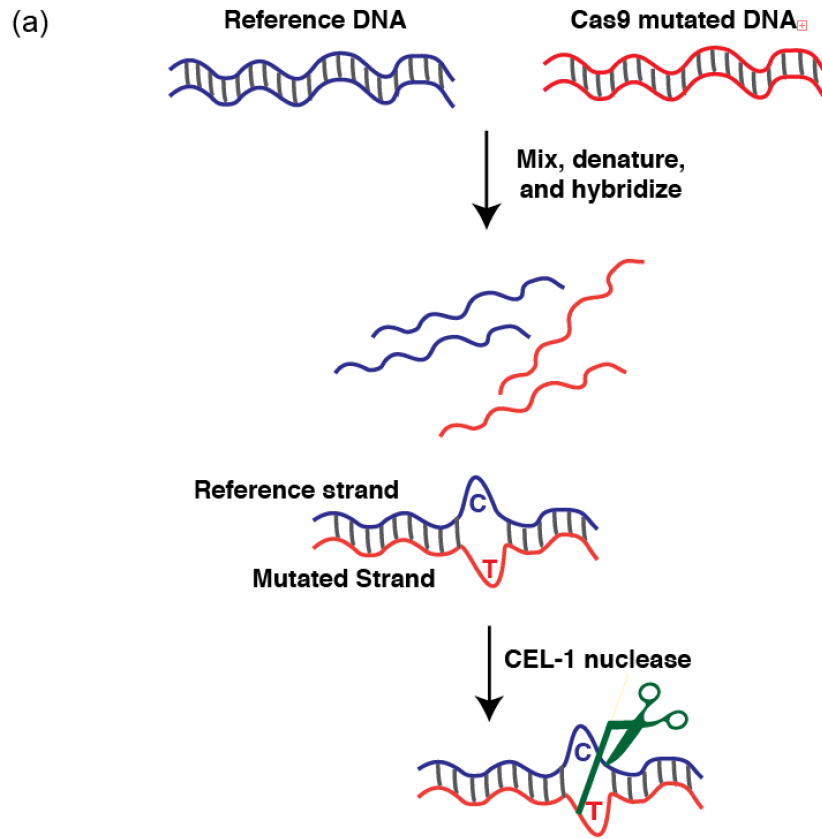


Figure 4.3 Mutation detection using Cel-I nuclease: mechanism and DNA gel visualization

a) Unmutated reference DNA and cas-9 treated mutated DNA are mixed, heated, and reannealed such that individual single strands can bind to each other. Reannealed DNA heteroduplexes that contain one strand from reference DNA and one strand from mutated DNA will result in a physical kink. Cel-I nuclease recognizes this atypical structure and cleaves at the site of mutation. The resulting cleavage products are analyzed by gel electrophoresis. **b)** MEF2c candidate gene targeted by cas-9 confirms presence of mutations. After PCR amplification of a 585bp amplicon containing the gRNA directed site, the SURVEYOR assay was run as shown in first panel. Lanes 2,3,4 are three different samples transfected with LentiCRISPRV2 with gRNA directed toward MEF2c. The last lane is unmutated control DNA. As expected, the DNA with cas-9 generated mutations is Cel-cleaved and results in the cleavage of 585bp into 471bp and 114bp products. In contrast, unmutated DNA is not cleaved and runs as a single band at 585bp.

Figure 4.4

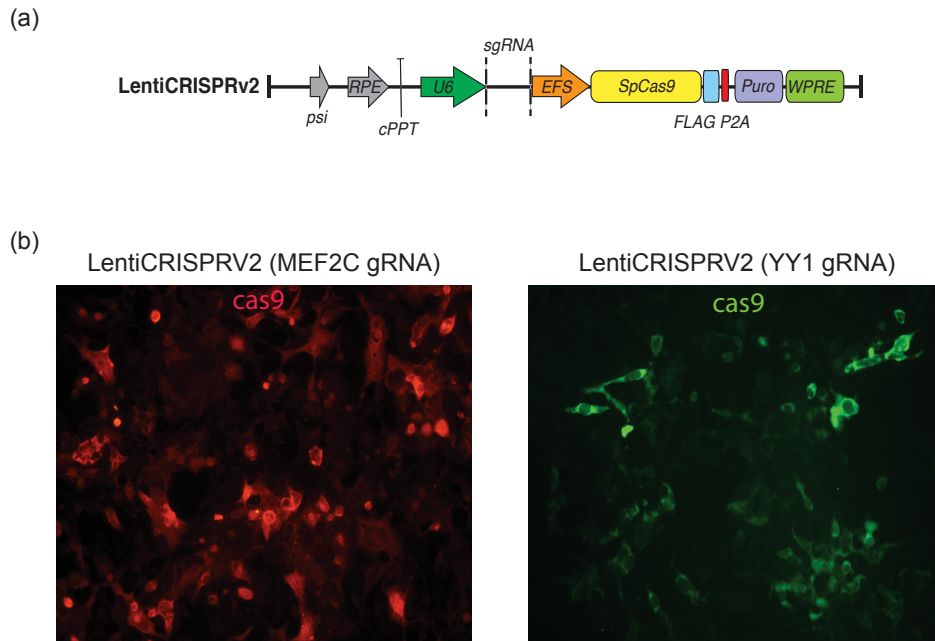


Figure 4.4 LentiCRISPRV2 transduction and cas9 expression

a) LentiCRISPRV2 construct for gRNA integration. Cas9 is driven by EFS (truncated Elongation Factor alpha) promoter, and gRNA is driven by ubiquitous U6 RNA polymerase promoter. **b)** HEK293 transduced by packaged lentivirus for 5 days indicates positive cas9 expression from viral infection. Representative images from two candidate gene targets: MEF2c (left) and YY1 (right)

Figure 4.5

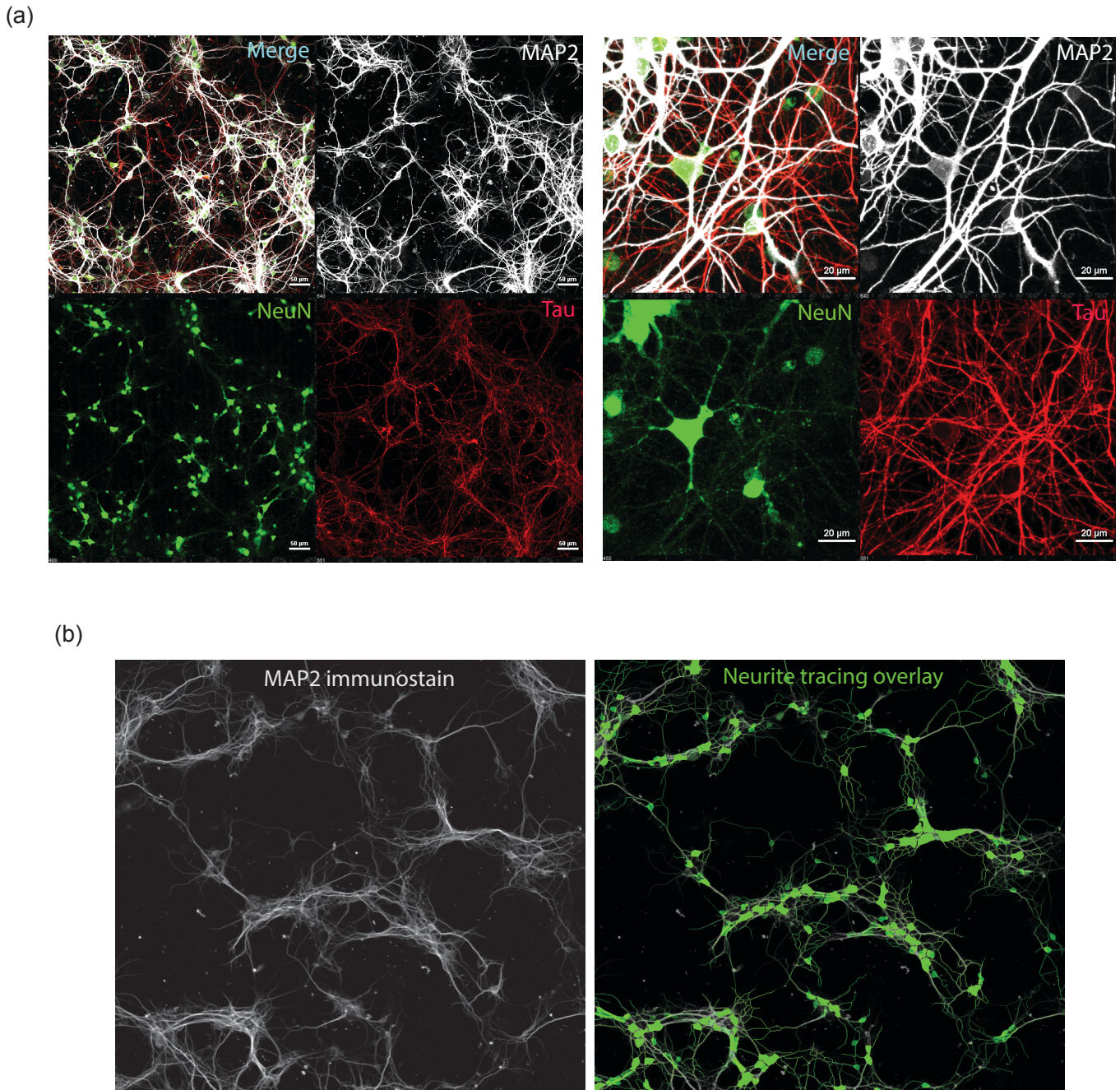


Figure 4.5 Immunostaining of DIV6 primary cortical neurons and ImageXpress generated neurite overlay

a) Left: 20X confocal images of immunostained plates for screening. NeuN labels neuronal nuclei, Map2 dendrites and Tau axons Right: 40X magnification shows distinct neurite staining by Tau and Map2 **b)** ImageXpress confocal images are run through an optimized neurite tracing analysis function and a representative neurite overlay is shown in green. The automated tracing is of high fidelity for both Map2 and Tau immunostains.

Table 4.3

Candidate Comparison	Mean difference in axon length per neuron (μm , control relative to knockout)	Effect of knockout	Bonferroni adjusted p-value
Ctrl vs. MEF2c	-15.59	increased axonal sprouting	> 0.9999
Ctrl vs. YY1	-41.62	increased axonal sprouting	0.0329
Ctrl vs. WAP	-50.53	increased axonal sprouting	0.003
Ctrl vs. Casp14	-27.35	increased axonal sprouting	0.675
Ctrl vs. Nat8l	-24.11	increased axonal sprouting	> 0.9999
Ctrl vs. Crx	-40.03	increased axonal sprouting	0.2405
Ctrl vs. NeuroG3	58.82	decreased axonal sprouting	0.0002
Ctrl vs. Otx2	-48.09	increased axonal sprouting	0.0469
Ctrl vs. NGFR	39.23	decreased axonal sprouting	0.213
Ctrl vs. EphA10	-26.1	increased axonal sprouting	0.9012
Ctrl vs. Nat8l(2)	-38.22	increased axonal sprouting	0.1067
Ctrl vs. NGFR(2)	42.45	decreased axonal sprouting	0.0635
Ctrl vs. SOSTDC1(5)	10.83	decreased axonal sprouting	> 0.9999
Ctrl vs. Otx2(2)	-50.38	increased axonal sprouting	0.0077
Ctrl vs. Zbtb32	-8.957	increased axonal sprouting	> 0.9999
Ctrl vs. Crx(2)	8.224	decreased axonal sprouting	> 0.9999

Table 4.3 Neurite outgrowth candidate screen: Tau label for axons

Table 4.4

Candidate Comparison	Mean difference in dendrite length per neuron (μm , control relative to knockout)	Effect of knockout	Bonferroni adjusted p-value
Ctrl vs. MEF2c	-7.832	increased dendritic outgrowth	> 0.9999
Ctrl vs. YY1	-24.67	increased dendritic outgrowth	0.0012
Ctrl vs. WAP	-19.43	increased dendritic outgrowth	0.0312
Ctrl vs. Casp14	-8.411	increased dendritic outgrowth	> 0.9999
Ctrl vs. Nat8l	-6.71	increased dendritic outgrowth	> 0.9999
Ctrl vs. Crx	2.359	decreased dendritic outgrowth	> 0.9999
Ctrl vs. NeuroG3	33.55	decreased dendritic outgrowth	< 0.0001
Ctrl vs. Otx2	15.12	decreased dendritic outgrowth	0.6174
Ctrl vs. NGFR	24.54	decreased dendritic outgrowth	0.0206
Ctrl vs. EphA10	-29.02	increased dendritic outgrowth	0.0002
Ctrl vs. Nat8l(2)	-6.329	increased dendritic outgrowth	> 0.9999
Ctrl vs. NGFR(2)	17.31	decreased dendritic outgrowth	0.0914
Ctrl vs. SOSTDC1(5)	-42.01	increased dendritic outgrowth	< 0.0001
Ctrl vs. Otx2(2)	-25.08	increased dendritic outgrowth	0.0012
Ctrl vs. Zbtb32	-36.26	increased dendritic outgrowth	< 0.0001
Ctrl vs. Crx(2)	-11.62	increased dendritic outgrowth	> 0.9999

Table 4.4 Neurite outgrowth candidate screen: MAP2 label for dendrites

4.5 Methods

Fluidigm qPCR

Independent cohorts of animals were generated for FACS isolation of RSC FG+ cells from stroke only and stroke+limb overuse groups, and RSC NCAM+ control cells. After FACS purification of the cell populations of interest, cDNA was generated for the Fluidigm qPCR studies. Validated qPCR primers were selected from PrimerBank (<https://pga.mgh.harvard.edu/primerbank/>) for all 40 candidate genes and 3 housekeeping genes. In addition to GAPDH, two additional housekeeping genes *sdha* and *ywhaz* were chosen as previous studies indicated their robustness in the setting of ischemia (Gubern *et al.*, 2009). T_a for all primers was 55°C. A 48x48 microfluidic chamber was used to run 12 samples by 40 gene targets. Since input cDNA is low, Fluidigm uses a 14-cycle pooled-target preamplification step to increase target concentration prior to chip run (Citri *et al.*, 2012). This step is particularly necessary for targets with fewer than 1000 copies/uL of sample, as our samples likely fell into this range (RNA input was on the order of hundreds of pg/uL). 5uL samples were run on the 48x48 chip run using 35X PCR cycle with 10min hotstart. Transcript fold change was calculated using $2^{[Ct(Sdha \text{ housekeeping gene}) - Ct(\text{target})]}$.

CRISPR/cas9 guide-RNA design:

LentiCRISPRV2 CRISPR/cas9 constructs previously developed for viral application (gift from Feng Zhang, (Sanjana *et al.*, 2014; Shalem *et al.*, 2014)) were used for in-vitro axonal sprouting assay. Guide RNAs 20-22bps were designed using CHOPCHOP (<https://chopchop.rc.fas.harvard.edu/>) and Benchling (<https://benchling.com/editor>). Specific gRNA selection was prioritized by high sensitivity and specificity. Two gRNAs were designed for

each candidate gene, and SURVEYOR assays (IDT) were performed for mutation detection. qPCR to confirm transcript knockdown was also performed to ensure efficiency of the cas9 platform.

Lentivirus packaging:

LentiCRISPRV2 with respective gRNA inserts were cotransfected with PAX2 (AddGene12260) and pVSVg (AddGene 8454) packaging plasmids into HEK 293FT cells (Invitrogen) via calcium phosphate transfection. Since LentiCRISPRV2 does not itself have a fluorescent reporter, a positive control plasmid was used for transfection confirmation and viral production (CMV-EGFP AddGene 19319). Virus was collected over 48 hours, PEG precipitated, and functionally titered at 10^8 - 10^9 viral particles /mL. Lentivirus transduction was confirmed for CRISPR viruses by infecting Hek293 cells in 24 well format and immunostaining for cas9 (Mouse, Cell Signaling, 1:250).

In-vitro neuronal outgrown screen:

Primary mouse cortical neurons were prepared from P3 C57/BL6 mice. Briefly, mouse pups were euthanized on ice and a midline incision of the scalp and underlying translucent skull revealed the brain for removal. Under a dissecting microscope, meninges were carefully removed, cortices shelled off from underlying white matter, and detached from hippocampal formation. The sensorimotor cortex was isolated, quartered, and collected in 4 °C HBSS (calcium and magnesium free). After dissections, cortical tissue chunks were transferred to a dissociation solution of preheated 37 °C HBSS + 0.2%w/v papain solution (Worthington Biochemical), and digested for 12 min with occasional tube inversion. DNase I and FBS were added after the dissociation to detach tissue chunks and stop the papain reaction, respectively. The resulting cell suspension was passed through a 70um cell strainer and counted. Cells were plated into NbActiv medium (BrainBits, USA)

at 30K/well in a 96well plate (Ibidi, Germany) coated with poly-d-lysine (Sigma, USA). All conditions were tested in double or triple replicates.

24 hours after seeding at DIV1, CRISPR/cas9 lentivirus was used to transduce cells at an MOI of 8-20. On DIV5, cells were fixed in 2% PFA and immunostained using Tau (Millipore, Mouse, 1:1000), MAP2 (Abcam, Chicken, 1:1000), and NeuN (Abcam, Rabbit, 1:1000). Tau labels axonal processes, MAP2 dendrites, and NeuN neuronal cell bodies. Donkey secondary antibodies (JacksonImmuno, PA) against Mouse (cy3), Chicken (cy5), and NeuN (cy2) were used at 1:400 for fluorescent conjugation. After the last wash, cells were left in cold PBS for in-well imaging on the ImageXpress confocal microscope (Molecular Devices, UCLA Molecular Shared Screening Resource).

ImageXpress confocal image acquisition and MetaExpress data analysis:

Systematic image acquisition parameters were set for automation of plate imaging on the ImageXpress platform. 16 images were taken from each well at 20X for unbiased sampling across all conditions. Cy2, cy3, and cy5 channels were used on the confocal for acquiring NeuN, Tau, and MAP2 signals, respectively. All raw .tif image files were saved onto the core server from which downstream MetaExpress analyses were performed. MetaExpress software was used for quantification of total neuronal outgrowth, cell number, and average neuronal outgrowth (a division of the two parameters). Neurite tracing was optimized by converting color images to 8bit files and configuring cell body size, neurite signal intensity to background ratios, and maximum neurite thickness. Tracing overlays were visually confirmed to be high fidelity coverage of the original fluorescent image. Total quantitative metrics were exported to excel and differences among multiple means were assessed by one-way ANOVA followed by Tukey-Kramer's *post hoc* tests using

GraphPad Prism version 6 (GraphPad Software). Significance was corrected for by using Bonferroni's multiple comparisons p-values.

4.6 References:

- Abe, N., Cavalli, V., 2008. Nerve injury signaling. *Current opinion in neurobiology* 18, 276-283.
- Beurdeley, M., Spatazza, J., Lee, H.H., Sugiyama, S., Bernard, C., Di Nardo, A.A., Hensch, T.K., Prochiantz, A., 2012. Otx2 binding to perineuronal nets persistently regulates plasticity in the mature visual cortex. *The Journal of neuroscience : the official journal of the Society for Neuroscience* 32, 9429-9437.
- Carmichael, S.T., Archibeque, I., Luke, L., Nolan, T., Momiy, J., Li, S., 2005. Growth-associated gene expression after stroke: evidence for a growth-promoting region in peri-infarct cortex. *Experimental neurology* 193, 291-311.
- Chaldakov, G.N., Tonchev, A.B., Aloe, L., 2009. NGF and BDNF: from nerves to adipose tissue, from neurokines to metabokines. *Riv Psichiatr* 44, 79-87.
- Chandran, V., Coppola, G., Nawabi, H., Omura, T., Versano, R., Huebner, E.A., Zhang, A., Costigan, M., Yekkirala, A., Barrett, L., Blesch, A., Michaelovski, I., Davis-Turak, J., Gao, F., Langfelder, P., Horvath, S., He, Z., Benowitz, L., Fainzilber, M., Tuszynski, M., Woolf, C.J., Geschwind, D.H., 2016. A Systems-Level Analysis of the Peripheral Nerve Intrinsic Axonal Growth Program. *Neuron* 89, 956-970.
- Cheng, A.W., Wang, H., Yang, H., Shi, L., Katz, Y., Theunissen, T.W., Rangarajan, S., Shivalila, C.S., Dadon, D.B., Jaenisch, R., 2013. Multiplexed activation of endogenous genes by CRISPR-on, an RNA-guided transcriptional activator system. *Cell research* 23, 1163-1171.
- Cho, S.W., Kwak, S., Woolley, T.E., Lee, M.J., Kim, E.J., Baker, R.E., Kim, H.J., Shin, J.S., Tickle, C., Maini, P.K., Jung, H.S., 2011. Interactions between Shh, Sostdc1 and Wnt signaling and a new feedback loop for spatial patterning of the teeth. *Development* 138, 1807-1816.
- Citri, A., Pang, Z.P., Sudhof, T.C., Wernig, M., Malenka, R.C., 2012. Comprehensive qPCR profiling of gene expression in single neuronal cells. *Nature protocols* 7, 118-127.

- Cong, L., Ran, F.A., Cox, D., Lin, S., Barretto, R., Habib, N., Hsu, P.D., Wu, X., Jiang, W.,
Marraffini, L.A., Zhang, F., 2013. Multiplex genome engineering using CRISPR/Cas systems.
Science 339, 819-823.
- Dahlman, J.E., Abudayyeh, O.O., Joung, J., Gootenberg, J.S., Zhang, F., Konermann, S., 2015.
Orthogonal gene knockout and activation with a catalytically active Cas9 nuclease. *Nature
biotechnology* 33, 1159-1161.
- Dancause, N., Barbay, S., Frost, S.B., Plautz, E.J., Chen, D., Zoubina, E.V., Stowe, A.M., Nudo, R.J.,
2005. Extensive cortical rewiring after brain injury. *The Journal of neuroscience : the official journal
of the Society for Neuroscience* 25, 10167-10179.
- Dickson, B.J., 2002. Molecular mechanisms of axon guidance. *Science* 298, 1959-1964.
- Ding, B., Kilpatrick, D.L., 2013. Lentiviral vector production, titration, and transduction of primary
neurons. *Methods in molecular biology* 1018, 119-131.
- Doudna, J.A., Charpentier, E., 2014. Genome editing. The new frontier of genome engineering with
CRISPR-Cas9. *Science* 346, 1258096.
- Geraerts, M., Willems, S., Baekelandt, V., Debyser, Z., Gijssbers, R., 2006. Comparison of lentiviral
vector titration methods. *BMC biotechnology* 6, 34.
- Gilbert, L.A., Horlbeck, M.A., Adamson, B., Villalta, J.E., Chen, Y., Whitehead, E.H., Guimaraes, C.,
Panning, B., Ploegh, H.L., Bassik, M.C., Qi, L.S., Kampmann, M., Weissman, J.S., 2014.
Genome-Scale CRISPR-Mediated Control of Gene Repression and Activation. *Cell* 159, 647-
661.
- Gubern, C., Hurtado, O., Rodriguez, R., Morales, J.R., Romera, V.G., Moro, M.A., Lizasoain, I.,
Serena, J., Mallolas, J., 2009. Validation of housekeeping genes for quantitative real-time
PCR in in-vivo and in-vitro models of cerebral ischaemia. *BMC molecular biology* 10, 57.

- Hsu, P.D., Lander, E.S., Zhang, F., 2014. Development and applications of CRISPR-Cas9 for genome engineering. *Cell* 157, 1262-1278.
- Ikeda, K., Nukumi, N., Iwamori, T., Osawa, M., Naito, K., Tojo, H., 2004. Inhibitory function of whey acidic protein in the cell-cycle progression of mouse mammary epithelial cells (EpH4/K6 cells). *J Reprod Dev* 50, 87-96.
- Ishino, Y., Shinagawa, H., Makino, K., Amemura, M., Nakata, A., 1987. Nucleotide sequence of the iap gene, responsible for alkaline phosphatase isozyme conversion in Escherichia coli, and identification of the gene product. *J Bacteriol* 169, 5429-5433.
- Karlstetter, M., Walczak, Y., Weigelt, K., Ebert, S., Van den Brulle, J., Schwer, H., Fuchshofer, R., Langmann, T., 2010. The novel activated microglia/macrophage WAP domain protein, AMWAP, acts as a counter-regulator of proinflammatory response. *Journal of immunology* 185, 3379-3390.
- Lin, C.Q., Dempsey, P.J., Coffey, R.J., Bissell, M.J., 1995. Extracellular matrix regulates whey acidic protein gene expression by suppression of TGF-alpha in mouse mammary epithelial cells: studies in culture and in transgenic mice. *The Journal of cell biology* 129, 1115-1126.
- Ma, W., Yan, R.T., Mao, W., Wang, S.Z., 2009. Neurogenin3 promotes early retinal neurogenesis. *Mol Cell Neurosci* 40, 187-198.
- Mali, P., Yang, L., Esvelt, K.M., Aach, J., Guell, M., DiCarlo, J.E., Norville, J.E., Church, G.M., 2013. RNA-guided human genome engineering via Cas9. *Science* 339, 823-826.
- Nelson, C.E., Hakim, C.H., Ousterout, D.G., Thakore, P.I., Moreb, E.A., Castellanos Rivera, R.M., Madhavan, S., Pan, X., Ran, F.A., Yan, W.X., Asokan, A., Zhang, F., Duan, D., Gersbach, C.A., 2016. In vivo genome editing improves muscle function in a mouse model of Duchenne muscular dystrophy. *Science* 351, 403-407.

- Nielsen, J.V., Thomassen, M., Mollgard, K., Noraberg, J., Jensen, N.A., 2014. Zbtb20 defines a hippocampal neuronal identity through direct repression of genes that control projection neuron development in the isocortex. *Cerebral cortex* 24, 1216-1229.
- Overman, J.J., Carmichael, S.T., 2014. Plasticity in the injured brain: more than molecules matter. *The Neuroscientist : a review journal bringing neurobiology, neurology and psychiatry* 20, 15-28.
- Overman, J.J., Clarkson, A.N., Wanner, I.B., Overman, W.T., Eckstein, I., Maguire, J.L., Dinov, I.D., Toga, A.W., Carmichael, S.T., 2012. A role for ephrin-A5 in axonal sprouting, recovery, and activity-dependent plasticity after stroke. *Proceedings of the National Academy of Sciences of the United States of America* 109, E2230-2239.
- Ran, F.A., Hsu, P.D., Wright, J., Agarwala, V., Scott, D.A., Zhang, F., 2013. Genome engineering using the CRISPR-Cas9 system. *Nature protocols* 8, 2281-2308.
- Sanjana, N.E., Shalem, O., Zhang, F., 2014. Improved vectors and genome-wide libraries for CRISPR screening. *Nat Methods* 11, 783-784.
- Shalem, O., Sanjana, N.E., Hartenian, E., Shi, X., Scott, D.A., Mikkelsen, T.S., Heckl, D., Ebert, B.L., Root, D.E., Doench, J.G., Zhang, F., 2014. Genome-scale CRISPR-Cas9 knockout screening in human cells. *Science* 343, 84-87.
- Sharma, A., Moore, M., Marcora, E., Lee, J.E., Qiu, Y., Samaras, S., Stein, R., 1999. The NeuroD1/BETA2 sequences essential for insulin gene transcription colocalize with those necessary for neurogenesis and p300/CREB binding protein binding. *Mol Cell Biol* 19, 704-713.
- Simon-Arecas, J., Dopazo, A., Dettenhofer, M., Rodriguez-Tebar, A., Garcia-Segura, L.M., Arevalo, M.A., 2011. Formin1 mediates the induction of dendritogenesis and synaptogenesis by neurogenin3 in mouse hippocampal neurons. *PLoS one* 6, e21825.

- Sperry, R.W., 1963. Chemoaffinity in the orderly growth of nerve fiber patterns and connections. *Proceedings of the National Academy of Sciences of the United States of America*, 703-710.
- Sugiyama, S., Di Nardo, A.A., Aizawa, S., Matsuo, I., Volovitch, M., Prochiantz, A., Hensch, T.K., 2008. Experience-dependent transfer of Otx2 homeoprotein into the visual cortex activates postnatal plasticity. *Cell* 134, 508-520.
- Tabebordbar, M., Zhu, K., Cheng, J.K., Chew, W.L., Widrick, J.J., Yan, W.X., Maesner, C., Wu, E.Y., Xiao, R., Ran, F.A., Cong, L., Zhang, F., Vandenberghe, L.H., Church, G.M., Wagers, A.J., 2016. In vivo gene editing in dystrophic mouse muscle and muscle stem cells. *Science* 351, 407-411.
- Wahl, A.S., Omlor, W., Rubio, J.C., Chen, J.L., Zheng, H., Schroter, A., Gullo, M., Weinmann, O., Kobayashi, K., Helmchen, F., Ommer, B., Schwab, M.E., 2014. Neuronal repair. Asynchronous therapy restores motor control by rewiring of the rat corticospinal tract after stroke. *Science* 344, 1250-1255.
- Wen, J., Kawamata, Y., Tojo, H., Tanaka, S., Tachi, C., 1995. Expression of whey acidic protein (WAP) genes in tissues other than the mammary gland in normal and transgenic mice expressing mWAP/hGH fusion gene. *Mol Reprod Dev* 41, 399-406.

CHAPTER 5.

GDF10 IS A MOLECULAR SIGNAL FOR POST-STROKE AXONAL SPROUTING AND IMPROVED MOTOR RECOVERY

5.1 Introduction

In 2010, Li and colleagues published the first study in the field to systematically map the molecular “sprouting transcriptome” after stroke. This landmark study showed that peri-infarct neuronal sprouting after stroke occurs through coordinated signaling systems. Brain injury induces secreted factor signaling in the extracellular environment, cell-intrinsic cytoplasmic cascades, and nuclear transcriptional responses. One key finding was that axonal sprouting as a molecular process differs by age. In sprouting neurons isolated from the aged brain at 7 days after stroke, one of the most highly upregulated genes was Growth and Differentiation Factor 10, or GDF10 (Li *et al.*, 2010). GDF10 emerged as a leading candidate for mechanistic analysis because it is a secreted factor found in the highly dynamic peri-infarct cortex, it has growth promoting roles in development, and signals through transforming growth factor B receptors (TGFBR) that can be pharmacologically targeted.

In these series of studies, we show that GDF10 gain of function produces increased axonal sprouting in-vitro and in-vivo. Further, in-vivo delivery of the GDF10 protein brain during the recovery period increases motor improvement after injury in a mouse model of ischemic stroke. In this post-stroke role, GDF10 signals through the Smad2/3 pathway. RNA-Seq analysis of GDF10 signaling reveals that it is a process distinct from other CNS injury-related, developmental, and other adult plasticity paradigms. Finally, the translational potential for these findings are significant because GDF10 upregulation in peri-infarct cortex is found across rodent, monkey, and human brain. We hope to move these findings toward therapeutic targeting after stroke.

5.2 Results

GDF10 increases axonal sprouting in-vitro and in-vivo

Since GDF10 was identified bioinformatically from peri-infarct sprouting neurons (Li *et al.*, 2010), the first step in these studies was to confirm its mechanistic role in promoting the sprouting phenotype. Primary mouse cortical neurons age P4 exhibited increased axonal outgrowth upon GDF10 addition to the growth medium compared to control medium alone (Fig 5.1a). Knockdown of GDF10 using siRNA inhibits axonal outgrowth from primary cortical neurons, a culture model system where GDF10 is expressed in neurons that have undergone the plating process (Fig 5.1b). Next, GDF10 protein delivery from hydrogel formulated for extended release increased axonal sprouting compared to delivery of an inert protein control, cytochrome C. In particular, the sprouting occurred in an anterior direction to the motor cortex, toward premotor cortex (Fig5.2a). Conversely, siRNA knockdown of GDF10 significantly inhibits cortical axonal sprouting after stroke, producing a pattern of connections that resembles the non-stroke, normal brain (Fig. 5.1b).

Does GDF10 axonal sprouting result in synaptic contacts in reorganizing circuits? To answer this question, we performed immunofluorescent colocalization analysis of the pre- and post-synaptic markers VGLUT2 and Homer1. These studies indicate that BDA-labeled sprouting neurons contain the pre-synaptic glutamatergic marker in tight association with the post-synaptic marker Homer1 (Fig 5.3). Analyses were performed in premotor cortex, a region of the motor system with increased axonal sprouting as indicated by in cortical mapping studies (Fig5.2b).

GDF10 increases motor functional recovery after stroke

Next, we aimed to understand if GDF10-induced axonal sprouting promotes functional recovery. After GDF10 protein or GDF10 targeted siRNA delivery to the peri-infarct cortex, we tested mice on forelimb motor tasks using the stroke-affected forelimb. This is the same ipsilesional

cortex in which axonal sprouting was measured. The grid walking, cylinder and pasta handling tasks are motor tests that measure gait, exploratory forelimb use and skilled control of thin pasta pieces, respectively (Overman *et al.*, 2012; Tennant *et al.*, 2010).

Stroke produces impairments in forelimb motor control for an extended period: at least 11 weeks (pasta handling) or 15 weeks after stroke (cylinder, gridwalking) (Fig. 5.4). GDF10 treatment starting 1 week after stroke enhances recovery beginning from 3 weeks post-stroke (Fig. 5.4). With GDF10 delivery, mice performed at the level of non-stroke motor control by 5 weeks after stroke. Remarkably, GDF10 siRNA significantly reduces the normal process of recovery after stroke, beginning 1-3 weeks after delivery. No significant changes in motor performance were observed among animals treated with inert protein or scrambled siRNA controls. Thus, administration of GDF10 protein improves motor recovery after stroke and knocking down GDF10 levels significantly decreases functional recovery. These behavioral data point toward an important endogenous role for GDF10 in recovery after stroke, and furthermore, also suggest that the neuronal sprouting mapped *in vivo* (Fig 5.2a) may represent formation of functional neural circuits that cause behavioral improvement.

GDF10 is expressed in the peri-infarct cortex across species

Initially, GDF10 was identified in the rat brain as an upregulated gene found in peri-infarct sprouting neurons (Li *et al.*, 2010). Further Immunohistochemical analyses across a range of species, mouse macaque and human, indicate that GDF10 upregulation after stroke is conserved across different vertebrates (Fig 5.5). Furthermore, cellular phenotyping alongside GDF10 immunostaining indicates that it is expressed in neurons and seen extracellularly, as it is a secreted protein. Microglia and astrocytes do not upregulate GDF10 after stroke (Fig 5.6).

GDF10-induces a molecular transcriptome distinct from other CNS injury, developmental, and learning-related paradigms

Next, we aimed to identify the molecular systems behind post-stroke GDF10-induced axonal sprouting and functional recovery. Using the FACS approach developed in the RSC-PMC studies (Chapter 3), neurons were isolated from GDF10+stroke, stroke alone, normal control and developmental P4 cortex. The number of reads ranged from 64,602,785 to 107,291,640 and the uniquely mapped reads ranged from 43,087,682 to 85,407,243. The differentially expressed genes were analyzed using a false discovery rate (FDR) threshold of <0.1 .

We used unsupervised genome-wide principal component analysis to compare our data from GDF10 and stroke to other plasticity transcriptomes. These transcriptomes include cortical neuron outgrowth during development, the cortical critical period, mouse growth cones, P7 to P28 mouse neurons, motor cortex after spinal cord injury, retina after optic nerve crush, contralateral cortex after stroke, and learning and memory paradigms in hippocampus and medial prefrontal cortex (Table 5.1). Original microarray or RNA-Seq data from published array files were compiled, normalized, controlled for batch effect and statistically compared to the present data sets for cortical neurons from stroke, stroke+GDF10, no stroke control and P4.

The greatest difference in the analyzed conditions is between adult cortical neurons (from control, stroke and stroke+GDF10 conditions) and cortical neurons from the developmental age of P4 (Figure 5.7). This indicates that growth states in adult and developmental neurons are transcriptionally more different from each than cortical neuron transcription before and after injury (and +/- GDF10). This finding also challenges an idea that “regeneration recapitulates development.” Although earlier single gene studies showed overlap between isolated axonal developmental and axonal regeneration genes (Ng *et al.*, 1988), unsupervised cluster analysis across transcriptomes confirms that the adult and neonatal gene expression transcriptomes cluster according to age and

stage of development (Fig 5.7). After this distinction, the most unique transcriptome is stroke+GDF10 vs. stroke. In addition, stroke and stroke+GDF10 transcriptomes cluster closely together with a partial relationship to retina 12 hours after optic nerve crush. Stroke+GDF10 or stroke-alone transcriptomes lie distant from mouse growth cone, mouse cortical critical period and corticospinal and callosal postnatal neuronal transcriptomes, which themselves do cluster together. These clustering analyses indicate that GDF10 induces a distinct transcriptional profile after stroke, more closely related to stroke without GDF10 treatment than to the transcriptomes derived from neuronal development, CNS injury and learning and memory paradigms.

GDF10, a molecular signal for axonal sprouting in the adult brain after stroke, regulates a unique transcriptome that consists of a smaller number of genes from that seen during the initial process of neurodevelopmental axonal sprouting. Consistent with other studies (Li *et al.*, 2010), these data show that axonal outgrowth genes vary according to age of the brain, and the initial process of axonal sprouting in neurodevelopment in general is quite different molecularly from neuronal growth in the adult state. IPA network analyses indicate that Stroke+GDF10 highly regulates Axonal Guidance, PTEN and PI3K signaling (Fig 5.8) pathways after stroke. GDF10 delivery after stroke downregulates PTEN canonical signaling and upregulates PI3K canonical signaling (Table 5.2). There is precedent in the field for PTEN and SOCS3 inhibition of axonal sprouting in the adult CNS; their knockout in optic nerve and spinal cord injury increases axonal sprouting after injury (Liu *et al.*, 2010; Sun *et al.*, 2011). GDF10 also differentially regulates axonal guidance molecules including Ephrin A3, T α 1tubulin, Beta-II-tubulin, VEGF_d, neuropilin 1, SOCS3 and downstream molecules in the Rho and Rac pathways (Table 5.2). Together, these delineated molecules may represent a potential mechanism of action for GDF10 in axonal sprouting after stroke.

5.4 Discussion

The last two and a half decades have produced compelling studies that show the peri-infarct neurons are placed into a growth state after stroke. Much research has since focused on overcoming the growth inhibitory environment of the adult brain; relatively less basic science is known about promoting the intrinsic growth state in the post-stroke brain. In the present studies, we show that GDF10 is an important player that induces axonal sprouting and improves recovery after stroke. GDF10 is a growth promoting molecule upregulated in peri-infarct cortex after stroke in the rodent, monkey and human brain (Fig 5.5). We find that it is a potent initiator of axonal sprouting in the peri-infarct cortex. The sprouted neurons also support synaptogenesis in premotor cortex and are correlated with improved functional motor recovery after stroke. GDF10 is a divergent member of the bone morphogenetic protein (BMP)/transforming growth factor- β (TGF β) superfamily (Cunningham *et al.*, 1995), and signal through TGF β receptors (TGF β R) (Akhurst and Hata, 2012). It activates a unique transcriptional program that in part works through PTEN and SOCS3 inhibition. Though GDF10 mRNA is strongly expressed in the developing brain (Soderstrom and Ebendal, 1999), the current study is the first to identify a role for GDF10 in the adult brain or after CNS injury.

Axonal mapping studies of the peri-infarct cortex after GDF10 induction leads to increased sprouting toward premotor cortex, a motor system area previously associated with functional recovery after stroke (Overman *et al.*, 2012; Zeiler *et al.*, 2013). Although we did not perform electron microscopy (EM) studies of synapse terminals, the tight association of pre- and post-synaptic markers suggests GDF10-induced axonal sprouting may support excitatory synaptogenesis. Future studies of these specific synapses using EM and electrophysiological (i.e. paired pulse recoding) or optogenetic functional circuit mapping will more fully elucidate the mechanisms of functional rewiring.

Axonal sprouting after stroke shares similarities with the neuronal morphology changes in learning and memory paradigms, optic nerve and spinal cord regeneration and neurodevelopment. From this perspective, we wanted to further probe the molecular similarities between these morphologically related but functionally disparate plasticity paradigms. By comparing transcriptomes that represent different plasticity states throughout development and adulthood, we find that the expression profile of post-stroke sprouting neurons lie distant from cortical developmental profiles, but in part overlaps with an optic nerve injury profile. RNA-Seq analyses of GDF10-induced neurons indicate that PTEN and SOC3 pathways are inhibited. This represents a mechanistic connection with findings in the optic nerve and spinal cord regeneration fields (Du *et al.*, 2015; Sun *et al.*, 2011).

In total, we highlight the mechanistic roles of GDF10 related plasticity in the post-stroke brain. GDF10 is a growth-promoting factor with widely conserved expression after injury. This finding, coupled with our discovery of GDF10-induced anatomic plasticity and functional recovery, may signal high translational potential for molecular delivery in future stroke therapies.

5.4 Chapter 5. Figures

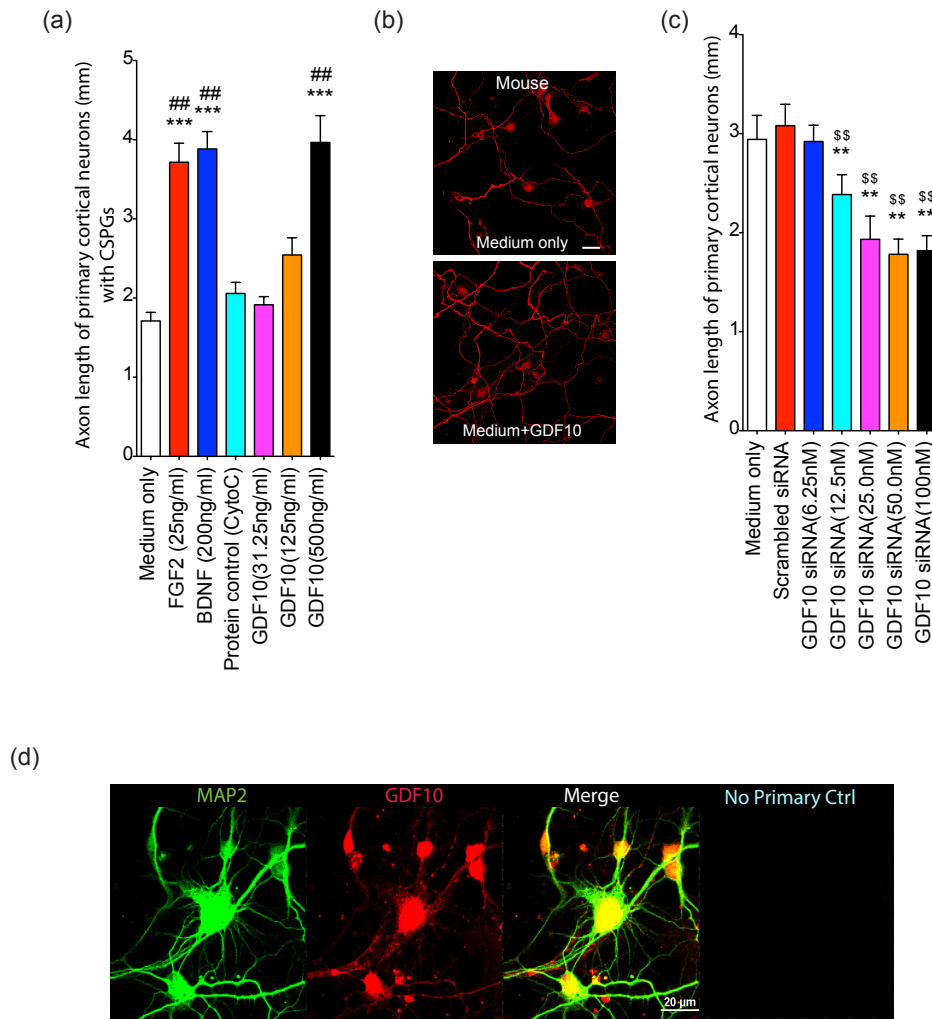


Figure 5.1 GDF10 enhances axonal outgrowth in primary neurons *in vitro*

(a) Axonal outgrowth in P4 mouse primary cortical neurons. Wells were plated with CSPG before cell growth to mimic extracellular inhibition in adult CNS. Axon length was measured after 3d in culture. Cyto C = cytochrome C, a protein control for the addition of growth factor, used in the *in vivo* studies (Fig. 4a). The whiskers show the minimum and maximum values. (b) P4 cortical neurons stained with SMI-312 after 2 additional days culture in medium alone or medium + GDF10 (500ng/ml). Scale bar represents 20µm. (c) P4 mouse primary cortical neurons treated with siRNA targeted toward GDF10 or scramble siRNA control. siRNA between 12.5-100nM produced significant decrease in neuron outgrowth. Independent cultures per condition and, in each culture, four wells repeating the condition. $**P < 0.01$ compared with medium only; $##P < 0.01$ compared with scrambled + GDF10; $$$P < 0.05$ compared with scrambled siRNA. All conditions were tested in quadruplicate, in two separate experiments. **a**, $F(6, 105) = 7.220$; **b**, $F(6, 105) = 8.384$; **c**, $F(6, 105) = 22.44$. All observations were normalized to the number of NeuN⁺ cells in each sample. Statistical testing was repeated-measures ANOVA followed by Tukey-Kramer's *post hoc* test (a–c) or one-tail unpaired *t* test (e).

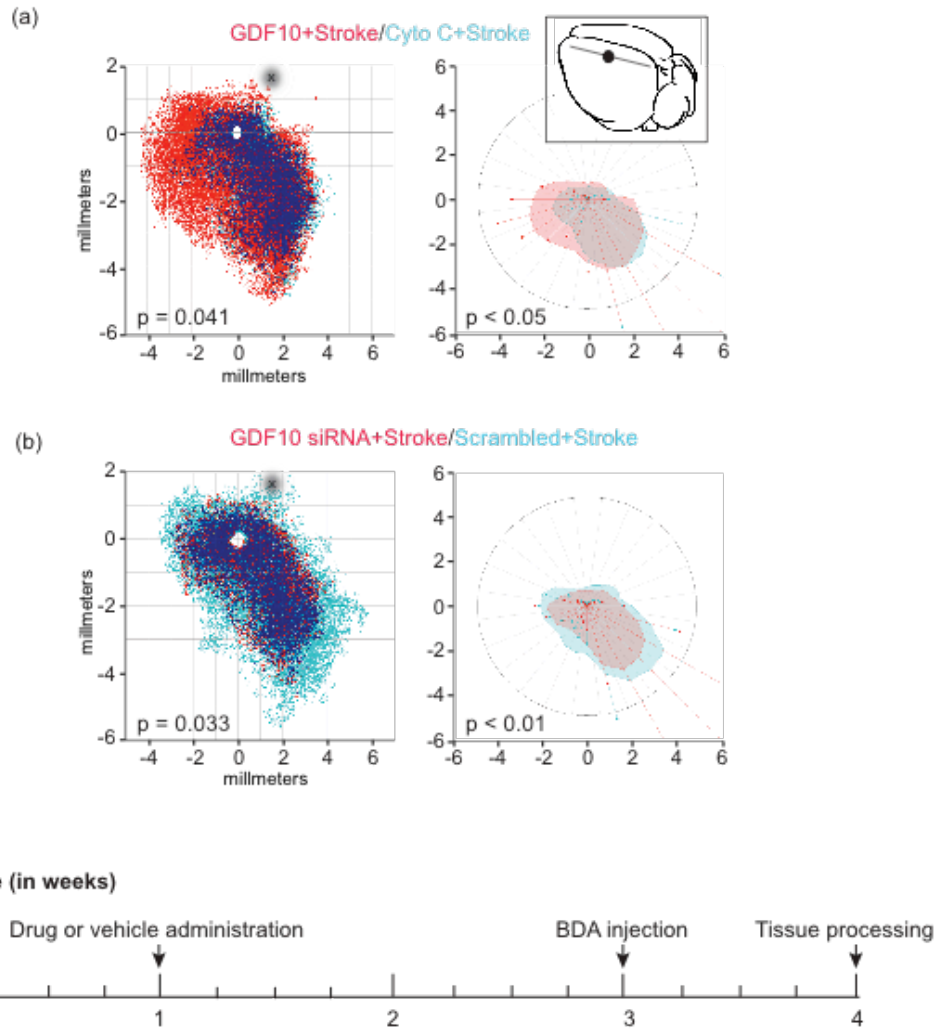


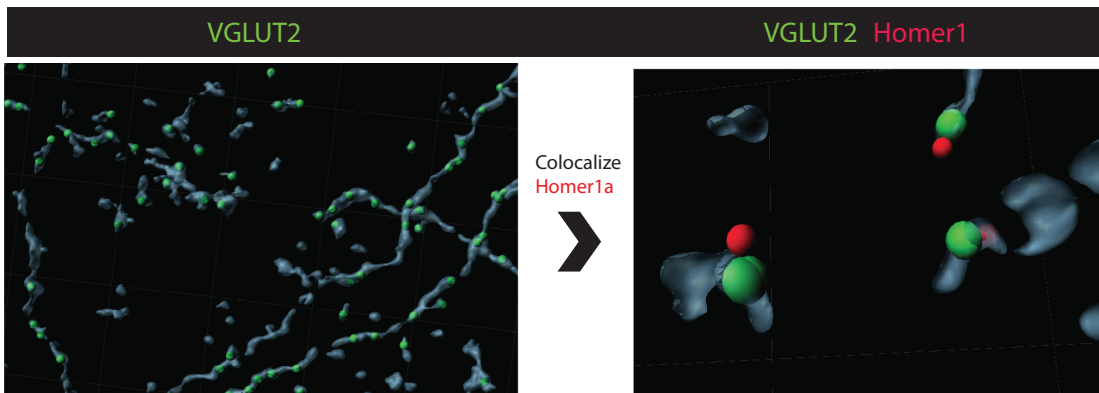
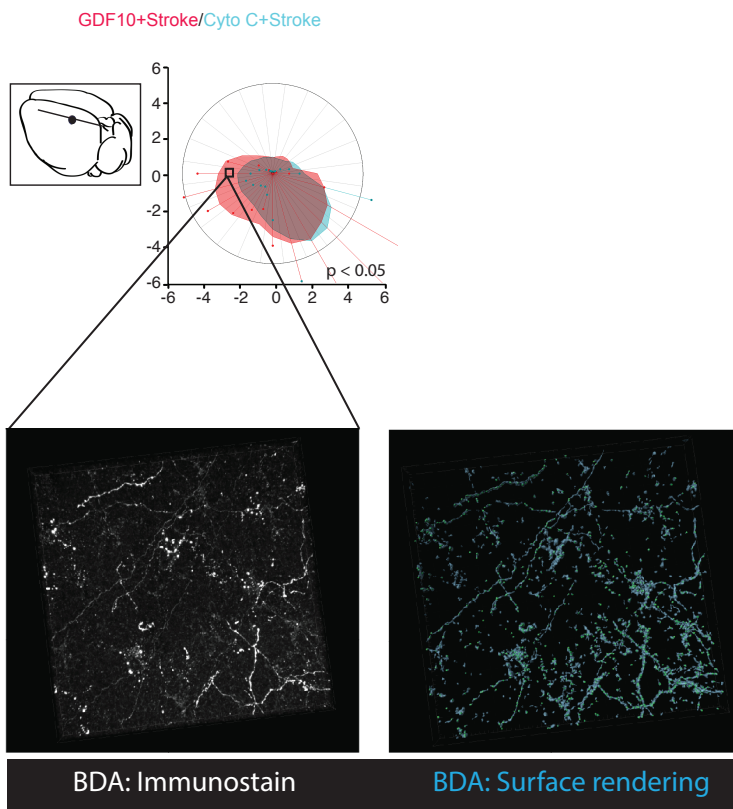
Figure 5.2 GDF10 promotes axonal connections in peri-infarct cortex after stroke

a) Left: quantitative cortical mapping of connections in layers II/III of the flattened mouse cortical hemisphere ipsilateral to the forelimb motor cortex in stroke with protein control (Cyto C) (blue, $n=8$), GDF10+stroke (red, $n=8$) and areas of dense overlap of these two conditions (dark blue). x and y axes are distances in millimeters from the center of the BDA tracer injection (empty circle). P value is Hotelling's T^2 test. Right: Polar plot of connections of forelimb motor cortex projections relative to the tracer injection in forelimb motor cortex as the origin. Filled polygons represent the 70th percentile of the distances of all BDA-labeled connections from the injection site in each segment of the graph. Weighted polar vectors represent the median vector multiplied by the median of the normal distribution of the number of points in a given segment of the graph. P value is Watson's nonparametric two-sample U^2 test. Inset shows schematic lateral view of mouse brain. The horizontal line shows the position in which neuronal label was quantified.

(b) Left: quantitative cortical mapping of GDF10 knockdown in stroke. Right: polar plots of GDF10 siRNA and scrambled siRNA after stroke. Data are presented as in **a**. The gray shaded circle in **a** and **b** indicates the center of the stroke site.

(c) Timeline of stroke surgery, drug/control delivery, BDA labeling, and tissue analysis

a)



b) Video: Synaptic connections identified in peri-infarct cortex after GDF10 treatment
http://www.nature.com/neuro/journal/v18/n12/fig_tab/nn.4146_SV1.html

Figure 5.3 Synaptic connections are formed in peri-infarct cortex after GDF10 treatment

a) Synaptic analysis was performed in the same peri-infarct tissues from animals used for BDA axonal sprouting maps in Fig. 4a) and b). Presynaptic VGLUT2 and postsynaptic Homer1 antibodies were used for identification of synaptic contacts. Marker colocalization analyses were performed on Imaris Imaging software (Bitplane, Version 8.1.1) by 1) creating a surface for BDA positive neurons 2) colocalizing presynaptic VGLUT2 within BDA surface 3) excluding postsynaptic Homer1 in BDA positive cells and 4) colocalizing presynaptic and postsynaptic datasets to $<0.75\mu\text{m}$. These analyses uniquely identify the synaptic connections formed by GDF10-induced sprouting cortical neurons after stroke (mapped in Fig. 4). **b)** Video through a 15um thick section of peri-infarct cortex taken at 100x. BDA surface is shown in light blue. VGLUT2 presynaptic marker is shown by green spots, and Homer1 postsynaptic marker in red spots.

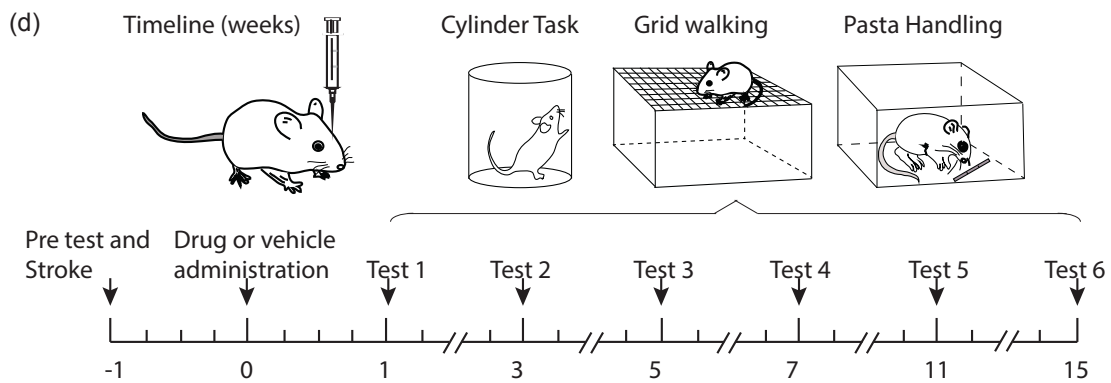
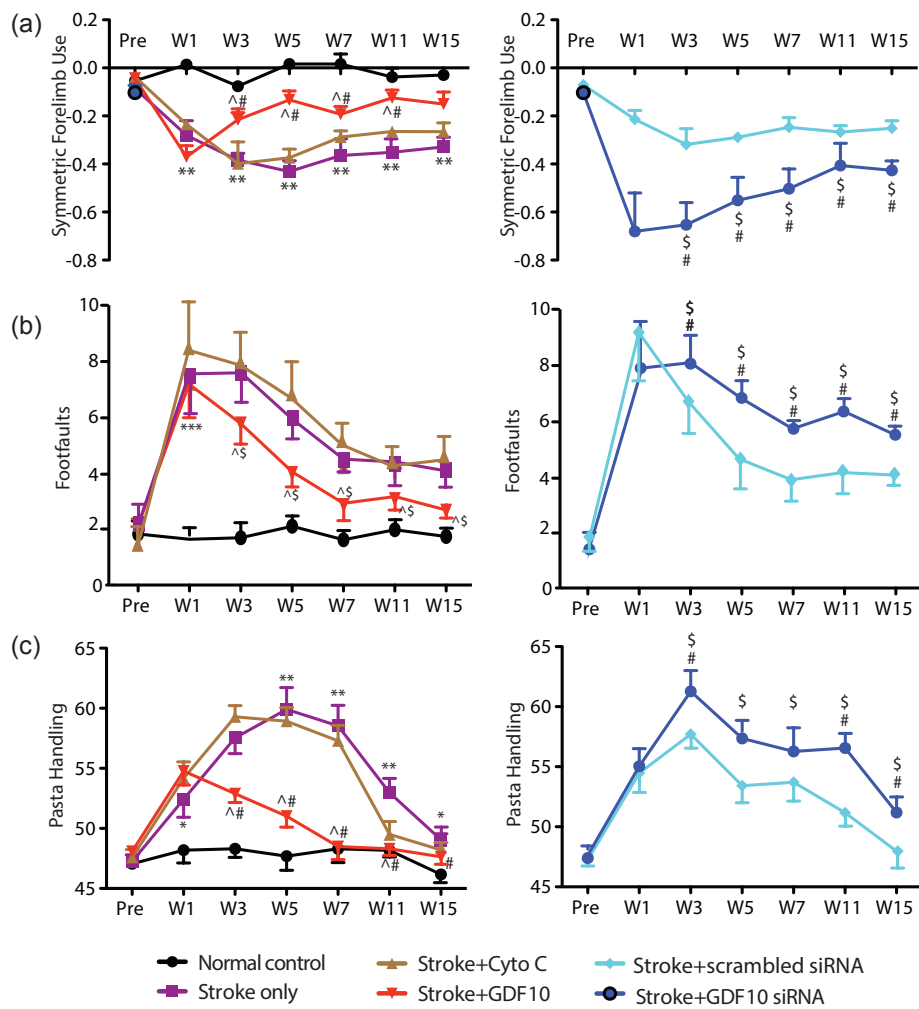
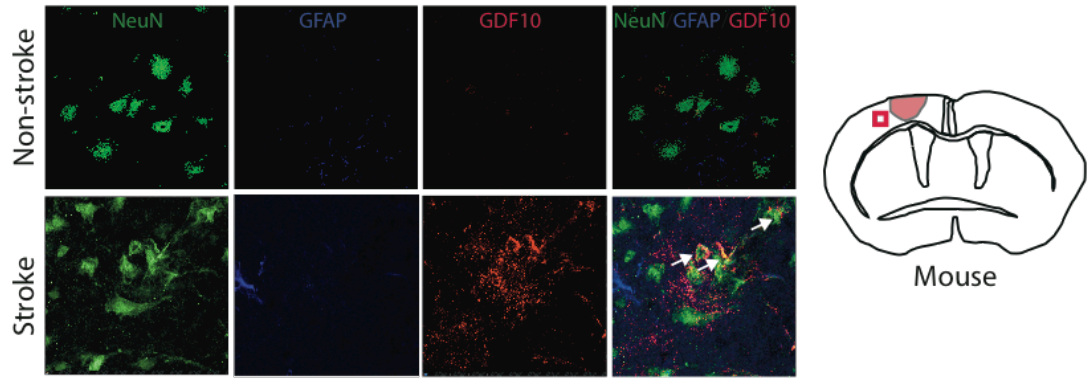


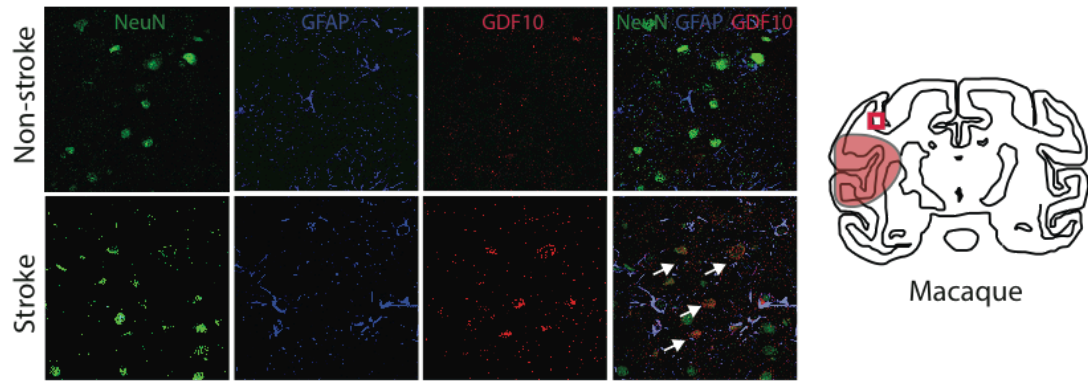
Figure 5.4 GDF10 promotes motor behavioral recovery after stroke

a) Cylinder test of forelimb symmetry in exploratory rearing (n=7 all conditions in behavioral testing). Y-axis shows bilaterally symmetric rearing as 0.0 and percent of left (unaffected) forelimb rearing as negative values. Left graph: Stroke causes a significant increase in the number of rears with the left forelimb. GDF10 treatment produces a significant recovery compared to stroke+vehicle (# = P<0.05) and stroke+cyto C (^ = P<0.05). Right graph: Stroke+GDF10 siRNA impairs the normal recovery seen in stroke+vehicle (# = p<0.01) and in stroke+scrambled siRNA (\$ = P<0.05). **(b)** Gridwalking test of forelimb function in gait. Y-axis is the number of footfaults of the forelimb contralateral to the stroke (right forelimb). Left graph: Stroke+GDF10 produces a significant recovery in forelimb function compared to stroke+cyto C (^ = P<0.05). Right graph: Stroke+GDF10 siRNA reduces the normal process of motor recovery after stroke (** = P<0.01, compared with stroke+vehicle) and impairs the forelimb function compared with stroke+scrambled siRNA (\$ = P<0.05). **(c)** Pasta handling task after stroke. Y-axis is the percentage of handling time using right forepaw relative to both paws. Delivery of GDF10 results in a significant recovery in forepaw use compared to delivery of protein control cyto C (^ = P<0.05). Injection of GDF10 siRNA complex significantly reduces right forepaw function compared to injection of the scrambled siRNA (\$ = p<0.05). In (a) $F(1.958, 11.75) = 22.07$; (b) $F(1.869, 11.21) = 10.70$; (c) $F(2.101, 12.61) = 9.382$. Error bars are SEM. Statistics are multiple comparisons ANOVA followed by Tukey-Kramer's post hoc test

(a)



(b)



(c)

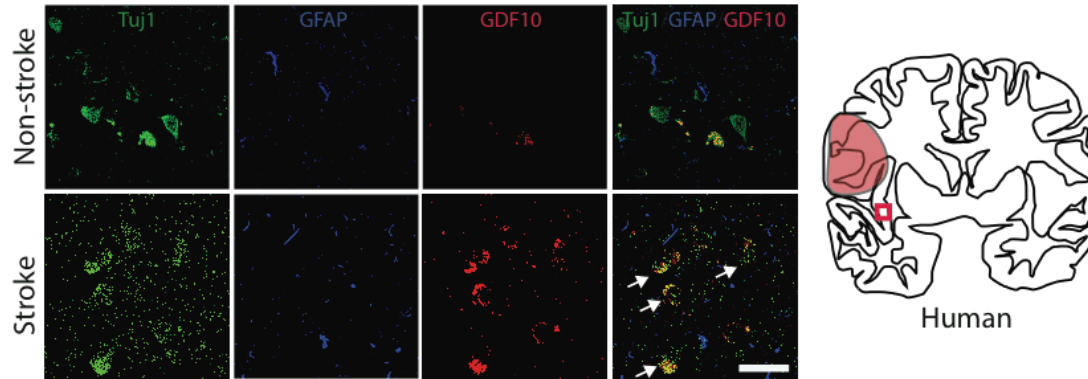
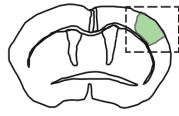


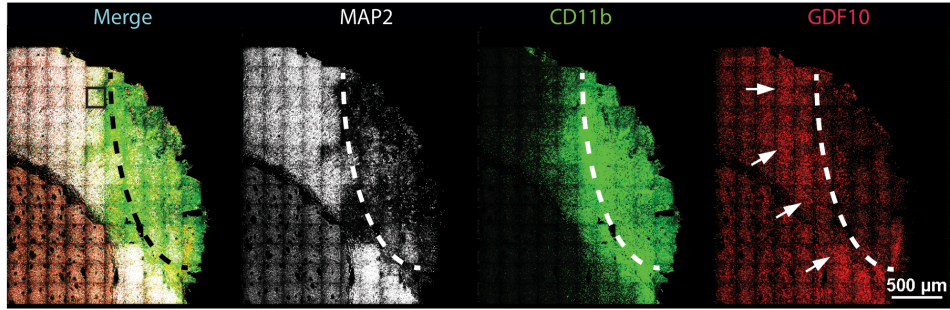
Figure 5.5 GDF10 is expressed in rodent, monkey and human peri-infarct tissue after stroke

a) Immunohistochemical staining in peri-infarct cortex in mice 7 d after stroke ($n = 5$). GDF10 staining (red) was apparent in peri-infarct tissue, overlapping with NeuN staining (green). Arrows in bottom right panel indicate representative NeuN+, GDF10+ cells. **b)** Immunohistochemical staining in peri-infarct cortex in non-human primate ($n = 2$ stroke, $n = 3$ control) 2d after stroke. Data are presented as above. Arrows in bottom right indicate double-labeled NeuN+, GDF10+ neurons after stroke. **c)** Immunohistochemical staining in human control ($n = 4$) and stroke ($n = 7$). Arrows indicate neurons labeled with both GDF10 and either NeuN or TuJ1 after stroke. In this human case, the stroke is chronic, or greater than 3 months after the event. Scale bar in the bottom right panel represents 50um and applies to all photomicrographs.

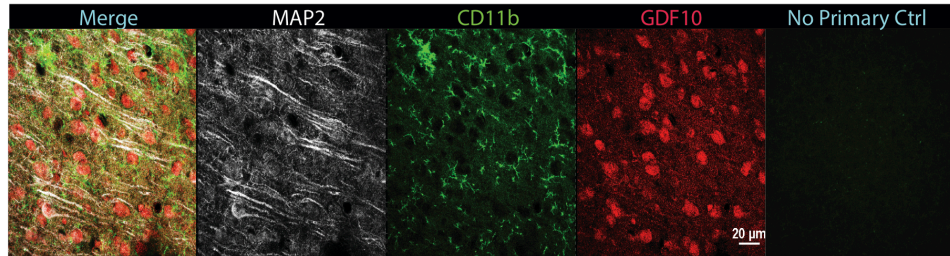
Figure 5.6



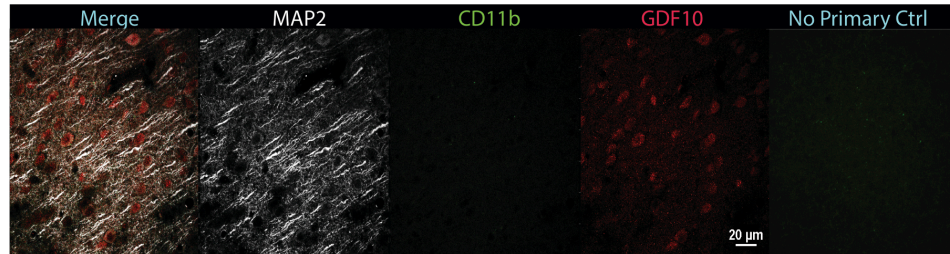
a) Stroke infarct and ipsilesional cortex (hemispheric overview)



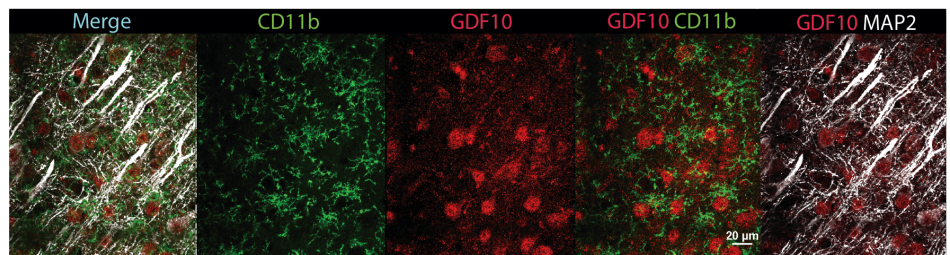
b) Peri-infarct Cortex (60X)



c) Contralateral Cortex Control (60X)



d) GDF10 upregulated in peri-infarct neurons and excludes microglial/macrophages



e) Extracellular GDF10 adjacent to infarct area near surviving neurites

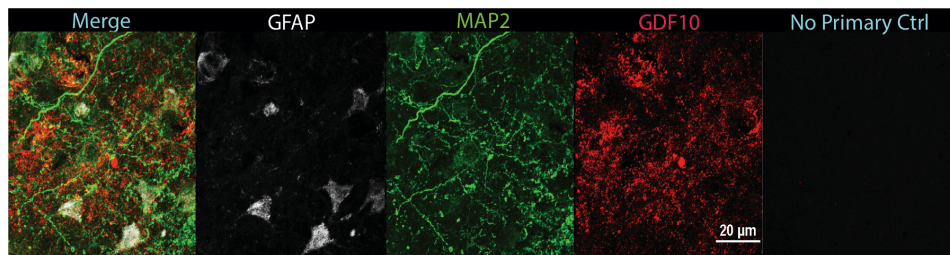


Figure 5.6. GDF10 is upregulated in peri-infarct cortex neurons and extracellular space after stroke

a) GDF10 protein expression in the ipsilateral hemisphere after stroke. This low magnification photomicrograph of the ipsilesional hemisphere shows axonal loss, as indicated by loss of MAP2, in the stroke core. GDF10 is induced in the cortex bordering the stroke core, as seen by the increased intensity of staining (arrows). The stroke core contains an abundance of microglia and macrophages, labeled by CD11b. **b)** GDF10 expression in the peri-infarct cortex. Image is taken from the region of interest indicated by box in panel a). GDF10 protein expression is upregulated compared to contralateral control in 1c). **c)** GDF10 expression in the non-injured cortex from the contralateral hemisphere. GDF10 has a sparse low level of endogenous expression. This indicates that GDF10 induction is specific to cortex immediately adjacent to the site of stroke injury. In the absence of stroke, CD11b is not induced in the control cortex. **d)** GDF10 expression in the peri-infarct colocalizes to neurons labeled with MAP2 and excludes microglia and macrophages. GDF10 immunoreactivity is present in MAP2+ neuronal somas and in dendrites. GDF10 does not colocalize with CD11b+ microglia/ macrophages. **e)** Secreted GDF10 is also found in the extracellular space in the peri-infarct cortex near surviving axons (MAP2).

Table 5.1

Study name	Species	Platform	Reference
Developing Cortical Efferent Neurons	Mouse	microarray	Arlotta, P., Molyneaux, B.J., Chen, J., Inoue, J., Kominami, R. & Macklis, J.D. Neuronal subtype-specific genes that control corticospinal motor neuron development in vivo. <i>Neuron</i> . 45 , 207-21. (2005)
Mouse Cortical Neurons: P7, P16, P28	Mouse	microarray	Cahoy, J.D. <i>et al.</i> A transcriptome database for astrocytes, neurons, and oligodendrocytes: a new resource for understanding brain development and function. <i>J Neurosci</i> 8 , 264-78 (2008).
Growth cone	Mouse	microarray	Zivraj, K.H. <i>et al.</i> Subcellular profiling reveals distinct and developmentally regulated repertoire of growth cone mRNAs. <i>J Neurosci</i> 30 , 15464-78 (2010).
Critical Period Mouse (P28)	Mouse	microarray	Lyckman, A.W., <i>et al.</i> Gene expression patterns in visual cortex during the critical period: synaptic stabilization and reversal by visual deprivation. <i>Proc Natl Acad Sci U S A</i> 105 , 9409-14 (2008)
Retinal ganglion transection or crush	Rat	microarray	Agudo, M., <i>et al.</i> Time course profiling of the retinal transcriptome after optic nerve transection and optic nerve crush. <i>Mol Vis</i> 14 , 1050-63 (2008).
Exercise and Hc memory enhancement	Rat	microarray	Inoue, K., Unpublished GEO data set. http://www.ncbi.nlm.nih.gov/geo/query/acc.cgi?acc=GSE45813
Motor cortex SCI	Rat	exon array	Jaerve, A., Schiwy, N., Schmitz, C., Mueller, H.W. Differential effect of aging on axon sprouting and regenerative growth in spinal cord injury. <i>Exp Neurol</i> 231 , 284-94 (2011)
Fear conditioning medial PFC	Mouse	Hiseq 2000	Bero, A.W., <i>et al.</i> Early remodeling of the neocortex upon episodic memory encoding. <i>Proc Natl Acad Sci U S A</i> 111 , 11852-7 (2014)
Contralateral cortex stroke	Rat	BeadChip	Zai, L., <i>et al.</i> Inosine alters gene expression and axonal projections in neurons contralateral to a cortical infarct and improves skilled use of the impaired limb. <i>J Neurosci</i> 29 , 8187-97 (2009).

Table 5.1 Sources of expression profiles for transcriptomic overlay analyses

Figure 5.7

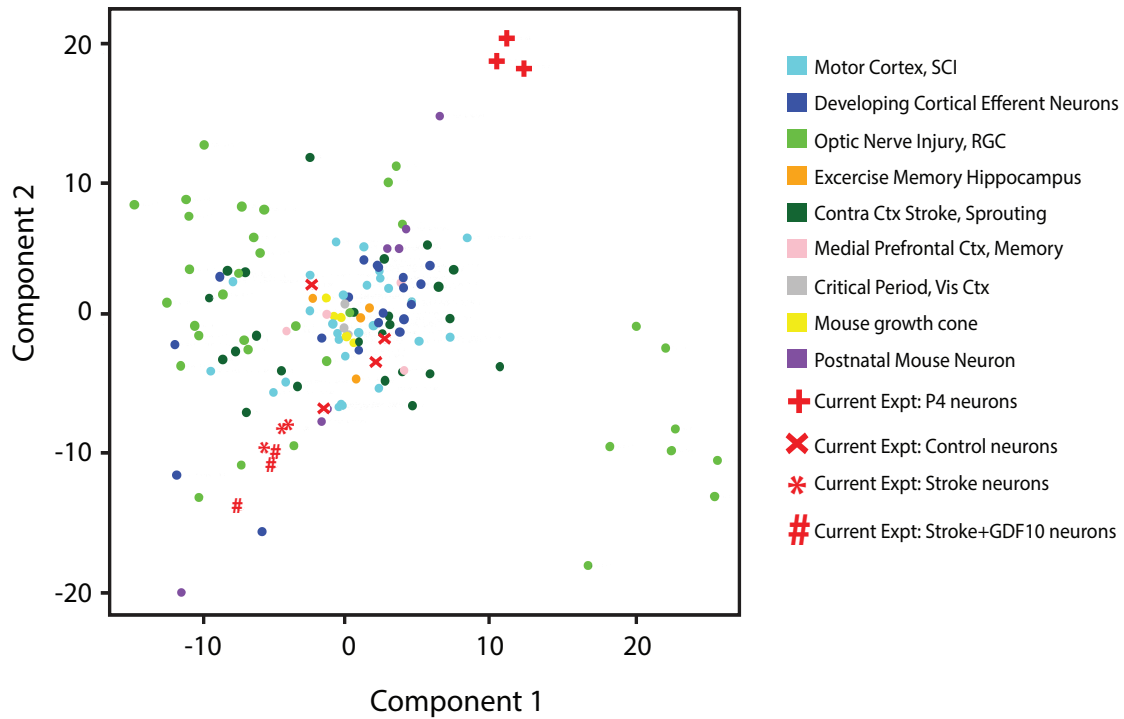


Figure 5.7 Molecular transcriptome comparisons across stroke, developmental, learning and memory and other CNS injury profiles

Genome wide associations of Stroke+GDF10 transcriptome to learning and memory, neurodevelopmental and CNS injury transcriptomes. Current experiment stroke+/- GDF10 expression profiles lay distant from developmental profiles and partially overlap with optic nerve regeneration profiles. Statistical testing was Fisher's exact p value, Benjamini Hochberg correction for multiple comparisons and principle component analysis across datasets from 10 transcriptomic studies (Table 5.1).

Figure 5.8

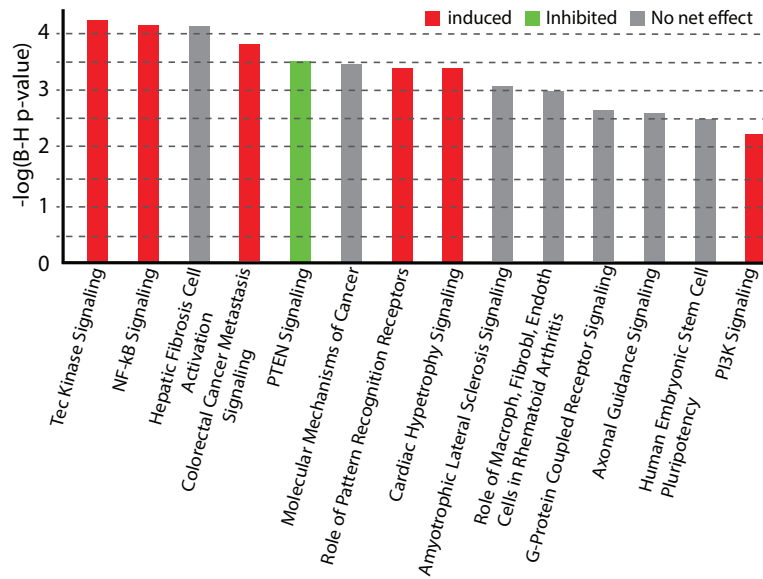


Figure 5.8 GDF10 canonical signaling pathways

Top canonical pathways significantly regulated in Stroke+GDF10 vs. Stroke. Y-axis is inverse log of p value corrected for multiple comparisons in Benjamini-Hochberg (B-H) test. Significance is set to a B-H $p < 0.05 = -\log(\text{B-H } p\text{-value})$ of 1.3. Red is net upregulation of the genes in this pathway; green is net downregulation. Grey is mixed up or downregulation in pathway genes such that there is not net trend.

Table 5.2

PI3K and PTEN Pathway Components in Stroke+GDF10 vs Stroke

Symbol	Log Ratio	Symbol	Log Ratio
<i>PPP3R2</i>	4.616	<i>FYN</i>	-1.542
<i>PDGFRB</i>	4.023	<i>IRS1</i>	-1.568
<i>TNFRSF11A</i>	3.488	<i>PIK3R3</i>	-1.753
<i>TLR4</i>	2.689	<i>TGFBR1</i>	1.737
<i>PTPRC</i>	2.646	<i>INPPL1</i>	-1.706
<i>PIK3CD</i>	2.424	<i>CASP3</i>	-1.615
<i>ITGA4</i>	2.235	<i>CNKSR3</i>	-2.073
<i>PIK3CG</i>	2.233	<i>FGFRL1</i>	-2.019
<i>LYN</i>	1.748	<i>PLCD1</i>	-3.573
<i>ITPR2</i>	-1.454	<i>FASLG</i>	-5.479

Table 5.2. Differentially regulated genes within PTEN and PI3K pathways and fold change

Table 5.3

Symbol	Entrez Gene Name	Gene Symbol	Log Ratio
ARHGEF6	Rac/Cdc42 guanine nucleotide exchange factor (GEF) 6	NM_152801	1.996
ARHGEF7	Rho guanine nucleotide exchange factor (GEF) 7	NM_017402	-1.369
BMP5	bone morphogenetic protein 5	NM_007555	8.086
BMP6	bone morphogenetic protein 6	NM_007556	4.009
EFNA3	ephrin-A3	NM_010108	-3.280
FIGF	c-fos induced growth factor (vascular endothelial growth factor D)	NM_010216	4.538
FYN	FYN proto-oncogene, Src family tyrosine kinase	NM_008054	-1.542
GNA14	guanine nucleotide binding protein (G protein), alpha 14	NM_008137	5.834
GNG4	guanine nucleotide binding protein (G protein), gamma 4	NM_010317	-2.855
IGF1	insulin-like growth factor 1 (somatomedin C)	NM_184052	3.191
ITGA4	integrin, alpha 4 (antigen CD49D, alpha 4 subunit of VLA-4 receptor)	NM_010576	2.235
MICAL1	microtubule associated monooxygenase, calponin and LIM domain containing 1	NM_138315	-2.110
NRP1	neuropilin 1	NM_008737	1.878
PIK3CD	phosphatidylinositol-4,5-bisphosphate 3-kinase, catalytic subunit delta	NM_008840	2.424
PIK3CG	phosphatidylinositol-4,5-bisphosphate 3-kinase, catalytic subunit gamma	NM_020272	2.233
PIK3R3	phosphoinositide-3-kinase, regulatory subunit 3 (gamma)	NM_181585	-1.753
PLCD1	phospholipase C, delta 1	NM_019676	-3.573
PPP3R2	protein phosphatase 3, regulatory subunit B, beta	NM_001004025	4.616
PTCH2	patched 2	NM_008958	6.952
SDCBP	syndecan binding protein (syntenin)	NM_016807	1.265
SOCS3	suppressor of cytokine signaling 3	NM_007707	-1.662
TUBA1A	tubulin, alpha 1a	NM_011653	-1.910
TUBB2B	tubulin, beta 2B class IIb	NM_023716	-1.874

Table 5.3 Axonal guidance genes differentially regulated by GDF10

5.5 Methods

Mouse model of stroke

Animal procedures were performed in accordance with the US National Institutes of Health Animal Protection Guidelines and the University of California Los Angeles Chancellor's Animal Research Committee. Focal cortical strokes on adult C57BL/6 male mice weighing 20–25 g (2–4 months old, Charles River Laboratories) were produced by photothrombosis at surgery as previously described (Lee et al., '07; Overman et al., '12). Briefly, under isoflurane anesthesia, mice were placed in a stereotactic apparatus with the skull exposed through a midline incision, cleared of connective tissue, and dried. A cold light source (KL1500 LCD; Carl Zeiss MicroImaging, Inc.) attached to a 40× objective was used to produce a 2-mm diameter focal stroke upon light illumination. Prior to illumination, 0.2 ml of Rose Bengal solution (10 mg/ ml in normal saline; Sigma) was administered i.p. After 5 min, the brain was illuminated through the intact skull for 15 min. The mice were then sutured along the scalp, removed from the stereotactic frame (**Model 900**, David Kopf Instruments), and allowed to recover. Body temperature was maintained at 37.0 °C with a heating pad throughout the operation. Control animals received no stroke.

Non-human primate model of stroke

Non-human primate tissues are taken from a previously reported stroke neuroprotection study in which stroke animals did not receive study drug (saline control, Bahjat et al., '11, n=3 stroke, n=2 control, non-stroke). Adult, male rhesus macaques (*M. mulatta*) were single-housed indoors in double cages on a 12:12-hour light/dark cycle, with lights-on from 0700 to 1900 hours, and at a constant temperature of 24°C±2°C. Laboratory diet was provided bidaily (Lab Diet 5047, PMI Nutrition International, Richmond, IN, USA) and supplemented with fresh fruits and vegetables.

Drinking water was provided ad libitum. The animal care program is compliant with federal and local regulations, regarding the care and use of research animals and is Association for Assessment and Accreditation of Laboratory Animal Care accredited. All experiments were approved by the Institutional Animal Care and Use Committee.

The right MCA (distal to the orbitofrontal branch) and both anterior cerebral arteries were exposed and occluded with vascular clips for 60 min. Animals were given ketamine (~10 mg/kg, intramuscular injection) and then intubated and maintained under general anesthesia using 0.8% to 1.3% isoflurane vaporized in 100% oxygen. A blood sample was taken and a venous line was placed for fluid replacement. An arterial line was established for blood pressure monitoring throughout the surgery and to maintain a mean arterial blood pressure of 60 to 80 mm Hg. End-tidal CO₂ and arterial blood gases were continuously monitored to titrate ventilation to achieve a goal CO₂ pressure of 35 to 40 mm Hg. Postoperative analgesia consisted of intramuscular hydromorphone HCl and buprenorphine. Animals were euthanized 2 d after stroke and tissue fixed in formaldehyde.

Human stroke

The cases selected for examination in this study are a retrospective, convenience sample of autopsy cases from a clinicopathologic study of cognitively normal subjects, those with subcortical ischemic vascular dementia (SIVD) or Alzheimer's disease (AD). Written informed consent for autopsy was obtained from all subjects or legal next-of-kin. From this larger database, cases selected for detailed microscopy included those with definable large artery infarcts determined by expert neuropathologic assessment of H&E stained sections. Sections from 7 of stroke and 4 control cases were evaluated.

GDF10 protein, GDF10 siRNA administration and BDA injection

GDF10 protein was delivered from the stroke cavity with a hyaluronan plus heparin sulfate hydrogel (Extracel-HP, Glycosan BioSystems) injected 7 d after stroke (A-P, 0.0 mm; M-L, 1.5 mm; D-V, 1.0 mm) (Paxinos and Watson, 2001). Six microliters of hydrogel impregnated with recombinant GDF10 (1.33 mg/ml, $n = 8$) (cat. no. 1543-BP-025/CF, R&D Systems), or protein control cytochrome C (Cyto C) (1.33 mg/ml, $n = 8$) (C2506-50MG, Sigma) was implanted into the stroke core. Three GDF10 siRNA duplex (cat. nos. MSS236596, MSS236597, MSS236598; Invitrogen) and negative control samples (12935-200, Invitrogen) were used to determine protein knockdown *in vitro* using day 4 postnatal mouse cortical primary neurons (Brewer and Torricelli, 2007; Xu *et al.*, 2012). The combination of MSS236597 and MSS236598 siRNA produced the greatest knockdown in GDF10 protein expression. This GDF10 siRNA ($n = 8$) or scrambled control siRNA ($n = 8$) duplex with RNAiMAX (cat. no. 13778-075, Invitrogen) (6 μ l) was introduced at 150 nM directly into the stroke cavity (A/P, 0.0 mm; M/L, 1.5 mm; D/V, 1.0 mm) (Paxinos and Watson, 2001) 7 d after stroke. At day 21 after stroke or 14 d after GDF10 protein, GDF10 siRNA or Cyto C injection, each mouse received an injection of 300 nL of 10% BDA (Sigma) into the forelimb motor cortex (A/P, 1.5 mm; M/L, 1.75 mm; D/V, 0.75 mm) (Paxinos and Watson, 2001). At 28 d after stroke, mice were perfused with paraformaldehyde and the cortex removed, flattened and sliced to 40 μ m tangentially (Li *et al.*, 2010; Overman *et al.*, 2012).

Behavioral Assessment

Mice (6-8 per group) were tested once on the grid-walking, cylinder and pasta eating tasks 1 week before surgery to establish baseline performance levels. Animals were tested at week 1, 3, 5, 7, 11 and 15 after stroke. Treatments were administered as for the axonal sprouting studies: GDF10+stroke, Protein control (Cyto C)+stroke, GDF10 siRNA+stroke and Sham+stroke. Assessment on the grid-walking, cylinder and pasta eating tasks were performed as previously

described (Allred and Jones, 2008; Overman *et al.*, 2012). Behaviors were scored by observers who were masked to the treatment group of the animals.

FACS

Tissue and cell preparation:

Male C57BL/6 mice age 4 months were anesthetized with isoflurane, decapitated, and cortical tissue removed from underlying white matter. Peri-infarct cortex (for stroke groups) or homologous sensorimotor cortex (for non-stroke groups) was dissected using a double tissue punch method: a ring of cortical tissue 750µm wide was isolated between two concentric circular tissue punches (3.0mm and 1.5mm in diameter) to exclude necrotic stroke core. P4 postnatal sensorimotor cortex was isolated using only one 1.5mm tissue punch. Cortical tissue was enzymatically digested and triturated based on a published protocol (Brewer and Torricelli, 2007). Briefly, cortical tissue was equilibrated for 8 minutes and digested for 30 min at 30°C and 190 rpm in 6 mL papain solution (12 mg/mL). Complete Hibernate buffer (BrainBits) was used to maintain neural metabolites and pH during tissue dissection and digestion. Glutamate antagonists kynurenic acid and AP5 were added to minimize excitotoxicity (Ozdinler and Macklis, 2006). Tissue was triturated into 6 mL suspension and loaded onto density gradient column (4 mL of 12.4% OptiPrep in Hibernate), and centrifuged for 15 min at 900g at 22°C. The bottom 5 mL was collected and washed 2X at 400g for 5 min before antibody staining. Two cortices were pooled for each of the 12 FACS samples. 6 animals per group (stroke alone, stroke + 7d GDF10, Adult WT, P4 WT) were coupled into 3 samples each for a total of 12 samples across the 4 experimental groups for FACS analysis.

Cell sorting and RNA extraction:

Prior to flow cytometry, all cell suspensions were stained for neuronal marker NCAM (Mouse; NCAM-1/CD56 Allophycocyanin MAb, 10µL antibody/10⁶ cells, FAB7820A R&D Systems,) for 20

min at 25°C, and washed twice with HABG. Samples were maintained on ice during FACS isolation. APC sort gates were set using positive and negative controls prior to neuron sorting. Neurons were collected via FACS (FACsARIA, Becton Dickinson, UCLA FACS Core) directly into 400 uL lysis buffer for RNA isolation. Total RNA was extracted using RNA-Microprep kit (Zymo-Research) and eluted into 7 uL ddH₂O. RNA-quality was verified (RIN>7) on an Agilent Bioanalyzer.

Spinal Cord Injections:

As previously described in Chapter 2 Methods.

RNA-Seq and Bioinformatics of other neuronal transcriptomes

Total RNA from FACS-isolated cells from each condition (n=6) was pooled in 2 brains per sample. Total RNA was amplified and converted into double-stranded DNA, which is typically between 200 and 300 bp (Ovation RNA-Seq System v2, NuGen, San Carlos, CA) that was further processed with the Ovation UltraLow kit (NuGen). RNA libraries were prepared using a NuGen Ovation Ultra Low Mass kit for paired-end 2x50 RNA-sequencing (HiSeq2000, UCLA ICNN core). After library preparation (Encore NGS Library System I, NuGen) amplified double-stranded cDNA was fragmented into 300 bp (Covaris-S2, Woburn, MA). DNA fragments (200 ng) were end-repaired to generate blunt ends with 5' phosphatase and 3' hydroxyls and adapters ligated. The purified cDNA library products were evaluated using the Agilent Bioanalyzer (Santa Rosa, CA) and diluted to 10 nM for cluster generation in situ on the HiSeq paired-end flow cell using the CBot automated cluster generation system. Three samples at a time, all samples were multiplexed into single pools and run in 9 lanes total of Paired-End 2 x 100 bp flow cells in HiSeq 2000 (Illumina, San Diego, CA).

Six Libraries for RNA-Seq were prepared using the NuGen Ovation UltraLow library preparation protocol (NuGen Technologies, Inc.) and sequenced using an Illumina HiSeq 2500 sequencer across 10 lanes of 100bp-paired-end sequencing, corresponding to 3 samples per HiSeq 2500 lane. After demultiplexing, we obtained between 50 and 79 million reads per sample. Quality control was performed on base qualities and nucleotide composition of sequences. Alignment to the *M. musculus* (mm9) refSeq (refFlat) reference gene annotation was performed using the STAR spliced read aligner (Dobin et al., '12) with default parameters. Additional QC was performed after the alignment to examine: the level of mismatch rate, mapping rate to the whole genome, repeats, chromosomes, and key transcriptomic regions (exons, introns, UTRs, genes). One control sample failed QC and was excluded from analysis. Between 67 and 85% of the reads mapped uniquely to the mouse genome. Total counts of read-fragments aligned to candidate gene regions were derived using HTSeq program (www.huber.embl.de/users/anders/HTSeq/doc/overview.html) and used as a basis for the quantification of gene expression. Only uniquely mapped reads were used for subsequent analyses. Across the samples >25% of the annotated genes have been detected by at least 50 reads. Following alignment and read quantification, we performed quality control using a variety of indices, including sample clustering, consistency of replicates, and average gene coverage.

Differential expression analysis was performed using the EdgeR Bioconductor package (Robinson et al., '10), and differentially expressed genes were selected based on False Discovery Rate (FDR Benjamini Hochberg-adjusted p values) estimated at ≤ 0.1 (or 10% FDR). 3 samples from stroke, stroke+GDF10, P4 and 2 samples from control were compared. Clustering and overlap analyses were performed using Bioconductor packages within the statistical environment R (www.r-project.org/).

Genes that were differentially expressed false discovery rate (FDR) < 10% were submitted to Cluster 3.0 for hierarchical clustering analysis (Euclidian distance, centroid linkage clustering) and visualized using Java TreeView. Differentially expressed genes were further analyzed by molecular pathway analysis and canonical signaling systems (IPA, Redwood City, CA). Briefly, for IPA analyses the genes regulated in each specific category, filtered to only include genes $\leq 10\%$ FDR, were compared to all genes known to be involved in a given molecular pathway or canonical signaling system in a large curated database of molecular interactions. Fisher's exact p value was calculated by IPA to determine a statistically different relationship of a data set in the WT, stroke+/-GDF-10, and P4 cortical transcriptomes to chance representation of these genes. For the upstream analysis there are 4 values that go into the Fisher's exact p-value calculation with Benjamini Hochberg correction for multiple comparisons.

For genome-wide association testing, individual data from .cell, SRA or Excel files was obtained for each experiment (Table5.1). The gene symbol was located for each probe and average expression computed for duplicated genes. The data was combined with RNA-Seq data from this study and variance stabilization transformation normalization performed.

5.6 References:

- Akhurst, R.J., Hata, A., 2012. Targeting the TGFbeta signalling pathway in disease. *Nat Rev Drug Discov* 11, 790-811.
- Allred, R.P., Jones, T.A., 2008. Maladaptive effects of learning with the less-affected forelimb after focal cortical infarcts in rats. *Experimental neurology* 210, 172-181.
- Brewer, G.J., Torricelli, J.R., 2007. Isolation and culture of adult neurons and neurospheres. *Nature protocols* 2, 1490-1498.
- Cunningham, N.S., Jenkins, N.A., Gilbert, D.J., Copeland, N.G., Reddi, A.H., Lee, S.J., 1995. Growth/differentiation factor-10: a new member of the transforming growth factor-beta superfamily related to bone morphogenetic protein-3. *Growth Factors* 12, 99-109.
- Du, K., Zheng, S., Zhang, Q., Li, S., Gao, X., Wang, J., Jiang, L., Liu, K., 2015. Pten Deletion Promotes Regrowth of Corticospinal Tract Axons 1 Year after Spinal Cord Injury. *The Journal of neuroscience : the official journal of the Society for Neuroscience* 35, 9754-9763.
- Li, S., Overman, J.J., Katsman, D., Kozlov, S.V., Donnelly, C.J., Twiss, J.L., Giger, R.J., Coppola, G., Geschwind, D.H., Carmichael, S.T., 2010. An age-related sprouting transcriptome provides molecular control of axonal sprouting after stroke. *Nature neuroscience* 13, 1496-1504.
- Liu, K., Lu, Y., Lee, J.K., Samara, R., Willenberg, R., Sears-Kraxberger, I., Tedeschi, A., Park, K.K., Jin, D., Cai, B., Xu, B., Connolly, L., Steward, O., Zheng, B., He, Z., 2010. PTEN deletion enhances the regenerative ability of adult corticospinal neurons. *Nature neuroscience* 13, 1075-1081.
- Ng, S.C., de la Monte, S.M., Conboy, G.L., Karns, L.R., Fishman, M.C., 1988. Cloning of human GAP-43: growth association and ischemic resurgence. *Neuron* 1, 133-139.

- Overman, J.J., Clarkson, A.N., Wanner, I.B., Overman, W.T., Eckstein, I., Maguire, J.L., Dinov, I.D., Toga, A.W., Carmichael, S.T., 2012. A role for ephrin-A5 in axonal sprouting, recovery, and activity-dependent plasticity after stroke. *Proceedings of the National Academy of Sciences of the United States of America* 109, E2230-2239.
- Ozdinler, P.H., Macklis, J.D., 2006. IGF-I specifically enhances axon outgrowth of corticospinal motor neurons. *Nature neuroscience* 9, 1371-1381.
- Paxinos, G., Watson, K.B.J., 2001. *The Mouse Brain in Stereotaxic Coordinates 2nd ed.* . Academic Press: San Diego.
- Soderstrom, S., Ebendal, T., 1999. Localized expression of BMP and GDF mRNA in the rodent brain. *Journal of neuroscience research* 56, 482-492.
- Sun, F., Park, K.K., Belin, S., Wang, D., Lu, T., Chen, G., Zhang, K., Yeung, C., Feng, G., Yankner, B.A., He, Z., 2011. Sustained axon regeneration induced by co-deletion of PTEN and SOCS3. *Nature* 480, 372-375.
- Tennant, K.A., Asay, A.L., Allred, R.P., Ozburn, A.R., Kleim, J.A., Jones, T.A., 2010. The vermicelli and capellini handling tests: simple quantitative measures of dexterous forepaw function in rats and mice. *Journal of visualized experiments : JoVE*.
- Xu, S.Y., Wu, Y.M., Ji, Z., Gao, X.Y., Pan, S.Y., 2012. A modified technique for culturing primary fetal rat cortical neurons. *J Biomed Biotechnol* 2012, 803930.
- Zeiler, S.R., Gibson, E.M., Hoesch, R.E., Li, M.Y., Worley, P.F., O'Brien, R.J., Krakauer, J.W., 2013. Medial premotor cortex shows a reduction in inhibitory markers and mediates recovery in a mouse model of focal stroke. *Stroke; a journal of cerebral circulation* 44, 483-489.

CHAPTER 6.

INTEGRATION OF FINDINGS AND FUTURE OUTLOOK

After ischemic stroke, we find that overuse of the stroke-affected limb during the recovery period leads to marked axonal sprouting from retrosplenial cortex to premotor cortex. Studies in rodents, primates, and humans have previously demonstrated that premotor cortex is functionally involved in limb rehabilitation and post-stroke recovery (Cramer *et al.*, 1997; Dancause *et al.*, 2005; Johansen-Berg *et al.*, 2002; Overman *et al.*, 2012; Seitz *et al.*, 1998), but the specific structural changes that occur within premotor circuits remain unknown. The current study is the first to map a key circuit that mediates premotor cortical reorganization during limb overuse, and identifies retrosplenial cortex as an important origin for sprouting afferent projections into premotor cortex. Although not functionally tested within this body of work, rudimentary formation of this circuit may be partially responsible for the limited amount of “spontaneous recovery” after stroke (without limb overuse). However, we find that this RSC-PMC connection is vastly enhanced upon CIMT-like overuse, an activity-based behavioral therapy that improves long-term motor recovery. We also perform a connection-specific RNA-Seq expression profile study of the retrosplenial population of neurons uniquely connected to PMC after limb overuse, and identify 160 significant genes that characterize this circuit. Some molecular candidates like MEF2C and have previous roles in activity-dependent plasticity, but many are indeed novel to the field of injury-induced plasticity. These circuit and molecular findings start to bridge mechanisms of activity-dependent plasticity and neural repair plasticity. Lastly, in-vitro screening of 15 candidates highlights several candidate genes that increase neuronal outgrowth, and has prioritized a next tier of targets for in-vivo investigation.

As perhaps with all basic science ventures, the findings answer a few questions but open the floodgates for even more hypotheses. In the initial neuroanatomical mapping phase of this work, we

find that limb overuse drives increased premotor connectivity from three regions, two of which remain mysterious in this post-stroke context: the insular cortex and lateral somatosensory areas. Like retrosplenial cortex, the insular cortex is highly multimodal and plays the role of an integration center for somatosensory, motor, and emotional processing. In humans, the insular cortex is divided into social-emotional, sensorimotor, olfacto-gustatory, and cognitive networks that have unclear neuroanatomical connectivity (Kurth *et al.*, 2010). How behavioral therapy after stroke modulates these networks is unknown. On the other hand, sensory cortex reorganization has been studied after stroke and is functionally linked to increased motor recovery in the hand after CIMT (Laible *et al.*, 2012). The distant somatosensory areas likely engage an intermixed population of spared sensorimotor circuits during recovery, but the finer mechanisms will require deeper study. Lastly, the retrosplenial cortex (RSC) is a complex structure with anatomical subdivisions (i.e. granular vs. agranular RSC) that may differentially contribute to recovery after different types of stroke. While studies are starting to describe learning and memory mechanisms in the retrosplenial cortex (Cowansage *et al.*, 2014; Czajkowski *et al.*, 2014), exploring the RSC after stroke and other brain injuries is a subfield in its infancy.

Chapters 3 and 4 delve into the RSC-PMC molecular profile and screen top candidate genes for mechanistic contributions to neuronal outgrowth. From unbiased genome-wide transcriptome comparison analyses, we learned that this activity-induced post-stroke circuit is molecularly distinct from developmental and other CNS injury profiles. Transcriptome overlay analyses in Chapter 5's GDF10 studies echo these distinctions (Li and Nie, 2016). Together, these findings diverge from the idea that “regeneration recapitulates development.” While early studies in CNS regeneration looked at genes that were inspired by molecules from neuronal development (EphrinA5, Sema3a) or PNS injury (GAP43), larger datasets from our lab and others are now showing the uniqueness of the regenerating CNS neuron in the adult. An outstanding question from the transcriptomic work is

how relative gene expression changes are actually reflected in the transcriptome or proteome of a sprouting neuron. Moreover, how do epigenetic contributions to plasticity fit into the diverse neural repair landscape? Outside of focused gene or protein studies, the field still lacks rigorous and systematic studies in these pre- and post- transcriptional areas. Finally, in contrast to somal gene expression, recent advances in basic neuroscience highlight the importance of the “axonal transcriptome,” comprised of RNA-protein complexes (ribonucleoproteins) transported along microtubules. Emerging studies find that these transcripts are locally translated and have specific roles in axonal physiology, guidance and survival, and injury-induced regeneration (Doron-Mandel *et al.*, 2016; Rishal and Fainzilber, 2014; Ross *et al.*, 2011; Wu *et al.*, 2005). A look into this transported transcriptome has not been conducted in the post-stroke sprouting neuron, nor for that matter in other highly arborized cells that contribute to injury-response and plasticity such as microglia and astrocytes.

As we learn more about the confluence of mechanisms that contribute to recovery after stroke and other brain injuries (including axonal and dendritic plasticity, intrinsic neurophysiological changes, angiogenesis and stem cell recruitment), another big question is: how and when do we deliver potential combinatorial therapies to enhance these endogenous mechanisms of repair? Studies in the vein of the IPA upstream analyses may help generate targets that are master regulators or potent initiators of neural repair cascades that are targetable early in the recovery period. Alternatively, approaches to manipulate various downstream target genes within the same window (i.e. neurotropic viruses with large carrying capacities) will need to be developed for in-vivo delivery. Multiplexed CRISPR/cas9 knockout and activation platforms (Dahlman *et al.*, 2015; Platt *et al.*, 2014) are also starting to address this constraint. But even when all the technology is available and reliable, we will still need to continue the reductionist’s approach to answering basic questions about the intricate mechanisms of adult axonal sprouting. For example, even if we can deliberately turn on

all the intrinsic mechanisms for axonal sprouting after stroke, will it path-find correctly and lead to meaningful plasticity? Or may this lead to an overdrive state (or in the worst case scenario, a neoplastic state) that could have been prevented by a titrated growth signal? Will the “right” wiring also need experience-dependent input? This dissertation includes studies that broach upon a couple of these ideas by examining how plasticity mechanisms after injury can interface with activity-dependent processes driven by behavioral experience.

One long-standing question in the neural repair field has been: How are PNS and CNS regeneration related, and why is CNS regeneration so inhibited? One reasonable postulate is that CNS and learning and memory plasticity evolved from more basic forms of sensorimotor plasticity in response to injury. The latter includes mechanisms of the PNS, which largely innervates musculature that directly allows one to respond to external stimuli in the physical world. The PNS also regenerates more readily, perhaps given its extra-cranial vulnerability to injury and its critical innervation of muscles that need to be functionally intact for evolutionary survival. On the other hand, the CNS and in particular the brain, not only contains areas for primary sensory and motor processing, but it also dedicates “tissue real-estate” for higher order processing like multi-sensory integration, memory and cognition, and emotional processing. This multitude of functional areas is in principal organized by a coordination of hardwired and experience-dependent gene expression during neurodevelopment. However after development, the cortex has necessarily evolved sophisticated inhibitory mechanisms to limit aberrant plasticity in the adult brain in exchange for maintenance of efficient and reinforced functional networks. Of course, the healthy adult brain is capable of much learning and memory, though this occurs usually through fine-tuning synaptic contacts and strengths, rather than through tremendous circuit reorganization structurally. Stroke injury perturbs this anatomic and functional tranquility, awakens a unique set of intrinsic growth pathways, and concomitantly opens the door for experience-dependent circuit shaping in the adult.

From this perspective, we can view clinical CIMT as an activity-based therapy that engages the dynamic post-stroke CNS in new learning paradigms. Perhaps it is not surprising that plasticity profiles from injured neocortex will include a subset of PNS genes but also recruit novel players during CNS regeneration and behavioral therapy. While the basic mechanisms of axonal sprouting and motor practice and learning have traditionally been studied independently, our findings illuminate how these two processes interface at the circuit and molecular levels during the recovery period after stroke.

Future scientific studies are necessary to more fully understand post-injury plasticity in the adult brain. A lingering general question in post-injury structural plasticity is: do axotomized and spared neurons differentially contribute to sprouting after stroke? Recent evidence suggests that enhanced sprouting in injury-spared circuitry may be an untapped source for functional recovery (Jin *et al.*, 2015). The scope of our present work does not include examining if spared or injured RSC projections form the connection to PMC. Moreover, the RSC-PMC mapped after limb overuse is a circuit whose functional activity has not yet been tested in post-stroke CIMT. One potential study is to use the transgenic “Tet-Tag” mouse, in which c-fos drives EGFP production to label active circuits during a specific time window (Reijmers *et al.*, 2007), to visualize RSC and PMC neuronal activity during forelimb overuse after stroke. The advantage of this approach over calcium or voltage-sensitive imaging is that subsequent tissue analyses can be done to colocalize task-specific active neurons with neuronal tracers or immunostained candidate molecules. Based on the neuroanatomical maps and associated functional improvement after limb overuse, we might expect to see enhanced activity in this circuit only in rehabilitated animals, or in the context of in-vivo manipulation of the genes that drive this connection. Moreover, the RSC-PMC circuit has not been studied at all in nonhuman primates or patients, and may be differentially recruited across other species during behavioral shaping after injury. Alternatively, it is entirely possible that the exact

connection does not form at all in the human brain after stroke, and in this case we will have used it as a heuristic substrate to learn about the mechanisms that drive a unique, plastic connection after murine stroke. In trusting of basic science, we aspire that some of the molecular insights may continue to build a greater appreciation for CNS regeneration.

Stroke is a common disease that can occur almost anywhere in the brain. In the cortex, we are starting to learn how the 6-layered structure, nested in unitary microcircuits, long-range horizontal connections, and sub-cortically diving fibers has remarkable ways of rewiring in response to injury. This process has inherent limitations in the adult brain, but there is a beauty to its ontology, and exciting scientific endeavors are still enlightening us on the system's biological malleability. To quote Alexander Pope, we must continue to think and learn deeply, "or taste not the Pierian spring," the Muses' infinite source of knowledge of art and science (Pope, 1711). At the end of this odyssey of a project, I am left with more awe and wonderment of the brain than when I started graduate school. I look forward to continuing peering into this mysterious organ as my career begins.

*"A little learning is a dang'rous thing;
Drink deep, or taste not the Pierian spring:
There shallow draughts intoxicate the brain,
And drinking largely sobers us again.
Fir'd at first sight with what the Muse imparts,
In fearless youth we tempt the heights of arts,
While from the bounded level of our mind,
Short views we take, nor see the lengths behind,
But more advanc'd, behold with strange surprise
New, distant scenes of endless science rise!
So pleas'd at first, the tow'ring Alps we try,
Mount o'er the vales, and seem to tread the sky;
Th' eternal snows appear already past,
And the first clouds and mountains seem the last;
But those attain'd, we tremble to survey
The growing labours of the lengthen'd way,
Th' increasing prospect tires our wand'ring eyes,
Hills peep o'er hills, and Alps on Alps arise!"*

*Alexander Pope
Essay on Criticism (Part II), 1711*

6.1 References

- Cowansage, K.K., Shuman, T., Dillingham, B.C., Chang, A., Golshani, P., Mayford, M., 2014. Direct reactivation of a coherent neocortical memory of context. *Neuron* 84, 432-441.
- Cramer, S.C., Nelles, G., Benson, R.R., Kaplan, J.D., Parker, R.A., Kwong, K.K., Kennedy, D.N., Finklestein, S.P., Rosen, B.R., 1997. A functional MRI study of subjects recovered from hemiparetic stroke. *Stroke; a journal of cerebral circulation* 28, 2518-2527.
- Czajkowski, R., Jayaprakash, B., Wiltgen, B., Rogerson, T., Guzman-Karlsson, M.C., Barth, A.L., Trachtenberg, J.T., Silva, A.J., 2014. Encoding and storage of spatial information in the retrosplenial cortex. *Proceedings of the National Academy of Sciences of the United States of America* 111, 8661-8666.
- Dahlman, J.E., Abudayyeh, O.O., Joung, J., Gootenberg, J.S., Zhang, F., Konermann, S., 2015. Orthogonal gene knockout and activation with a catalytically active Cas9 nuclease. *Nature biotechnology* 33, 1159-1161.
- Dancause, N., Barbay, S., Frost, S.B., Plautz, E.J., Chen, D., Zoubina, E.V., Stowe, A.M., Nudo, R.J., 2005. Extensive cortical rewiring after brain injury. *The Journal of neuroscience : the official journal of the Society for Neuroscience* 25, 10167-10179.
- Doron-Mandel, E., Alber, S., Oses, J.A., Medzihradzsky, K.F., Burlingame, A.L., Fainzilber, M., Twiss, J.L., Lee, S.J., 2016. Isolation and analyses of axonal ribonucleoprotein complexes. *Methods Cell Biol* 131, 467-486.
- Jin, D., Liu, Y., Sun, F., Wang, X., Liu, X., He, Z., 2015. Restoration of skilled locomotion by sprouting corticospinal axons induced by co-deletion of PTEN and SOCS3. *Nat Commun* 6, 8074.

- Johansen-Berg, H., Rushworth, M.F., Bogdanovic, M.D., Kischka, U., Wimalaratna, S., Matthews, P.M., 2002. The role of ipsilateral premotor cortex in hand movement after stroke. *Proceedings of the National Academy of Sciences of the United States of America* 99, 14518-14523.
- Kurth, F., Zilles, K., Fox, P.T., Laird, A.R., Eickhoff, S.B., 2010. A link between the systems: functional differentiation and integration within the human insula revealed by meta-analysis. *Brain Struct Funct* 214, 519-534.
- Laible, M., Grieshammer, S., Seidel, G., Rijntjes, M., Weiller, C., Hamzei, F., 2012. Association of activity changes in the primary sensory cortex with successful motor rehabilitation of the hand following stroke. *Neurorehabilitation and neural repair* 26, 881-888.
- Overman, J.J., Clarkson, A.N., Wanner, I.B., Overman, W.T., Eckstein, I., Maguire, J.L., Dinov, I.D., Toga, A.W., Carmichael, S.T., 2012. A role for ephrin-A5 in axonal sprouting, recovery, and activity-dependent plasticity after stroke. *Proceedings of the National Academy of Sciences of the United States of America* 109, E2230-2239.
- Platt, R.J., Chen, S., Zhou, Y., Yim, M.J., Swiech, L., Kempton, H.R., Dahlman, J.E., Parnas, O., Eisenhaure, T.M., Jovanovic, M., Graham, D.B., Jhunjhunwala, S., Heidenreich, M., Xavier, R.J., Langer, R., Anderson, D.G., Hacohen, N., Regev, A., Feng, G., Sharp, P.A., Zhang, F., 2014. CRISPR-Cas9 knockin mice for genome editing and cancer modeling. *Cell* 159, 440-455.
- Pope, A., 1711. *An essay on criticism (1st ed.)*: London.
- Reijmers, L.G., Perkins, B.L., Matsuo, N., Mayford, M., 2007. Localization of a stable neural correlate of associative memory. *Science* 317, 1230-1233.
- Rishal, I., Fainzilber, M., 2014. Axon-soma communication in neuronal injury. *Nature reviews. Neuroscience* 15, 32-42.

- Ross, J.R., Porter, B.E., Buckley, P.T., Eberwine, J.H., Robinson, M.B., 2011. mRNA for the EAAC1 subtype of glutamate transporter is present in neuronal dendrites in vitro and dramatically increases in vivo after a seizure. *Neurochemistry international* 58, 366-375.
- Seitz, R.J., Hoflich, P., Binkofski, F., Tellmann, L., Herzog, H., Freund, H.J., 1998. Role of the premotor cortex in recovery from middle cerebral artery infarction. *Archives of neurology* 55, 1081-1088.
- Wu, K.Y., Hengst, U., Cox, L.J., Macosko, E.Z., Jeromin, A., Urquhart, E.R., Jaffrey, S.R., 2005. Local translation of RhoA regulates growth cone collapse. *Nature* 436, 1020-1024.